U-Pbages and provenance of detrital zircon from metasedimentary rocks of the nya-ngezie and bugarama groups (dr congo): a key for the evolution of the mesoproterozoic kibaran-burundian orogen in central africa

Manon Villeneuve, A. Gaertner, C. Kalikone, N. Wazi, M. Hofmann, U. Linnemann

21 03 2019.

U-Pb ages and provenance of detrital zircon from metasedimentary rocks of the Nya-Ngezie and Bugarama groups (D.R. Congo): A key for the evolution of the Mesoproterozoic Kibaran-Burundian Orogen in Central Africa.

M. Villeneuve[1], A. Gärtner[2], C. Kalikone[3], N. Wazi [3], M. Hofmann[2], U. Linnemann[2]

[1]Aix-Marseille Univ., CNRS, IRD, INRA, Coll. France, CEREGE, Aix-en-Provence, France. Email: michel.villeneuve65@gmail.com,

[2] Senckenberg Naturhistorische Sammlungen Dresden, Museum für Mineralogie und Geologie, Sektion Geochronologie, GeoPlasma Lab, Königsbrücker Landstraße 159, 01109 Dresden, Germany, andreas.gaertner@senckenberg.de, mandy.hofmann@senckenberg.de, ulf.linnemann@senckenberg.de

[3] Université officielle du Sud Kivu, Bukavu. R.D. Congo, kalichrist@gmail.com, robertwazi@yahoo.fr

Abstract

The Kibaran Belt is one of the major Mesoproterozoic orogens formed between 1.4 and 1.0 Ga during the Rodinia assembly. Despite several decades of geologic investigations, correlations, evolution, and geodynamic models are still under debate. Modern studies distinguish the north-eastern Karagwe-Angkole Belt (KAB) and the southern Kibaran Belt (KIB). A further distinction of the KAB and the poorly studied northwestern Kivu Belt (KVB) has to be suggested. Latest researches in the KAB agree with a separation between a lower unit formed prior to 1375 Ma, and late tectono-magmatic events around 1250 Ma. The KIB model considers a continental collision starting at ~1.25 Ga with latest tectonic events at ca. 1.00 Ga. A more precise correlation was achieved by U-Pb age determinations on detrital zircon from six samples of the metasedimentary Nya-Ngezie and Bugarama groups. Both of them occur along the Congo,

Rwanda and Burundi borders and have frequently been used for interregional correlations despite their unknown age. Detrital zircon grains indicate Archaean to Mesoproterozoic inheritance for the Upper Nya-Ngezie Group (ca. 2800 to ca. 1120 Ma) and a similar age range for the lower Bugarama Group (ca. 2850 to ca. 1207 Ma). Accordingly, the two latest Kibaran-Burundian events of sedimentary deposition and tectonic overprint are younger than ca. 1207 and ca. 1120 Ma. This is inconsistent with prior age estimates for the bulk of formations in the vicinity. Thus, the time frame for the deposition of the numerous formations that have previously been correlated to the Nya-Ngezie and Bugarama groups has to be re-examined. New radiometric data indicate two formations in the western KVB that are younger than in the eastern KAB. Additionally, the detrital zircon record indicates significantly changing source rocks of the Nya-Ngezie deposits through time. Resulting correlations with the belts of the Kibaran-Burundian Orogen, suggest four geological “units”, seven tectonic events, five tectono-sedimentary cycles and two different geodynamic “models”. Additionally, three early, middle and late Kibaran belts are proposed. This allows proposing a reconciling model including a plate tectonic model to the West (KVB and KIB) and a coeval extensive model in the early stage of this orogen (KAB). Finally, the relationships between the N-S elongated structures belonging to the late Kibaran, late pan-African and modern rifting events in the same area are discussed.

Key Words: Mesoproterozoic orogen, Kibaran Belt, Central Africa, U-Pb geochronology, detrital zircon, lithostratigraphic correlations, geodynamic models, rift precursor

1 Introduction

The Kibaran Orogen of Central Africa is supposed to have been formed between 1.4 and 1.0 Ga. Therefore, it is among those orogenic belts like the Grenvillian in North America

(McLelland et al., 2001) or the Sunsas and Rondonian-San Ignacio in South America (Cordani et al., 2000), which were involved in the assembly of the Rodinia supercontinent between ca. 1.3 and 0.9 Ga (Li et al., 2008). The Kibaran belts extend from the Katanga region of southeastern Congo to Uganda through the Kivu province of eastern Congo, Burundi and Rwanda (fig. 1a). Despite numerous geological studies and radiometric age determinations in Katanga (Cahen, 1954; Cahen and Snelling, 1966; Cahen et al., 1984; Kampunzu, 2001; Kokonyangi et al., 2001), in Kivu (Boutakoff, 1939; Safianikoff, 1950; Peeters, 1956; Villeneuve, 1977; Villeneuve and Guyonnet-Benaize, 2006), in Rwanda and Burundi (Gérards and Ledent, 1970; Lavreau and Liégeois, 1982; Klerkx et al., 1984; Tack et al., 1990, 1994; Fernandez-Alonso and Theunissen, 1998; Deblond et al., 2001; Brinckmann et al., 2001; Tack et al., 2010; Fernandez-Alonso et al., 2012), in NW Tanzania (Ikungura et al., 1990, 1992; Boniface et al., 2014), and in Uganda (Vernon-Chamberlain and Snelling, 1972; Buchwaldt et al., 2008; Link et al., 2010), there are important debates concerning the Kibaran belts evolution. This applies particularly for geologists who worked in the western countries, e.g. the D.R. Congo, and those who worked in eastern countries like Burundi, Rwanda, and Uganda.

One debate concerns the number and timing of tectonic events. For Kampunzu et al. (1998a) as well as for Villeneuve and Chorowicz (2004), there are three main tectonic events accompanied by granitic intrusions around 1380, 1250 and from 1100 to 1000 Ma. Other authors propose a termination of the Kibaran Orogen at around 1.26 Ga (Rumvegeri, 1987, 1989), 1.25 Ga (Pöhl, 1994; Brinckmann et al., 2001), or 1.20 Ga (Pöhl, 1992). However, there is a general agreement about a post tectonic intrusive event, characterised by granitoids bearing cassiterite, wolframite, columbo-tantalite, and rare earth minerals, between 1.0 Ga and 0.94 Ga (Caron et al., 1986).

A second debate concerns the geodynamic interpretation. Kampunzu et al. (1986), Rumvegeri (1989) and Debruyne et al. (2015), who worked in the southern and western areas of the orogen (DRC), favoured a classical subduction / collisional model, while Klerkx et al. (1984), Tack et al. (2010), and Fernandez-Alonso et al. (2012), who worked in the eastern areas (Rwanda and Burundi), favoured an extensional basinal model.

A third debate concerns the age of the Kibara Belt's basement. In the Nya-Ngezie area, it was first ascribed to the Ruzizian Group, which supposedly occurred coeval to the Eburnean Orogeny at ca. 2.0 Ga (figs. 1 and 2; Boutakoff, 1939; Safianikoff, 1950). More recent studies limited the area of the Ruzizian outcrops drastically. However, Lavreau (1985) revealed the presence of Palaeoproterozoic Ruzizian terranes in the Lower Burundian (Kibaran) granitised basement. Villeneuve and Chorowicz (2004) considered a single basement in the northern part of the belt, where the Ruzizian and the Lower Burundian system with granitoid intrusions around 1375 Ma cannot be differentiated. These rocks are covered by several sedimentary formations that were folded and metamorphosed prior to the emplacement of 1.0 to 0.9 Ga old tin bearing granitoids (Cahen et al., 1967, 1984).

The process of putting the Kibaran Orogeny in a global context resulted in numerous proposals for stratigraphic correlations. This applies particularly for correlations between the southern Kibaride Belt (KIB), the northern Kivu (KVB), and Karagwe Ankolean (KAB) belts that are separated by the SE-NE striking Ubendian-Ruzizian high. Contemporary authors (Tack et al., 2010; Fernandez-Alonso et al., 2012) conclude that the northeastern part of the Kibaran orogens is different from the southern part. They proposed to distinguish the KIB in southern Katanga (former Shaba) from the KAB in Burundi, Rwanda, and Uganda. The complexity of the northwestern part of the Kibaran orogens, corresponding to the Kivu province of Congo, justifies

a differentiation of the KVB from the KAB. This approach considers the fact that there is no continuity in the field, no stratigraphic land mark level, and no sufficient radiometric age data to propose consistent correlations between the KAB and KVB that are separated by sediments and lavas of the "East African Rift". The closest area between them is Nya-Ngezie, which is separated from the adjacent countries of Rwanda and Burundi by the Ruzizi River. This area was carefully studied by Villeneuve (1977).

In order to clarify the above-mentioned debates U-Pb age determinations on detrital zircon have been performed on six samples from the Nya-Ngezie area south of the Kivu Lake (figs. 1 and 2). This area has formerly been used as referential stratigraphic scale for the Burundian formations, which there are capped by the pan-African "Itombwe" trench (Villeneuve, 1977; Cahen et al., 1979; Villeneuve, 1987). The new results suggest two latest Kibaran-Burundian depositional events of siliciclastic sediments younger than 1250 Ma, which were subsequently tectonised around or after 1111 ± 38 Ma. Finally, the existence of a Ruzizian "ghost" basement can be proposed for the vicinity.

2 Regional geological setting and previous geochronological framework

2.1 In the northern Kibaran belts (KVB and KAB). Figure 1b (Villeneuve and Chorowicz, 2004, modified) shows a schematic map of the northern part of the Kibaran belts (KVB and KAB). Several sedimentary belts, indicated by green colour, have a N-S general trend, while only few are E-W. Most of them are resting upon metamorphic basement inliers (yellow colour). According to Tack et al. (2010), the eastern part contains two domains: An eastern domain (ED) comprising sedimentary deposits on top of an Archaean basement, limited to the east of Rwanda and Burundi, and a western domain (WD) with sedimentary basins deposited on top of metamorphic inliers older than 1375 Ma (Tack et al., 1994). Both domains are separated by

a narrow transition zone (TZ, Tahon et al., 2004), including mafic to ultramafic sills of the Kabanga-Muzingati intrusive province (KM). A-type granitoid magmatism was found in two sites in the Gitega-Makebuko-Bukiasari (GMB) alignment of central Burundi that occurs in close spatial association with some KM mafic / ultramafic complexes and the TZ. However, emplacement ages of the KM complexes and A-type granitoid massifs of the GMB alignment seem not to be coeval.

A N-S-elongated structure (in blue colour) cropping out west of the Kivu Lake, is ascribed to the pan-African orogen (Villeneuve, 1977; Cahen et al., 1979).

These belts are bound to the east and to the north, by the Neoarchaean Tanzanian Craton and Kibalian Shield (3.0 to 2.5 Ga), themselves covered by Late Proterozoic sediments. To the south they are bound by the ca. 2.0 Ga Ubendian and Ruzizian belts. The KVB was first covered by the Palaeozoic sediments of the Karoo Group and then by Mesozoic sediments of the Congo Basin. Cenozoic sediments and volcanic lavas related to the "East African Rift" are limited to the central area separating the KVB from the KAB. Since the beginning of the twentieth century, two main units have been distinguished in the KVB and KAB by Salée (1928) and Salée et al. (1939): the metamorphic Ruzizian basement, and the overlying metasedimentary Urundian (former name of Burundian) formations. The latter authors provide the first geological map and also the first lithostratigraphic scale of these countries. In this scale the Urundian was divided into three formations, which are from base to top: U1, U2 and U3. U1 is mainly made of shale or micaschist, U2 comprises mostly quartzites, and U3 is again dominated by shale. This trilogy has been used and sometimes abused by successors, which were unable to distinguish common shale and quartzite alternations from the very Urundian trilogy. Boutakoff (1939) and successors (Safianikoff, 1950; Cahen, 1954; Peeters, 1956) ascribed the basement inliers to the

Palaeoproterozoic. In the KAB of Rwanda and Burundi, most of the granitic intrusions display early Mesoproterozoic ages (Lavreau and Liégeois, 1982; Cahen et al., 1984; Klerkx et al., 1984, 1987; Tack et al., 2010). Four groups of granitic episodes can be distinguished: G1 (1370 ± 25 Ma), G2 (1308 ± 25 to ~1250 Ma), G3 (1094 ± 50 Ma), and G4 (977 ± 18 Ma). Furthermore, Klerkx et al. (1984, 1987) reported an Rb/Sr isochron age of 1185 ± 59 Ma for some granitoids exposed in Burundi and Lavreau and Liégeois (1982) reported a tectono-metamorphic event at 1111 ± 38 Ma. The latter is likely linked to the NW-SE (D2) tectonic phase in central Rwanda. Several attempts have been performed to establish a synthetic lithostratigraphic succession as well in Rwanda (Baudet et al., 1988) as in Burundi (Radulescu, 1981), and even in the Kivu area (Villeneuve and Chorowicz, 2004). The most used succession in Rwanda and Burundi is that of Baudet et al. (1988), which distinguished four lithostratigraphic groups. However, radiometric ages (Tack et al.,2010) led to the distinction of the ED comprising two groups from the WD with four groups.

2.2 First geologic investigations in ***the Kivu Belt (KVB)*** were undertaken by mining companies and the Geological Survey of Congo Belge (SGCB). They distinguished between two main units: the Ruzizian and the Urundian based on their grade of metamorphism. At this time, no consistent discontinuities were found between them. Later on Lhoest (1946), who mapped the Itombwe syncline in the Luemba area of southern Kivu, evidenced an Urundian – now Burundian – syncline superimposed to a Ruzizian basement. Lhoest (1964) extended the eastern flank of this syncline to the Nya-Ngezie area, while Peeters (1956) did not found any unconformity at all and extended the Itombwe formations until Rwanda. Initially, the N-S trending Itombwe Syncline at Luemba (Lhoest, 1946), was linked to the Mesoproterozoic Urundian. Then, Villeneuve (1987) showed that there are two different superimposed synclines of which the lower one is linked to a

Kibaran, whereas the upper one is linked to a pan-African trench. Consequently, the western unconformity observed by Lhoest (1964) at Kasika on the northwestern part of the Itombwe Syncline is not similar to that observed by Villeneuve (1976) at Nya Kasiba on its northeastern side. The first one is related to the base of the Mesoproterozoic Burundian terranes, while the second one is linked to the base of the pan-African Itombwe Group. In order to avoid any further confusion, the upper likely pan-African structure is considered as "Itombwe Syncline" in the following text, while the lower one is named "Luemba Syncline" (Villeneuve and Chorowicz, 2004). The northwestern Kivu area from the Mt. Kahusi to Walikale was initially investigated by Blaise (1934) and Boutakoff (1939), who applied the Salée (1928) lithostratigraphy. More recent work on that area was published by Kampunzu (1981), Rumvegeri et al. (1985), Rumvegeri (1987), and Mugaruka Bibentyo et al. (2015). The western edge of the Kivu Lake has been studied by Pasteels (1961), Blès (1972) and Villeneuve (1983a), who ascribed the metasedimentary formations to the early Burundian Group (Stenian), except a syncline filled with pink shale and feldspathic sandstone linked to the late Burundian (Blès, 1972). The northern Kivu area was studied by Legraye (1939), Lhoest (1940), Aguillaume et al. (1975), and Thibault (1982). The Burundian sedimentary succession was proven in two trenches with a detrital formation at the base and a volcanic complex on top. Tectonic structures are E-W and N-S. Previous studies carried out by Cahen et al. (1976) have detected an N-S folding trend prior to the E-W structuration.

The last paper devoted to the KVB (Villeneuve and Guyonnet-Benaize, 2006) uses support of remote sensing and led to the recognition of two formations in the basement: a metamorphic one at the base and several metasedimentary formations on top that are named the "Oso Formation" to the north (Masisi area) and the "Ulindi Formation" to the south (Mulungu

area). This is in accordance with the results published by Rumvegeri (1987) in the western Kivu area. Unfortunately, there is no radiometric age data at all on this basement.

The latest attempt to correlate the KVB and KAB (Villeneuve and Chorowicz, 2004) took the similarities in local lithologic successions into account, but the lack of "marker levels" like basal conglomerates associated to unconformities prevent any robust correlations and the paucity of radiometric data in the Kivu area is a major problem. The first radiometric ages were obtained by Monteyne-Poulaert et al. (1962) and Cahen and Ledent (1979) by the Rb/Sr method (520 ± 9 Ma and 989 ± 28 Ma, respectively). U-Pb data on detrital zircon from metasediments performed by R. Armstrong (Kampunzu et al., 2003a and Kampunzu et al., 2003b) have not yet been published owing to the sudden death of A.B. Kampunzu, in 2004.

2.3 The Nya-Ngezie area is a key area of the Kivu geology and was first studied by Boutakoff (1939). He ascribed the western epimetamorphic rocks to the Mesoproterozoic Burundian Group (e.g. Kibaran Orogen) and the eastern metamorphic rocks to the Palaeoproterozoic Ruzizian system (e.g. Ubendian Belt) by reference to the local Ruzizi River. Peeters (1956) interpreted this terrain as a monoclinal succession with a moderate dip of 45° to the NE. This led to the hypothesis that the western epimetamorphic rocks are older than the eastern micashists and gneisses. Our own studies in this area show the existence of an unconformity along the eastern edge of the Itombwe Syncline (Villeneuve, 1976) and differ from the preceding interpretation of the basement. This basement is considered to contain two superimposed lithostratigraphic groups: the upper episedimentary Nya-Ngezie Group and the lower metamorphic Bugarama Group. The first one exhibits large, NW-SE trending structures, whereas the second one shows some E-W trending structures. Both are cross-cut by the N-S Itombwe Syncline. Correlations with the adjacent Rwanda area (Frautschi, 1973) led us to the ascription of these two basement formations

to the Burundian Group. Consequently, we concluded that the stratigraphic formations in the overlying Itombwe structures were Neoproterozoic to Cambrian in age (710 and 520 Ma, Villeneuve, 1977). This hypothesis was further supported by geochronologic investigations (Cahen et al., 1979; Kampunzu et al., 2003b). Owing to a general lack of radiometric data in the Nya-Ngezie area, the more regional correlations remained very speculative.

The geological scheme reported in figure 2 shows three main structural units, which are from the west to the east: the N–S trending unit (in yellow) corresponding to the "Itombwe Supergroup", the central NW-SE trending anticlines and synclines (in orange) corresponding to the Nya-Ngezie Group, and the NW-SE trending structures (in dark brown) corresponding to the Bugarama Group. The Neogene lavas of the African Rift are lying to the north. Thus, from the top to the base, four main units have been distinguished above the basement in this area:

- The modern alluvium and Neogene lavas consisting of basalts, basanites, hawaiites, and phonolites, studied by Pasteels et al. (1989), Kampunzu et al. (1998b) and Pouclet and Bellon (2016).

- The Itombwe Formation of Neoproterozoic-Cambrian age (Villeneuve, 1977, 1987).

- The Nya-Ngezie Group, which is made of rocks displaying a very low grade of metamorphism (Villeneuve, 1977).

- The Bugarama Group, which includes three formations (Villeneuve, 1977).

- A granitic pre-Bugarama basement is reported to the south of Kamanyola, but was not studied.

Two unconformities are separating these groups: the “Nya-Kasiba unconformity” between the Itombwe Formation and the underlying groups and the “Mount Kamashuli unconformity” between the Nya-Ngezie and Bugarama groups (Fig. 2).

The Itombwe Supergroup consists of conglomerate and schist at the base and mixtite and schist at the top. Rb/Sr age determinations on these sediments allowed Cahen et al. (1979) and Villeneuve (1987) to ascribe these formations to the Neoproterozoic pan-African Orogen of Katanga. Detrital zircon grains from the basal conglomerate indicate a ca. 710 Ma maximum age of sedimentation (Kampunzu et al., 2003b). The Itombwe Syncline was affected by only one tectonic event (D3), which caused the formation of N-S trending folds with a vertical axial schistosity (S3). Villeneuve (1977) divided this group in two formations: Nya Kasiba at the base and Tshibangu on the top. Only the latter exhibits several mixtite levels.

The Nya-Ngezie Group includes three formations, which are from the base to the top:

- The Bangwe Formation (600 m), which contains two quartzitic members separated by a phyllitic member. They display numerous sedimentary features as cross-beddings, ripple and scour-marks.

- The Mukubio Formation (1345 m) comprises quartzite, conglomerate, phyllite and quartz-phyllite. Banded, bicoloured millimetre-thick bedding is characteristic for the phyllites.

- The Mughera Formation (1000 m) consists of ferruginous sandstone (banded iron formations) with cross-bedding, monogenic conglomerate and banded phyllite. Intercalated “black sand” type sandstone beds were interpreted to be the product of sedimentary processes acting in an increasingly littoral environment (Chauvel and Villeneuve, 1987).

These rocks were affected by two tectonic events, termed D2 and D'2. D2 provides the main NW-SE trending succession of kilometric synclines and anticlines shown in the geological scheme (Fig. 2a). These deformations are represented at various scales varying from outcrops to thin sections. Axial planes of the NW-SE folds have a strong dip to the north (60° to 70°). Thus, the northern flanks are reverse, while the southern flanks are in "normal" position. These D2 deformation features represent the main structures in the underlying Bugarama Group. Additional D1 folds are observed in the folds of the lower Bugarama Group, but are absent in the Nya-Ngezie Group. D'2 deformations consist of numerous NE dipping reverse faults with a NE dip parallel to the axial plane of the D2 folds. These D'2 faults are visible at various scales, and are likely the result of south-westward thrusting events. Obviously, the D'2 event is considered as being associated with the last stage of the D2 tectonic event. D2 and D'2 deformations were not yet registered in the overlying Itombwe Group. On the contrary, the D3 folding of the Itombwe Group has been evidenced at various scales, in the Nya-Ngezie and Bugarama groups. D2, D'2 and D3 interferences are discussed in detail by Villeneuve (1977). In conclusion the D2 and D'2 tectonic events took place after the deposition of the Nya-Ngezie Group and prior to the deposition of the Itombwe Group.

Two metamorphic parageneses have been found in these rocks. They are related to the tectonic cleavages resulting from D2 and D3. Minerals are quartz, biotite, muscovite, and sericite, indicating a medium grade metamorphism.

According to Villeneuve (1977), the Bugarama and Nya-Ngezie groups have distinct sedimentary environments. The siliciclastic Nya-Ngezie Group is made of conglomeratic lenses embedded in coarse sandstone layers. These sandstones show abundant traces of streaming on the bedding surface, such as ripple- and scour-marks, cross-bedding, channel structures, etc. These

sedimentary traces are considered as characteristic of a littoral sedimentary environment. “Black sands” in the Mughera Formation, interpreted as beach placers by Chauvel and Villeneuve (1987), favour this hypothesis. Fig. 3 presents the direction measured for 80 ripple and scour marks of the Nya-Ngezie Group in their initial position before the D2 and D’2 tectonic deformations. Ripple marks are oriented NW-SE and WSW-ENE, while scour marks are perpendicular to the ripple marks. The scours indicate that the streams either came from the north or from the south. These data suggest that the siliciclastics of the Nya-Ngezie Group are made of immature sedimentary rocks that were most probably formed during the erosion of a belt. Conglomerates in the Nya-Ngezie Group include clasts, which were probably derived from the underlying Bugarama Group.

The Bugarama Group chiefly consists of metamorphic rocks, such as: phyllite, quartz-phyllite, micaschist, amphibolite, and gneiss. The Bugarama Group has been divided into three formations (Villeneuve, 1977, 1978), which are from the top to the base:

- The Mushenie Formation (1500 m) consists of quartz-phyllite with conglomerate, biotite-schist and brecciated quartzite with ferruginous matrix.

- The Kamanyola Formation (2300 m) is composed of interbedded grey to greenish metapelite with biotitic quartzite, garnet-micaschist, phyllite, and quartz-phyllite with numerous intercalated amphibolitic sills.

- The Kashenie Formation (> 225 m visible) is made of micaschist with garnet, biotite and magnetite, and calc-silicates.

Rocks of the Kamanyola and Kashenie formations experienced two important folding events. The first folds (D1) are visible in metric outcrops or in thin section (associated to a S1

cleavage), while the second folding (D2) is expressed on the map and corresponds to the NW-SE metric and kilometric structures. D2 is also present in the Nya-Ngezie Group. However, axes of decametric and kilometric folds trend more or less W-E in the Mushenie Formation. This also applies for the part of the Kamanyola Formation located in the core of the Mt. Bangwe anticline. Directions of the D1 fold axes are more or less E-W although the D1 folds are clearly reworked by the D2 folds and D'2 thrusts.

Mineral associations indicate a first paragenesis with quartz, biotite, muscovite sericite, garnet, and tourmaline linked to the S1 schistosity (greenschist facies). That indicates a moderate metamorphic grade. M2 and M3 paragenesis are associated to the D2 and D3 deformation and also indicate a low grade of metamorphism (greenschist facies).

The Kamanyola and the Kashenie formations exhibit a "flysh facies". The numerous doleritic sills parallel to the bedding corroborate the hypothesised flysch environment. The Mushenie Formation exhibits numerous lenses of conglomerate or breccia associated with ferruginous sandstone suggesting sedimentary deposits in a tectonic instable basin.

3 Radiometric data

3.1 Previous radiometric ages

The only published age determinations concern the Late Miocene (10 to 5 Ma) basalts dated by the K/Ar method (Pasteels et al., 1989; Pouclet and Bellon, 2016).

The first attempt to date the metasedimentary siliciclastic rocks from the Nya-Ngezie Group was undertaken by Kampunzu et al. (2003a) using detrital zircon from coarse-grained sandstone samples of the Bangwe Formation at the base of the Nya-Ngezie Group applying the SHRIMP method. The majority of the $^{207}Pb/^{206}Pb$ ages plots in a limited range between 1850 and

1950 Ma. Two significantly older zircons with concordant ages at 2290 ± 40 Ma and 2733 ± 11 Ma were also found. The youngest detrital zircon group has a concordant $^{207}Pb/^{206}Pb$ age of 1222 ± 28 Ma. However, due to the death of A.B. Kampunzu in 2004, the initial project to publish these results collapsed (Kampunzu et al., 2003a and 2003b, unpublished).

3.2 New radiometric ages

In 2013, four samples from the Nya-Ngezie Group were studied for their detrital zircon age patterns in order to control the previous data. To compare these results with the underlying Bugarama Group that is supposedly coeval with the Burundian groups of Rwanda and Burundi, two additional samples from the Bugarama Group were also studied for their detrital zircon age patterns. Biotite from another four samples from the Bugarama Group were analysed by the $^{40}Ar/^{39}Ar$ method in order to date the Kibaran metamorphism. But, only pan-African or Mio-Pliocene ages were found in 2015 by this approach. Thus, only the age data of detrital zircon of six samples is presented below.

3.3 Sampling

Four samples have been selected in the Nya-Ngezie Group:

NG1 (N2°41’39.9” / W28°53’51.8”) from the Bangwe Formation is a quartzite with ripple-marks collected at the Bushinga pass.

NG3 (N2°41’45.2” / W28°51’39.9”) from the Mukubio Formation is a banded quartz phyllite rock from the Bangwe Anticline.

NG4 (N 2°43'19.5"/ W28°50'06.6") and **NG2** (N2°42'43.8"/ W28°50'19.5") are both quartzitic sandstones from the Mughera Formation of the Mughera Syncline.

Two samples have been selected in the Bugarama Group:

NG5 (N2°41'86.0" / W28°57'02.0") is a grey micaschist from the lower part of the Kamanyola Formation, sampled along the road from Nya-Ngezie to Bujumbura.

NG6 (N2°42'23.0" / W28°58'00.0") is a garnet-bearing quartz micaschist from the Kashenie Group.

4 Methods

4.1 Sample preparation

Due to small sample sizes, not more than ca. 0.3 kg of each fresh sample was crushed in a jaw crusher. After this, the material was sieved for the 36 to 400 µm fraction. Heavy mineral separation from the latter was done using LST (lithium heteropolytungstate in water) prior to magnetic separation in the Frantz isomagnetic separator. Zircon grains for U-Pb dating were selected by hand-picking under a binocular microscope (ZEISS Stemi 2000-C). In order to get a representative selection of the overall zircon population, at least 120 zircon grains of all sizes, colours and morphologic types were randomly picked from each sample if possible (Fedo et al., 2003; Link et al., 2009). Nevertheless, some samples contained less than 120 grains. Subsequently, the zircons were mounted in resin blocks and polished to approximately half their thickness in order to expose their internal structure. Thus, CL-imaging was performed using SEM coupled to a HONOLD CL-detector operating with a spot size of 550 nm at 20 kV.

4.2 U-Pb age determination and Th-U measurement via LA-ICP-MS

In order to avoid mixed U-Pb ages resulting from different late-to postmagmatic or metamorphic influences, spots for isotope analyses were preferentially set on monophase growth patterns. U-Th-Pb isotopic analyses took place between 2013 and 2014 at the GeoPlasma Lab, Senckenberg Naturhistorische Sammlungen Dresden and were carried out via LA-ICP-MS (Laser Ablation with Inductively Coupled Plasma Mass Spectrometry) techniques. Therefore, a Thermo-Scientific Element 2 XR instrument coupled to a New Wave UP-193 Excimer Laser System was used (for data see electronic supplement, NG Radiometric tables). The mounts were put into a teardrop-shaped, low volume laser cell, produced by Ben Jähne (Dresden), for ablation. Due to its fast wash-out this cell allows sequential sampling of heterogeneous grains (e.g. growth zones) during time-resolved data acquisition. Single measurement of one spot is composed of approximately 15 s background acquisition followed by 30 s data acquisition. With respect on grain structure and size, the chosen spot sizes ranged between 25 (very few grains) and 35 µm. If necessary, correction of common-lead was carried out, based on the interference- and background-corrected ^{204}Pb signal and a model Pb composition (Stacey and Kramers, 1975). Judgement of necessity for correction depended on whether the corrected $^{207}Pb/^{206}Pb$ lay outside the internal errors of the measured ratios. A U-Pb analysis is concordant when it overlaps within uncertainty with the Concordia. So, it seems to be appropriate to exclude results with a low level of concordance ($^{206}Pb/^{238}U$ age / $^{207}Pb/^{206}Pb$ age × 100), but very large errors that overlap with the Concordia from interpretation. Thus, an interpretation with respect to the obtained ages was done for all grains within the concordance interval of 90-110 % ($^{206}Pb/^{238}U$ age / $^{207}Pb/^{206}Pb$ age × 100) which is often used (e.g. Spencer et al., 2016). Discordant analyses were generally interpreted with caution. Finally, raw data were corrected for background signal, common-Pb, laser induced elemental fractionation, instrumental mass discrimination, depth- and time-dependant elemental fractionation of Pb/Th and Pb/U by use of an Excel® spreadsheet program

developed by Axel Gerdes (Institute of Geosciences, Johann Wolfgang Goethe-University Frankfurt, Frankfurt am Main, Germany). The given uncertainties were propagated by quadratic addition of the external reproducibility obtained from the standard zircon GJ-1 (~0.6 % and 0.5-1.0 % for the $^{207}Pb/^{206}Pb$ and $^{206}Pb/^{238}U$, respectively) during individual analytical sessions and the within-run precision of each analysis. Each sequence started with five measurements of the GJ-1 zircon, followed by ten analyses of unknown grains, three spots on GJ-1 and so on. The obtained calculated Concordia ages for the GJ-1 reference zircon varied between 606.5 ± 2.6 and 606.8 ± 2.8 Ma (n_{total} = 428) for each analytical session (14 < n < 38 analyses per session), which is in line with the published ages (e.g. Jackson et al., 2004; Horstwood et al., 2016; and references therein). Concordia diagrams (2σ error ellipses) and concordia ages (95 % confidence level) were produced by using Isoplot/Ex 4.13 (Ludwig, 2001). The program Age Display (Sircombe, 2004) was employed to generate frequency as well as relative probability plots. For zircons with ages older than 1 Ga, $^{207}Pb/^{206}Pb$ ages were taken for interpretation, the $^{206}Pb/^{238}U$ ages for younger grains. Further details on analytical protocol and data processing are reported in Gerdes and Zeh (2006, 2009).

The general method for the age determination of rutile resembles that for zircon. A major aspect is the age discrepancy of the reference rutile as secondary standard when measured against a reference zircon as primary standard, which is likely caused by matrix effects (Luvizotto et al., 2009). Therefore, the ages and corresponding ratios of the unknown analyses have to be recalculated according to the deviation of the measured reference rutile ages from that given in the literature. In general, the use of a reference rutile as primary standard would be preferable, but as only the poorly defined SQR36 standard was available (Schmitt and Zack, 2012), it seemed to be a better choice to use the very well defined reference zircon GJ-1 as primary standard (Jackson et al., 2004). Ages received from the reference rutile measured against the GJ-1 standard had to

be corrected, for the obtained offset in age (1957 ± 7 Ma, n = 16, vs. 1998 ± 6 Ma and 2001 ± 7 Ma, (Schmitt and Zack, 2012).

5 Results

A total of 736 zircon grains was analysed for their U-Pb ages and 391 of them gave ages within an interval of concordance between 90 and 110% ("concordant" ages). If not explicitly mentioned, all following ages refer to zircon grains within this interval.

Age determinations from the Bugarama Group were done on samples NG5 and NG6. Sample NG6 yielded only two grains (of six dated) with ages at 1765 ± 24 Ma and 1889 ± 35 Ma. The paucity of concordant ages in NG6 and their occurrence in all samples (Fig. 4) limits the informative value of this sample with respect to provenance analysis. Unfortunately, the analysis of detrital rutile did not give any interpretable results. Forty five of 112 measured grains of sample NG5 yielded ages in a large span ranging from the Archaean (2820 ± 20 Ma) to the end of the Mesoproterozoic (1181 ± 69 Ma). Orosirian and Statherian ages occur frequently together with abundant Calymmian and Ectasian zircon ages. The youngest grain in NG5 shows an apparent age at 1181 ± 69 Ma, while the second youngest grain was dated at 1207 ± 28 Ma. Due to the large error of the youngest grain, which completely overlaps with the error of the second, the age at 1207 ± 28 Ma should be considered as the maximum age of deposition of the Bugarama Group. Anyway, the deposition is assumed to have happened in the post-1250 Ma Late Ectasian.

Age determinations from the Nya-Ngezie Group were done on samples NG1 (90/208 grains 90-110% conc.), NG2 (95/143 grains 90-110% conc.), NG3 (106/142 grains 90-110% conc.) and NG4 (53/114 grains 90-110% conc.). Detrital zircon age distribution patterns in NG1

of the Bangwe Formation and NG3 of the Mukubio Formation are very similar (Fig. 4). Both samples show an age peak around 1900 to 1800 Ma, while few zircon grains form a cluster with Kibaran ages between 1400 and 1200 Ma. However, NG1 exhibits some Archaean zircon ages comparable to those of NG5. Comparable ages were not found in NG3. NG2 and NG4 of the Mughera Formation have strong similarities with several age peaks between 1400 and 1100 Ma and zircon ages between 2200 and 1600 Ma. One grain of NG4 yielded an age around 2670 Ma that has no counterpart in NG2. The obtained detrital zircon age distribution patterns suggest a similar origin for sediments of the Bangwe (NG1) and Mukubio (NG3) formations. The age distribution patterns for the samples of the Mughera Formation (NG2, NG4) suggest a different origin. In any case, sedimentological investigations point to a source very proximal to the Nya-Ngezie area for the latter samples. Another major result concerns the maximum deposition ages of the Nya-Ngezie Group sediments Group, which are 1250 ± 18 Ma for NG1 (four youngest grains), 1216 ± 14 Ma for NG3 (five youngest grains), 1160 ± 19 Ma for NG4 (four youngest grains), and 1121 ± 14 Ma for NG2 (two youngest grains). These ages are consistent with the youngest ages (1222 ± 28 Ma) reported by Kampunzu et al. (2003a) in zircon grains from a sample located stratigraphically below NG1. Thus, the Nya-Ngezie Group is not older than 1250 Ma, and likely even as young as ca. 1120 Ma. The assumed age of the final deposition has to be set around 1000 Ma, which is the age of the first post-tectonic granites (Cahen et al., 1967, 1984).

A detailed list of all obtained radiometric results can be found in the supplementary tables, which are available from the journal website.

6 Discussion

Owing to the new results presented above, there are two main questions: 1) When was the likely time of deposition of the sediments and what is the age of the tectonic climax? 2) What is the potential origin of inherited zircons and location of potential source rocks?

6.1 Time of deposition of the Bugarama Group

The youngest detrital zircon grains at 1207 ± 28 Ma suggest a Stenian (Late Mesoproterozoic) age for the deposition of the Bugarama Group that was initially ascribed to the Ruzizian (Palaeoproterozoic) basement (Boutakoff 1939, Safianikoff 1950) or to the Burundian (Early to Middle Mesoproterozoic) by Villeneuve (1977) and Cahen et al. (1979). Previously, no metamorphic rocks younger than 1.25 Ga or 1.20 Ga have been reported in the KVB area except for the metamorphic rings linked to the tin bearing granites, which intruded during the Early Neoproterozoic (1000 Ma to 960 Ma, Cahen et al., 1967, 1984). With respect to the S1 folding and the metamorphism of the Bugarama Group prior to the deposition of the Nya-Ngezie Group, an older age has been expected. The 1121 ± 14 Ma of the youngest inherited zircon in the overlying Nya-Ngezie Group could be the age of the Bugarama metamorphism, which could be coeval to the D1 deformation.

6.2 Time of deposition on the Nya-Ngezie Group

The duration of deposition of the Nya-Ngezie Group remains unknown. However, it should be younger than the time bracket between 1121 ± 14 Ma (youngest inherited zircons) and the 1111 ± 38 Ma (Lavreau and Liégeois, 1982) which is the presumed age of the D2 tectonic event in Rwanda. In any case the D2 and D'2 tectonic events reported in the Nya-Ngezie Group are younger than 1121 ± 14 Ma and older than the ca. 710 Ma age, which is recorded in zircons from samples collected in the Nya-Kasiba basal conglomerates (Kampunzu et al., 2003b,

unpublished). Many authors, among them Caron et al. (1986), assume that D2 is younger than the widespread 960-1000 Ma tin bearing granites.

6.3 Possible source rocks

Despite they belong to two different groups there are some similarities between the detrital zircon age distribution patterns in samples NG6, NG1, and NG3 on one hand and NG5, NG4 and NG2 on the other. This could be caused by temporally changing delivery of siliciclastic detritus of potential source rocks.

The main question concerns the origin of the Archaean zircon grains identified in samples NG1, NG4, and NG5 and also by Kampunzu et al. (2003a) at the base of the Nya-Ngezie Group, because no Archaean outcrop has yet been described in the vicinity of the Nya-Ngezie area. A hidden Archaean massif is presumed elsewhere around, but a provenance from the Tanzanian Craton cannot be excluded. Furthermore, a provenance as recycled grains from the Palaeoproterozoic basement is also possible.

The Ruzizian basement with published ages between 2100 and 1700 Ma (Brick, 2011) is thought to have provided zircons in all six samples. Sedimentary investigations (Fig.3) indicate either a northern or a southern origin for the siliciclastic rocks. To the south, Cahen and Snelling (1966) obtained a Ruzizian Rb/Sr age at 1960 ± 170 Ma for the “Mojangjo” granite, cropping out in the north of Uvira (northern Tanganyika Lake). To the north, the nearest basement inlier with a Ruzizian age has been found at Runyinya (close to Butare) some 60 km away from the working area (Gerards and Ledent, 1970).

Mesoproterozoic zircon grains with ages between 1500 and 1200 Ma are present in every sample except NG6, which is likely due to the paucity of zircon in this sample. They can likely

be provided by the Burundian granitoids dated in Rwanda and Burundi. The closest dated granitic massifs crop out in northwestern Burundi (Brinckmann et al., 2001). Furthermore, the Kigarama / Akanyaru granite provided an Rb/Sr age of 1265 ± 45 Ma, and the Cibitoke / Kaburantwa granite yielded a U-Pb zircon age of 1210 ± 2 Ma. Both are considered as post tectonic by Brinckmann et al. (2001).

6.4 Conclusions from the new age determinations

Amongst the three main groups evidenced forty years ago (Villeneuve, 1977), the two lower have been correlated either to the Upper or Lower Burundian or also to the Ruzizian basement. Such discrepancies should be assigned to the lack of absolute age determinations. Now, it is known that the Nya-Ngezie and Bugarama groups belong to a late Kibaran-Burundian orogenic stage. Only the granitic basement cropping out in the lower Ruzizi valley is not yet dated but its linkage to the Bugarama Group metamorphism is strongly suspected (Brinckmann et al. 2001). This local study also confirms that a late metamorphic stage around 1120 Ma likely exists in the Kibaran-Burundian Orogen. The six new detrital zircon age spectra in the Nya-Ngezie and Bugarama groups provide useful information on the position of these two groups with respect to the western and eastern neighbouring terranes. Up to now, the stratigraphic position of these groups remained unclear with respect to the main western Burundian unit (Luemba-Bitale Supergroup), but the new data favours the hypothesis of a post-Luemba-Bitale deposition. These new age determinations also revealed a late molassic stage at the end of the Mesoproterozoic. This is interpreted as witness of late orogenic uplift and subsequent erosional processes. Contrary to Pöhl (1994), our results show that the Kibaran sedimentary deposition was not terminated at around 1.20 Ga. Thus, three groups of Kibaran belts can be distinguished: the early and middle

groups that are separated by the Luemba unconformity and the late group, which is cropping out in the Nya-Ngezie area and predates the opening of the pan-African Itombwe trough.

7 Correlations and consequences on the Kibaran-Burundian belts

Obviously, the new radiometric results have some consequences on the evolution of different parts of the Kibaran-Burundian belts. This applies particularly for the KVB, but also affects the adjacent KAB, KIB, and Irumide (IRB) belts under the assumption that the published stratigraphic correlations are more or less correct.

7.1 Consequences on the Kivu Belt (KVB)

The last attempt to correlate the formations of the eastern Kivu area, Villeneuve and Guyonnet-Benaize (2006) suggested four different Burundian units separated by three major unconformities. Out of the two lower units, ascribed to the Palaeoproterozoic and to the Lower Burundian (> 1380 Ma), they distinguished an Upper Burundian unit including the large majority of the Kivu trenches evidenced by Villeneuve and Chorowicz (2004) and the two groups of the Nya-Ngezie area. They considered two hypotheses depending on whether the Nya-Ngezie Group is older or younger than other formations of the Kivu area, classified as Upper Burundian. Furthermore, the Bugarama Group was correlated to the Lower unit of Lower Burundian age with respect to its metamorphism. However, the lack of radiometric data prevented any robust correlation. Now, taking into account the newly obtained radiometric data, we propose a revised correlation throughout the KVB. These correlations are based on the lithostratigraphic characteristics (four lithostratigraphic units), on the tectonic events (nine tectonic events), on the granitic magmatic events (four events), and on the metamorphic events (five events) that are explicitly explained in a separate paper devoted to the Kivu Belt, (Villeneuve et al., in progress).

The lithostratigraphic column presented in table I considers the correlations between the western and eastern Kivu units that are proposed elsewhere (Villeneuve et al., in progress). Apart from the two main units Kv1 and Kv2, considered by Villeneuve and Chorowicz (2004), two new units (Kv3 and Kv4) are delineated corresponding to the newly dated Bugarama and Nya-Ngezie groups, respectively. The metamorphic Bugarama Group is linked to the Bikangala Group (Rumvegeri, 1987), to the Masisi Group of the northern Kivu Lake, and likely to the "Burundien superieur" of Burundi as well as the Rugezi Group of the Burundian of Rwanda. In contrast, an equivalent to the metasedimentary Nya-Ngezie Group is only evidenced in the "serie supérieure" of the Kirotshe area (Blès, 1972). The lithological details of these four units and further parameters for the correlations are discussed in Villeneuve et al. (in progress).

Owing to the lack of robust radiometric studies, the relationships between the granitic bodies and the sedimentary deposits have not been debated here. The few granitic bodies dated by the Rb/Sr method (Nzombe, Kasika, Nyamakubi, Numbi, Kirumba, Kalehe, etc.) display a panel of pan-African ages, which are not in agreement with field observations (Pasteels, 1961; Blés, 1972; Burg et al., 1986; Villeneuve, 1987). According to Blès (1972), Burg et al. (1986), and Kampunzu et al. (1986) the Kasika and Mt. Hango granitoids are considered as post-Burundian despite they appear to be synkinematic with the Burundian host rocks. The best example of discrepancy between radiometric dating and field observations is the Kasika granite which looks like concordant with the Kv2 metasedimentary host rocks (Burg et al. 1986) but has been dated at about 986 ± 10 Ma by U-Pb on zircon (Tack et al., 2010). Another source of confusion is caused by similarities between the metamorphic events registered in the Bugarama Group (Kv3) and in the Kv2 unit rocks, since both metamorphic events resulted in quite similar lithologies and mineral compositions (sillimanite, kyanite, staurolite, garnet and biotite). All these granitic and metamorphic events are described in detail in the paper devoted to the KVB

(Villeneuve et al., in progress), but clearly, this area needs some more age determinations to be correctly correlated to the adjacent regions.

7.2 Consequences on the Karagwe Ankolean Belt (KAB)

The KAB includes Rwanda, Burundi, as well as parts of Uganda and Tanzania (Koegelenberg and Kister, 2014). The first synthetic paper devoted to the geology of Rwanda was published by Gerards and Ledent (1970), whereas the first synthetic map was coordinated by Ziserman (1983). Similar investigations have been performed in Burundi with the assistance of the Royal African Museum of Tervuren (Klerkx et al., 1984; Radulescu, 1981; Theunissen et al., 1991; Tack et al., 2010; Fernandez-Alonso et al., 2012). Between 1998 and 2001, the BGR (Hannover, Germany) conducted some geological and metallogenic studies in the northwestern part of Burundi adjacent to the Nya-Ngezie area (Brinckmann et al., 2001). Similar investigations have been performed in northern Rwanda by Pohl (1992, 1994). According to Tack et al. (1994), the KAB can be split in two parts: the eastern domain (ED or EED) and the western domain (WD or WID). Both are separated by a magmatic zone from each other (Tack et al., 1994, 2010; Fernandez-Alonso et al., 2012) called TZ by Tahon et al. (2004). The lithostratigraphic successions in the WD refer to the stratigraphic scale established by Baudet et al. (1988), which considers four groups: the Gikoro and Pindura groups at the base and the Cyohoha and Rugesi groups on top. Table I presents our attempt to correlate the Kivu Belt (KVB) to the WD and the ED. This table considers the five units (Kv1 to Kv4 plus K5) described in the Kivu Belt and their supposed counterpart (Ka1 to Ka5) in the Karagwe Ankole Belt. In conclusion of a meeting held in Tervuren in 1976 (Cahen et al., 1976), we admitted an equivalence of the Bugarama Group with the formations of Bugarama-Karengera evidenced in Rwanda (Frautschi, 1973), and with those cropping out in the Mabayi-Cibitoke area in Burundi. However, Radulescu (1981) ascribed

them to the Ruzizian basement in the geological map of Cibitoke. Later on, Theunissen (1989) classified these formations – called the Buganda-Ruhanda Complex – as the lower part of the Middle Burundian Group and ascribed the interbedded volcano-sedimentary Butahana-Murwi-Ngozoi and Mwokora formations to the upper part of the Middle Burundian Group. Subsequent geological investigations by Brinckmann et al. (2001) present a different interpretation. These authors assume an Upper Burundian relation for those terranes cropping out in areas in Burundi that are close to the Kamanyola and Kashenie localities. Two radiometric age determinations on the post tectonic granitoid of Cibitoke-Kabaruntwa (1210 ± 3 Ma and 1212 ± 2 Ma) were published by Brinckmann et al. (2001). This prevents us to correlate the Bugarama or the Nya-Ngezie Group with these adjacent Mesoproterozoic formations of Burundi, taking into account that zircon grains from these granites are included in the Bugarama sediments. A correlation with the Kv2 formations of Luemba, Bitale and Luntukulu fits better. Moreover, the Bugarama-Karengera Formation of Rwanda is thrust over the Bugarama Group. This thrust is exposed on the northern side of the Ruzizi River.

A correlation with the WD of Rwanda and Burundi by Fernandez-Alonso et al. (2012) linked the Bugarama Group to the Gikoro and Pindura groups. Likewise, the authors correlated the post 1375 Ma sedimentary deposits with the whole Nya-Ngezie Group. In our opinion these correlations should concern the Kv2 formations (including the Cyohoha and Rugesi groups) rather than the Nya-Ngezie Group (Kv4). This is more consistent with the 1300-1190 Ma detrital zircon ages found in samples NG2 and NG4. The last part of the KAB crops out in southern Uganda where the Karagwe-Ankolean units that cover the Palaeoproterozoic Kibalian / Ruwenzorian terranes (Westerhof et al., 2014). These metasedimentary and metamorphic formations are accompanied by large plots of “arena granites” (Wayland, 1920) which have been

dated in 1972 by the Rb/Sr isochron method and displayed ages between 1278 ± 58 Ma and 1146 ± 40 Ma (Vernon-Chamberlain and Snelling, 1972). However, new U-Pb age determinations on zircon from the same "arenas" massifs (Buchwald et al., 2008) show three age groups: one at around 1566 Ma, the second at about 1444 Ma and the third clusters between ca. 1368 and 1329 Ma. Thus, the Rb/Sr data is likely linked to later tectono-magmatic events rather than the emplacement of granitic intrusions.

Finally, lithostratigraphic correlations between the KVB and the KAB are exposed in table I. Surprisingly, no reliable counterpart of the Nya-Ngezie Group has been formally evidenced in the KAB throughout the geological literature, although the Upper Burundian Rugendo-Mabayi-Sagahanga Formation (Theunissen, 1989) exhibits some similarities with the Nya-Ngezie Group. Furthermore, the "Miyove" Formation is not older than 1250 Ma, and likely even as young as ca. 1120 Ma. This formation, which lies on top of the Rugesi Group, has been considered as a possible counterpart of the Nya-Ngezie Group. However, this Miyove Formation was involved in the Cyohoha and Rugesi tectonic events, and therefore should be associated to the Ka2.

In addition, two schematic cross sections have been drawn across the northern and southern parts of the KVB and KAB (Fig.5). They highlight the opposite vergence on both sides of the Kibaran Belt, on the Congo Craton to the west and on the Tanzanian Craton to the east. These cross sections show that the Kv1 and Ka1 units are capped by the Kv2 and Ka2 trenches. It has to be noted that the Kv4 unit does not crop out along these cross-sections.

7.3 Consequences on the Kibaride Belt (KIB)

The Kibara Mountains in the northern part of the Katanga province (Shaba) are among the first (de Magnée, 1935; Robert, 1938, 1944, 1951; Mortelmans, 1951; Van de Steen, 1959) and

the best studied areas of the Kibaran Orogen. It is also one of the first absolutely dated areas by geochronological methods (Cahen and Snelling, 1966; Cahen et al., 1967, 1972, 1984). The last studies conducted by Kokonyangi et al. (2001, 2004, 2005, 2006, and 2007) from the Lubumbashi University under the supervision of A.B. Kampunzu were completed by Debruyne et al. (2015). The Kibaran basement was dated in several places at around 2 Ga by Delhal and Liégeois (1982). The basement is capped by sandstones and volcanic tuffs especially in the Marungu area. The beginning of sedimentary deposition is ascribed to the Kibaran Orogeny and seems to have happened at around 1.4 Ga. In accordance to publications of the last two decades (Kokonyangi, 2006, 2007; Debruyne et al., 2015), the Kibara succession includes four main groups. They are from the base to the top: the Kiaora, Nzilo, Hakanson, and Lubudi groups. The Kiaora Group shows a strong cleavage (S1), which was acquired prior to the deposition of the Nzilo Group (Byamungu et al., 1979) and is linked to NE-SW structures to the south and E-W structures to the north. Magmatic rocks associated to the Kiaora Group display ages between 1.40 and 1.38 Ga (Kokonyangi et al., 2006). Such zircon ages have been recorded in sediments of the covering Nzilo Group and in the post-Kiaora Kataba conglomerate (1329 ± 32 Ma) according to Cahen et al. (1984) and Kokonyangi et al. (2007). According to Kampunzu et al. (1986) and Kokonyangi et al. (2006) the Kiaora Group underwent a second tectonic folding (associated to a S2 cleavage) with a NNE-SSW trend, which marks the only witness of a tectonic event registered in the three other groups. This second tectonic event is associated to a second magmatic event that likely occurred at around 1306 ± 35 Ma. Finally, according to Debruyne et al. (2015), a third magmatic event took place at around 1070 Ma (1079 ± 14 Ma and 1050 ± 50 Ma) prior to the intrusion of the post-Kibaran tin granites (1000 to 960 Ma) according to Cahen et al. (1967, 1984) and Kokonyangi et al. (2007).

According to the available radiometric data, the lithostratigraphic subdivisions for the KVB and KAB used in table I have been applied to the KIB. This underlines the lack of sedimentary deposition between 1250 or 1180 Ma and the first Katangian (Neoproterozoic) deposits. Nevertheless, numerous magmatic events were found and dated at around 1080 Ma (Debruyne et al., 2015). In table I only two units have been distinguished (Ki1 and Ki2) for the KIB and correlated to the lithostratigraphic units of the KVB and KAB. Thus, the Ki1 unit is correlated to the Kv1 and Ka1 units, while the Ki2 is thought to be linked to the Kv2 and Ka2. Sediments corresponding to the Bugarama (Kv3) and Nya-Ngezie (Kv4) groups are also lacking in the KIB.

In table I a large part of dated granitic intrusions have been reported. The age range of these granitic occurrences indicates that periods without granitic events are rather rare.

7.4 Consequences on the Ubendian Belt

Between the northern KVB / KAB and the southern KIB, there is an enigmatic NW-SE elongated structure setting on both sides of the Tanganyika Lake that straddles the DR Congo and Tanzania. In past times this structure was ascribed to the Ruzizian and now to the Ubendian Palaeoproterozoic belt (Dewaele et al., 2003, 2006). On the Congolese side, this NW-SE structure cuts the NS trending “Luiko syncline” considered as the southern part of the “Luemba syncline” now ranked in the Kv2 unit (Villeneuve and Guyonnet-Benaize, 2006) and shows a NW-SE sinistral strike-slip. On the Tanzanian side, a similar strike-slip movement is evidenced along the “Ufipa shear zone” (Theunissen, 1988a, 1988b). The age range of these granitic occurrences indicates that periods without granitic events are rather rare.

Apart from the Ubendian basement, which was well dated by Boven et al. (1999), several other formations have been described. Among them the “Itiaso metasedimentary group”, close to Mgambo, is intruded by the Kapalagulu Igneous Complex dated at 1392 ± 26 Ma (Boniface et al., 2014). To the southeast, the “Wakole terrane” exhibits detrital zircons dated at about 1.4 Ga and was subsequently metamorphosed at 1166 ± 14 Ma and 1007 ± 6 Ma (Boniface et al., 2014). Table I presents our correlations with the adjacent belts. The “Itiaso Group” is clearly an equivalent of the Kv1, Ka1 or Ki1 (= KI), but the southern Wakole terrane could be related to the Ka1, Ka2 or younger strata. The metasediments of the “Luiko syncline” are linked to the Kv2 unit. Until now, no counterpart of the Bugarama or Nya-Ngezie groups, have been found there, although main tectonic features can be related to the D1 and D2 events of the Nya-Ngezie area. This SE-NW lineament is one of the major tectonic features of this central African domain. It was active at various times from the formation of the Ubendian Belt (Palaeoproterozoic) to the ongoing Cenozoic East African rift system (Mac Connel, 1979; Chorowicz, 1983; Villeneuve, 1983b; Theunissen et al., 1996). Late Kibaran (Theunissen, 1988a) and pan-African (Theunissen et al., 1992) reworking have also been detected.

8 Discussion and synthetic framework (summarised in Table II)

Correlations between the different belts belonging to the “Kibaran System” allow us to propose some synthetic schemes of the whole Kibaran-Burundian Orogen. These synthetic proposals concern the lithostratigrahic scale, the tectonic and metamorphic events, the tectono-sedimentary cycles and the geodynamical models. The metamorphic events will be developed apart in another paper.

8.1 Unified lithostratigraphic scale

Although there are some stratigraphical differences between the main belts, the numerous similarities cannot be overlooked. Table I points out five lithostratigraphic units: KI to K5.

The *K1 unit* (with Kv1, Ka1 and Ki1) is represented in the three main belts (KVB, KAB, and KIB). Many authors agree with a stage of deposition that started around 1450 Ma and terminated with the main magmatic event dated at around 1375 Ma (Tack et al., 2010). Other authors prefer an extensive regime coeval with the 1360 ± 27 Ma magmatic events (Klerkx et al., 1984). There are some geological events between the end of the Ruzizian or Ubendian periods and the beginning of the Kibaran-Burundian stage like in the ED. Nevertheless, it would be better to begin the Kibaran Orogen by the opening of basins at about 1.4 Ga. Villeneuve and Chorowicz (2004) separated this lower unit from the overlying trenches. This hypothesis was then supported by radiometric dating (Tack et al., 2010; Fernandez-Alonso et al., 2012).

The *K2 unit* (Kv2, Ka2, and Ki2) is present in the KIB, KVB, and the KAB. Possibly, sediments of the "Luiko syncline" and the "Wakole terranes" cropping out in the Ubendian Belt (UBB) belong to this K2 unit. This unit is well studied in the KIB, although the main trenches of the KVB and KAB are linked to this unit. In the KVB and KAB, the lithostratigraphic succession of unit K2 is made of a coarse-grained siliciclastic formation interbedded between two pelitic or shaly formations that led to the trilogy of the Lower, Middle and Upper Urundian. Locally, this succession is capped by a molasse-like formation, e.g. the Miyove Formation of Rwanda, which sometimes was correlated with the above mentioned Nya-Ngezie Group.

The *K3 unit* (Kv3) is only known in the KVB and dated by our new radiometric results. A possible linkage of the Rugesi Group (KAB) to the K3 unit is not yet proven. Seemingly, the formations of the K2 unit may be confused with those of the K3 unit in many places due to similar petrographic characteristics. The deposition of the K3 unit began after ca. 1207 Ma and

terminated prior the deposition of the approximately 1121 ± 14 Ma old overlying Nya-Ngezie Group. Sedimentary deposition was not yet recognised in this time bracket outside the KVB.

The *K4* unit (Kv4) is mainly represented by the Nya-Ngezie Group of the KVB. The youngest zircon extracted from the Nya-Ngezie Group displays an age at 1121 ± 14 Ma, while the latest deposits should be older than the post-tectonic granites dated between ca. 976 and 912 ± 30 Ma, with mean ages around 960 Ma. There is only one isolated outcrop outside the KVB that could be linked to the Nya-Ngezie Group, lying in the northwestern part of the Kivu Lake.

The *K5* unit is associated to the post-Kibaran granites. The Banji Group of the Ubendian Belt could possibly be linked to this K5 unit (table I).

8.2 The main tectono-magmatic events (table II)

Owing to numerous studies all over the Kibaran Orogens since the beginning of the 20th century, there is neither a coherent nomenclature for the three belts, nor for their several parts. Each author has developed his own specific tectono-magmatic nomenclature with respect to local observations, which led to some confusion. The problem can exemplarily be shown for the discrepancies concerning the tectonic events in the Kivu area: the D1 and D2 tectonic events of Villeneuve (1977) correspond to the D2 of Rumvegeri (1984). On the other hand, the D1 of Blès (1972) is quite similar to the D1 of Klerkx et al. (1984) and different from the D1 of Rumvegeri (1984). Taking into account ages, direction and tectonic stress, eleven tectonic events have been distinguished throughout the Kibaran-Burundian belts (table II). In order to provide a coherent and common chronology for the whole series linked to the Kibaran-Burundian Orogen, each tectonic event has been renamed in the final list. From the earliest to the latest events we have

listed: Dx, D1-1, D1-2, D1-3, D2-1, D2-2, D2-3, D2-4, D3-1, D3-2, and D3-3. The D4 tectonic event is associated to the pan-African tectonic events.

Dx events predate the sediment deposition. They are ascribed to the basement tectonic framework and have various directions.

D1-1 structures are characterised by an E-W trend and could be related to the opening of oceans, particularly to the K01 (KAB aulacogen). **D1-2** structures show a NNE-SSW trend in the southern KIB, and are E-W in the KVB (Elila Belt). They are associated to a collisional event in these areas. **D1-3** is a tectonic event linked to a post tectonic extensive regime.

D2-1 (NNE-SSW trend), **D2-2** (NNW-SSE trend), **D2-3** (E-W trend), and **D2-4** (NW-SE trend) are associated to the folding and fracturing of the K2 basins. D2-1 is an extensional event associated to the opening of K2 basins. D2-2 and D2-3 are related to the folding of these basins. The D2-3 event is well exposed in three E-W bands: the *Luhule-Mobissio* band to the North, the *Rwate-Bilati* band to the NW of the Kivu Lake and the *Shabunda-Nzibira* band to the SW of the Kivu Lake. The Shabunda-Nzibira structure is clearly a pop-up structure, in which the D2-2 structures are refolded by D2-3 folds. Relationships between the various D2 deformations are not clearly understood.

D3-1 with an E-W trend corresponds to the folding and metamorphism of the Bugarama Group (K3). **D3-2** has an E-W to NW-SE trend is associated to the folding of the Nya-Ngezie Group (K4), while **D3-3** shows NW-SE strike slips and thrusting to the SW of the D2-2 structures of the Nya-Ngezie Group. These NW-SE striking faults are largely developed all over the Northern KAB and KVB.

D4 with an N-S trend is associated with the Neoproterozoic post-orogenic magmatic event and to the opening of the Neoproterozoic Itombwe half graben.

Noticeably, there are similarities in orientation of the D1-1, D2-3, and D3-1 structures. The same applies for D2-4 and D3-2 and D3-3. In the past (Cahen, 1954), every tectonic direction was related to a single tectonic event, which became much more complex since the widespread application radiometric dating.

Conjunction between the main tectonic events and the lithostratigraphic units generated at least five main unconformities (Un1 to Un5). **Un1** between the basement and unit 1 is supposed but not observed. However, there is an unconformity between the Bilati (Kv2) and the Kibalian basement. **Un2** corresponds to the "Luemba unconformity" underlain by the Luemba conglomerate. Further occurrences of the Un2 are at the western flank of the Luemba synclinorium. **Un3** corresponds to the unconformity between the Kv2 and Kv3 units and is yet only recognised on the Landsat images by Chorowicz and Mukonki (1980). **Un4** corresponds to the "Mt. Kamashuli unconformity" found in the Nya-Ngezie area (Villeneuve, 1977), whereas the "Nya-Kasiba unconformity" at the base of the Itombwe syncline is a part of the **Un5** group (Villeneuve, 1976). Despite several attempts, unconformities evidenced in the KAB have not yet been correlated to those of the KVB (Villeneuve and Chorowicz, 2004; Villeneuve and Guyonnet Benaize, 2006).

Such confusions also exist in the chronology of the granitic intrusions. Despite the first classification of Cahen et al. (1979), there are some large discrepancies between different authors and different countries. Since Blaise and Boutakoff (1934) it is known that granitic batholiths, like the Gondo Ya Bushema, cropping out west of the Kivu Lake, are composite and may include several intrusions of various ages. Blés (1972) notes that accordance between the magmatic

batholith and host structure does not necessarily indicate a synkinematic emplacement. The Kasika granite provides a good example (see above). On the other hand, the chronology of magmatic events is mainly based on radiometric data, although there are some discrepancies depending on the applied radiometric method. The best example concerns the "arena granites" of western Uganda, of which the Chitwe granite was dated by the Rb/Sr at 1146 ± 40 Ma (Vernon-Chamberlain and Snelling, 1972). The same rock dated by the U-Pb method on zircon yielded an age of 1568 ± 23 Ma (Buchwaldt et al., 2008). Similar results were found in the adjacent arena granites. Tables I and II show the main granitic bodies already dated in the region. No specific age clusters can be noted.

8.3 The main metamorphic events

The development of the metamorphic events related to the Kibaran Orogen is beyond the scope of this paper. Some of them are linked to the granitic intrusions or to the tectonic events. However, their grade of deformation is not correlated to their age. Metamorphic aureoles are present in every unit and the metamorphism could be more intense in the K3 than in the K1. An important period of "contact metamorphism" is related to the post collisional G4 granites. The sizes of metamorphic aureoles vary from hectometre to several kilometres away from the granitic massifs. The six main metamorphic events listed in table II will be developed elsewhere.

8.4 The main orogenic cycles

Considering the mentioned problems, we attempt to reconcile these local scales in table II. Five main "*tectono-sedimentary cycles*" including basin opening, sediment deposition and tectono-magmatic events, have been considered.

- *The first cycle (Cy1)* includes all formations belonging to the unit K1, which is terminated by the 1375 Ma Kibaran event (Tack et al., 2010). In the KAB it is represented by relict of E-W structures such as the Mugombwa anticline (Gérards, 1971) or the Rutunga structure (Nzojibwami, 1984). An extensive tectonic regime is considered in the KAB, meanwhile in the KIB and KVB this cycle seems to be ended by a compressive tectonic event.

- *The second cycle (Cy2)* began by accumulation of sedimentary deposits in N-S elongated trenches delineated by Villeneuve and Chorowicz, (2004). According to Blès (1972), Villeneuve (1983), and Klerkx et al. (1984) this could be linked to several N-S elongated basins intruded by large magmatic bodies inducing tangential isoclinal folds parallel to the bedding and inferred to the lower deposits (D2-1) during the extensional regime. These granites display several ages between 1360 and 1250 Ma. A set of compressive tectonic events (D2-2, D2-3, and D2-4) with various trends occurred between 1200 and 1180 Ma accompanied by several granitic intrusions (G2 or GR3). Thrust and strike-slip faults were commonly associated to the folds (Theunissen and Klerkx, 1980; Theunissen, 1984; Klerkx et al., 1984; Klerkx et al., 1987). The KVB has a quite similar evolution. A similar extensional regime in the KIB is terminated by a younger compressive tectonic event (1079 ± 14 Ma).

- *The third cycle (Cy3)* began with the deposition of the Bugarama Group after ca. 1180 Ma and was terminated by the D3-1 tectonic event reported by Villeneuve (1977) prior to the deposition of the Nya-Ngezie Group (post ca. 1120 Ma). The Masisi through is oriented N-S while the latest tectonic event exhibits E-W to WNW-ESE structures (Blès, 1972). This is likely the case for the Bugarama Basin. The meridional alignment of these two basins has to be noted. Up to now these basins are limited to the eastern part of KVB. This means: either these terranes

are not yet evidenced elsewhere or they are limited to the rift zone and should be interpreted as a basin opened in the middle part of the KVB and KAB assemblage.

- *The fourth cycle (Cy4)* is dated between ca. 1120 and ca. 1079 Ma and corresponds to the deposition and folding of the Nya-Ngezie Group. The D3-2 tectonic events are linked to the main E-W to NW-SE hectometric to kilometric folds of the Nya-Ngezie area, and to the large NW-SE shear zones crossing the KVB and the KAB. Very few sedimentary deposits are ascribed to this cycle. The latter is not consistent with a D3-1 doming followed by an erosional stage that would have been able to feed such E-W oriented basins. However, granitic intrusions, consistent with this tectonic event, are recorded in the KIB and in Tanzania.

- *The last cycle (Cy5)* corresponds to the "post Kibaran" magmatic event as proposed by several authors. The intra-cratonic intrusions were emplaced between ca. 975 and ca. 920 Ma (mean age around 960 Ma) and provide the main metallogenic occurrences, particularly in tin, tungsten, and coltan minerals. Meanwhile, the sediments of the Lindian and Malagarasian formations were deposited on both sides of the Kibaran-Burundian Belt. The exact time relationships between the NW-SE D3-3 structures and the post Kibaran-Burundian granites setting remain unknown. However, according to Dewaele et al. (2015) a Late Kibaran magmatic event occurred in the Maniema province (western KVB) between 1024 ± 5.5 Ma and 993 ± 1 Ma. It could be linked to an N-S shrinking that occurred before ca. 950 Ma, and thus, may be the trigger for the post orogenic granitic intrusions.

8.5 Geodynamical consequences (Table II)

Two opposite geodynamic models prevailed for a long time: i) the "mobile plate tectonic model" with oceanic subduction and continent / continent collision supported by Kokonyangi et

al. (2004) in Katanga and by Rumvegeri (1989) in the Kivu area; ii) the intra-continental (ensialic) model supported by the Klerkx et al. (1984, 1987) and others in Rwanda and Burundi. Owing to the lack of consistent radiometric dating, both models are considered as contemporaneous. However, the unique SSW-NNE trend led every author to consider his own conclusions as valid for the whole orogen. Considering these conclusions as representative of the local environment, we are looking for a "coordinated geodynamic model" taking into account that every local hypothesis is consistent. Table II presents the main characteristics of each cycle and their supposed geodynamic model only consistent for the KVB and KIB. Nine stages (a, b, c, d, e, f, g, h, i) have been distinguished in close relationship with the main orogenic cycles.

Kokonyangi et al. (2006) admitted a plate tectonic model operating before the D1-2 tectonic event (1380 Ma) and an intra-basinal regime between 1380 Ma (or 1375 Ma) and the D2-2 tectonic event in the KIB. According to Debruyne et al. (2015), the slab was subducted to the east underneath the Bangweulu Block, although no Mesoproterozoic rocks related to an orogenesis have been found. The latter was followed by the post collisional regime coeval with the intrusions of tin bearing granitoids around 960 Ma. This geodynamic model was supported by Kokonyangi has been revised by Debruyne et al. (2015). These authors considered a very long collisional stage between 1375 Ma and 1000 Ma that is highly questionable. A similar model was also considered for the KVB during cycle 1 by Rumvegeri (1985, 1987). Recent geochemical investigations on the Bunyakiri gneiss of the Lushasha Complex by Mugaruka Bibentyo et al. (2015) favoured an island arc setting which could be linked to this first geodynamic event (**a** and **b**, table II). The Lushasha Complex and the Elila Formation could be involved in this "subduction / collision" model although there are no witnesses of classical elements as ophiolite obduction, suture zones, and volcano-magmatic arcs to support a plate tectonic model ascribed to Cy1 as underlined by Liégeois (pers. comm.). Consequently, the slab vergence is unknown. In contrast,

such a model is excluded by Klerkx et al. (1984), Tack et al. (2010), and Fernandez-Alonso et al. (2012) in the KAB, where the sedimentary deposits are continuous during the Cy1 and Cy2. Thus, an extensional regime is favoured by them, from ca. 1400 Ma to ca. 1180 Ma. After this first collision in the KIB and KVB, an extensive regime is hypothesised everywhere during Cy2 (**c,** table II). The latter was terminated during a major tectonic event (**d**, table II). Then, the intra-crustal evolution of the Bugarama and Nya-Ngezie groups (Cy4 and Cy5) are illustrated in table II (**e, f, g, h**). After this last episode, a general tectonic reactivation of N-S elongated structures gave way to a large amount of post tectonic granitic bodies (Cy5) illustrated in table II (**i**). Although there are several tectono-metamorphic cycles, all are included in the Kibaran Orogeny.

8.6 A reconciling hypothesis

The synopsis visualised in table II allows us to launch a new hypothesis in order to reconcile the opposite geodynamic models proposed in the KIB / KVB against the model proposed in the KAB. A model similar to that of Dewey (1968) for the Atlantic Ocean including the opening of three aulacogens fits with our considerations. Such a model considers an aborted branch, and a large opening of the two other branches. Before the closure of the two latter branches convergence processes lead to the formation of a mountain belt.. This hypothesis relies on the Wichita and Marathon-Oklahoma rifts capped by the Variscan Ouachita Belt (King, 1975; Zolnai, 1986) in the southern part of the USA. This model seems to be the best solution to explain the different models between the KIB / KVB versus the KAB. The KAB could be an analogue of the aborted Proterozoic to Palaeozoic "Marathon-Oklahoma" aulacogen meanwhile the KIB and KVB could be compared to the Variscan Ouachita Belt. In our opinion this hypothesis deserves to be carefully examined.

8.7 Relationships between the modern rift structures and the Proterozoic basement.

A close relationship between the N-S pan-African troughs and the modern rift structures in the Kivu area has already been discussed by Villeneuve (1983b). The existence of a late Kibaran N-S trough located between the pan-African Itombwe trough and the Kivu Rift structures is a new possibility. This suggests that the ancestor of the modern rift is not linked to the pan-African period but is likely older and of potential Late Mesoproterozoic age.

Concluding remarks

In conclusion the new U-Pb age determinations on detrital zircons from six samples of the Bugarama and Nya-Ngezie groups have:

1) Shown the necessity to establish two new belts that occurred between the folding of the late Kibaran (1250-1200 Ma) and the intrusions of the G4 tin bearing granites (ca. 970 to ca. 920 Ma). The deposition of the lower Bugarama Group took place between 1207 ± 28 and 1121 ± 14 Ma. Meanwhile the upper Nya-Ngezie Group was deposited between 1121 ± 14 and 1111 ± 38 Ma. Inherited zircon grains from these two groups indicate several source rocks and noticeably sediments coming from the erosion of remote (or recycled) Archaean or Palaeoproterozoic materials.

2) Improved our understanding on the evolution of the Kivu area and allow us to decipher a KVB (Kivu Belt) different from the KAB (Karagwe-Ankolean Belt) and from the KIB (Kibaride Belt), in which the Bugarama and Nya-Ngezie groups are lacking.

3) Proposed the abandonment of the classical Burundian trilogy (Lower, Middle and Upper Burundian) which is still a matter of debate. For Rumvegeri (1991) the Lower and Middle Burundian correspond to our Unit II (K2) and the Upper Burundian to our Units III (K3)

and IV (K4) meanwhile for others, the Lower, Middle and Upper Burundian refer to formations included within unit II (K2).

These new data allows us to suggest a large set of correlations between the KAB and the KIB and even with the associate Kibaran Belts such as the Ubendian Trough of Tanzania. These correlations exposed in table I allow us to propose:

1) A new geological sketch map of the KAB and KVB areas (figure 1).

2) The distinction of four main lithostratigraphic units in the KVB, KAB, and KIB (table I).

3) The occurrence of eleven tectonic events (table II) between the D1-1 (pre-1380 Ma) and the D3-3 (around 1020 Ma) tectonic events.

4) The distinction of five tectono-sedimentary cycles (Cy1 to Cy5) associated to these tectonic events and to numerous magmatic and metamorphic events (table II). In addition nine (**a** to **i**) geodynamic stages are proposed in table II. A classical model of an active margin setting is accepted for the KVB and the KIB coeval with an "aulacogen" in the KAB (**a** and **b**). Then, several basins opened and closed from ca. 1360 to ca. 1050 Ma (**c** to **i**).

5) An additional contribution is to propose a hypothesis for reconciling the opposite geodynamic model between KIB / KVB and the KAB. Our hypothesis is based upon a "three branch model" of aulacogen opening followed by the closure of two of them by collisional processes in the KVB and the KIB, in their first stage of evolution. Consequently, the third branch (KAB) is considered as an aborted rift (aulacogen). This hypothesis is inspired by the model of Neoproterozoic to Palaeozoic aulacogens (i.e.: Marathon Aulacogen) of North America limited to the south by the Variscan belts (Ouachita Belt).

6) Another hypothesis considers the central part of the KVB and KAB assemblage occupied by the “Great Lakes” as a very old weakness zone which was successively reactivated in a narrow meridional zone. The latter also hosts the Late Mesoproterozoic Masisi and Bugarama basins, the Neoproterozoic anorogenic alkaline complex, the Itombwe through, and finally, the Neogene East African Rift. Analogues of the modern rift could be initiated at the end of the Kibaran Orogeny.

Of course, this simplified synthetic view has to be improved by more field and radiometric data, especially in the very poorly studied Kivu area where the main investigations have been performed before the year 2000. Many questions are unsolved, noticeably the relationships between the tectonic, magmatic, and metamorphic events. We are expecting that this synthetic view provides an interesting “working tool” for further studies.

Aknowledgements

We acknowledge the two reviewers Denis Thièblemont and Jean-Paul Liégèois who strongly improved this paper and also thank to Oceane Stchetinine for the drawing of tables.

References

Aguillaume, A., Colleau, A., Kabongo, K., 1975. Géologie du degré carré Lutunguru. Mission Nord-Kivu, 3eme campagne 1974, 1, Departement des Mines BRGM, Kinshasa, 18 pp.

Baudet, D., Hanon, M., Lemonne, E., Theunissen, K., 1988. Lithostratigraphie du domaine sédimentaire de la chaine Kibarienne au Rwanda. Annales de la Société géologique de Belgique 112, 225–246.

Blaise, F., 1934. Géologie des terrains situés au Nord-Ouest du lac Kivu. Annales de la Société géologique de Belgique, 17, 139–148.

Blaise, F., Boutakoff N., 1934. Note sur les differentiations de certains batholites granitiques du Kivu. Annales Societé. Géologique de Belgique 57, 1, 93–100.

Blès, J.L., 1972. Etude photo-interprétative et reconnaissance géologique et structurale de la zone exclusive de recherches Masisi-Saké. Note inédite, BRGM-SEREMI, 28 pp.

Boniface, N., Schenk, V., Appel, P., 2014. Mesoproterozoic high-grade metamorphism in pelitic rocks of the northwestern Ubendian belt: implications for the extension of the Kibaran intra-continental basins to Tanzania. Precambrian Research 249, 215–228.

Boutakoff, N., 1939. Géologie des territoires situés à l'Ouest et au Nord-Ouest du fossé tectonique du Kivu. Mémoires de l'Institut géologique de l'Université Louvain, Belgique, 9, 9-207.

Boven, A., Theunissen, K., Sklyarov, E., Klerkx, J., Melnikoff, A., Mruma, A., Punzalan, L., 1999. Timing of exhumation of a high-pressure mafic granulite terrane of the Paleoproterozoic Ubende belt (West Tanzania). Precambrian Research 93, 119–137.

Brick R.A. (2011). Palaeoproterozoic eclogite formation in Tanzania: a structural, geochronological, thermochronological and metamorphic study of the Usagaran and Ubende orogenic belts. Unpublished PhD thesis, University of Adelaide, 151 pp.

Brinckmann, J., Lehmann, B., Hein, U., Hohndorf, A., Musallam, K., Weiser, T., Timm, F., 2001. La géologie et la minéralisation primaire de l'Or de la chaine Kibarienne, Nord-Ouest du Burundi, Afrique orientale. Geologisches Jahrbuch D 101, 3–195.

Buchwaldt, R., Toulkeridis, T., Todt, W., Ucakuwun, E.K., 2008. Crustal age domains in the Kibaran belt of SW Uganda: Combined zircon geochronology and Sm-Nd isotopic investigation. Journal of African Earth Sciences 51, 4–20.

Burg, J.P., Rumvegeri, B.T., Kampunzu, A.B., Kapenda, D., 1986. Contraintes petro-structurales dans l'évolution de la chaine Kibarienne au Kivu (Zaire). UNESCO, Geology for Economic Development, Newsletters 5, 115–124.

Byamungu, B.R., Giordano, R., Kampunzu, A.B, Male, C.N., 1979. A propos du Kibarien (Precambrien moyen) de la région du barrage de Nzilo (Shaba, Zaire). Annales Faculté des Sciences, Université de Lubumbashi 2, 39–48.

Cahen, L., 1954. Géologie du Congo belge, Vaillant–Carmagne, Liège, Belgique, 577pp.

Cahen, L., Snelling, N.J., 1966. The geochronology of Equatorial Africa. North Holland, Amsterdam, 195 pp.

Cahen, L., Delhal, J., Deutsch, S., 1967. Rubidium-Strontium geochronology of some granitic rocks from the Kibaran belt (central Katanga, Republique of Congo). Annales du Musée Royal de l'Afrique Centrale, Sciences Géologiques 59, 1–65.

Cahen, L., Delhal, J., Deutsch, S., 1972. A comparison of the ages of granites of S.W. Uganda with those of the Kibaran of Central Shaba (Katanga), Rep. Zaire with some new isotopic

and petrogenetical data. Annalen / Koninklijk museum voor Midden-Afrika, Tervuren. Geologische wetenschappen 73, 45–67.

Cahen, L., Frautschi, J.M., Gérards, J., Lavreau, J., Theunissen, J., Villeneuve, M., 1976. Réunion de travail des 1, 2 et 3 septembre 1975: La géologie des terrains précambriens voisins du fossé tectonique occidental, spécialement dans les régions sises de part et d'autre de la partie sud du lac Kivu et du nord du lac Tanganyika, au Kivu, au Rwanda et au Burundi. Musée royal d'Afrique centrale, Tervuren, Belgique. Dept. Géologie Minéralogie, Rapport Annuel 1975, 143–170.

Cahen, L., Ledent, D., 1979. Précisions sur l'âge, la pétrogenèse et la position stratigraphique des «granites à étain» de l'Est de l'Afrique centrale. Annales de la Société géologique de Belgique 88, 33–49.

Cahen, L., Ledent, D., Villeneuve, M., 1979. Existence d'une chaine plissée protérozoïque supérieur au Kivu oriental (Zaïre). Données géochronologiques relatives au super groupe de l'Itombwe. Bulletin de la Société belge de géologie, de paléontologie et d'hydrologie 88, 71–83.

Cahen, L., Snelling, N.J., Delhal, J., Vail, J.R., Bonhomme, M., Ledent, D., 1984. The Geochronology and Evolution of Africa. Oxford University Press, Oxford, 512 pp.

Caron, J.P.H., Kampunzu, A.B., Lwango, B.L., Manteka, B., Nkanika, R.W., 1986. Les ressources minérales d'âge protérozoïque moyen en Afrique équatoriale et l'évolution géodynamique de la chaine Kibarienne. UNESCO, Geology for Economic Development, Newsletter 5, 139–152.

Chauvel, J.J., Villeneuve, M., 1987. Les quartzites ferrugineux rubanés du Précambrien du bassin de la Luzinzi (Zaïre): un dépôt de placer à titane, fer et zirconium. Sci. Geol. Bull., Strasbourg, France 40, 297–312.

Chorowicz, J., Mukonki, M.B., 1980. Apport géologique des images MSS Landsat du secteur autour du lac Kivu (Burundi, Rwanda and Zaire). Comptes Rendus de l'Académie des Sciences, Paris, 290, 1245–1247.

Chorowicz, J., 1983. The East African rift: early stage of a future oceanic opening? Bulletin des Centres de Recherches Exploration-Production Elf-Aquitaine, Pau, France 7, 155–162.

Cordani, U.G., Sato, K., Teixeira, W., Tassinari, C.G., Basei, M.A.S., 2000. Crustal evolution of the South American Platform. In: Cordani, U.G., Milani, E.J., Thomaz Filho, A., Campos, D.A. (eds.), Tectonic evolution of South America, 31st International Geological Congress, Rio de Janeiro, 19–40.

Deblond, A., Punzalan, L.E., Bowen, A., Tack, L., 2001. The Malagarasi supergroup of SE Burundi and its correlative Bukoban supergroup of NW Tanzania: Neo-and Mesoproterozoic chronostratigraphic constraint from Ar-Ar ages on mafic intrusive rocks. Journal of African Earth Sciences 32, 435–449.

Debruyne, D., Hulsboch, N., van Wilderode, J., Balcean, L., Vanhaeke, F., Muchez, P., 2015. Regional geodynamic context for the Mesoproterozoic Kibara belt (KIB) and the Karagwe-Ankole belt: Evidence from geochemistry and Isotopes in the KIB. Precambrian Research 264, 82–97.

Delhal, J., Liègeois, J.P., 1982. Le socle granito-gneissique du Shaba occidental (Zaïre). Petrographie et Geochronologie. Annales de la Société géologique de Belgique 105, 295–301.

De Waele, B. Wingate, T.D., Fitzsimons, M.T.D., Mapani, B.S.E., 2003. Untying the Kibaran knot: A reassessment of Mesoproterozoic correlations in southern Africa based on SHRIMP U-Pb data from the Irumide belt. Geology 31, 509–512.

Dewaele, S., Muchez, P., Burgess, R., Boyce, A., 2015. Geological setting and timing of the cassiterite vein type mineralization of the Kalima area (Maniema, Democratic Republic of Congo). Journal of African Earth Sciences 112, 1–14.

Link, P.K., Fanning, C.M., Beranek, L.P., 2009. Reliability and longitudinal change of detrital-zircon age spectra in the Snake River system, Idaho and Wyoming: An example of reproducing the bumpy barcode. Sedimentary Geology 182, 101–142.

Fedo, C.M., Sircombe, K.N., Rainbird, R.H., 2003. Detrital Zircon Analysis of the Sedimentary Record. In: Hanchar, J.M., Hoskin, P.W.O. (Eds.) Zircon. Reviews in Mineralogy and Geochemistry 53, 277–303.

Fernandez-Alonso, M., Theunissen, K., 1998. Airborne geophysics and geochemistry provide new insights in the intercontinental evolution of the Mesoproterozoic Kibaran belt (Central Africa). Geological Magazine 135, 203–216.

Fernandez-Alonso, M., Cutten, H., De Waele, B., Tack, L., Tahon, A., Baudet, D., Baritt, S.D., 2012. The Mesoproterozic Karagwe-Ankole belt (formerly the NE Kibara belt): The result of prolonged extensional intracratonic basin development punctuated by two short-lived far-field compressional events. Precambrian Research 216–219, 63–86.

Frautschi, J.M., 1973. Feuille Cyangugu. Rapp. Année 1972. Service Géologique du Rwanda, Ruhengeri, 7 pp.

Gérards, J., Ledent, D., 1970. Grands traits de la géologie du Rwanda, différents types de roches granitiques et premières données sur l'âge de ces roches. Annales de la Société Géologique de Belgique 93, 477–489.

Gérards, J., 1971. L'anticlinal de Mugombwa (Rwanda): un exemple de discordance majeure entre le Burundien et son socle. Musée royal d'Afrique centrale, Tervuren, Belgique. Dept. Géologie Minéralogie, Rapport Annuel 1970, 22–26.

Gerdes, A., Zeh, A., 2006. Combined U-Pb and Hf isotope LA-(MC-)ICP-MS analyses of detrital zircons: Comparison with SHRIMP and new constraints for the provenance and age of an Armorican metasediment in Central Germany. Earth and Planetary Science Letters 249, 47–61.

Gerdes, A., Zeh, A., 2009. Zircon formation versus zircon alteration–new insights from combined U–Pb and Lu–Hf in situ LA-ICP-MS analyses, and consequences for the interpretation of Archean zircon from the Central Zone of the Limpopo Belt. Chemical Geology 261, 230–243.

Horstwood, M.S.A., Košler, J., Gehrels, G., Jackson, S.E., McLean, N.M., Paton, C., Pearson, N.J., Sircombe, K., Sylvester, P., Vermeesch, P., Bowring, J.F., Condon, D.J., Schoene, B., 2016. Community-Derived Standards for LA-ICP-MS (U-Th-**Pb)** Geochronology – Uncertainty Propagation, Age Interpretation and Data Reporting. Geostandards and Geoanalytical Research 40(3), 311–332.

Ikungura, J.R., Bell, K., Watkinson, D.H., van Straalen, P., 1990. Geochronology and chemical evolution of granitic rocks, NE Kibaran (Karagwe-Ankolean) belt, NW Tanzania. In: Rocci, G., Deschamps, M., (eds.), Recent Data in Earth Sciences. Centre international de formation et échanges en Géosciences, Occasional, Publication 22, 97–99.

Ikungura, J.R., Reynolds, P.H., Watkinson, D.H., Bell, K., 1992. $^{40}Ar/^{39}Ar$ dating of micas from granites of NE Kibaran belt (Karagwe-Ankolean), NW Tanzania. Journal of African Earth Sciences 15, 501–511.

Jackson, S.E., Pearson, N.J., Griffin, W.L., Belousova, E.A., 2004. The application of laser ablation-inductively coupled plasma-mass spectrometry to in situ U-Pb zircon geochronology. Chemical Geology 211, 47–69.

Kampunzu, A.B., 1981. Le magmatisme du massif du Kahuzi (Kivu, Zaïre). Structure, pétrologie, signification et implication géodynamique. Doctoral thesis, Université du Zaire, Lubumbashi, 387 pp.

Kampunzu, A.B., Rumvegeri, B.T., Kapenda, D., Lubala, R.T., Caron, J.P., 1986. Les Kibarides d'Afrique centrale et orientale: une chaine de collision. UNESCO, Geology for Economic development Newsletter 5, 125–137.

Kampunzu, A.B., Kramers, J.D., Makutu, N.M., 1998a. Rb-Sr whole rocks ages of the Lueshe, Kirumba and Numbi igneous complexes (Kivu, DRC) and the break-up of the Rodinia supercontinent. Journal of African Earth Sciences 26, 29–36.

Kampunzu, A.B., Bonhomme, M.G., Kanika, M., 1998b. Geochronology of volcanic rocks and evolution of the Cainozoic Western Branch of the East African Rift System. Journal of African Earth Sciences 26, 441–461.

Kampunzu, A. B., 2001. Assembly and break-up of Rodinia. No link with Gondwana assembly. Gondwana Research 4, 647–650.

Kampunzu, A.B, Armstrong, R., Villeneuve, M., 2003a. Depositional age and provenance of the metasedimentary siliciclastic rocks of the Nya-Ngezie group (Congo): geological constraints, U-Pb detrital zircon geochronology and implications for the tectonic evolution of the Mesoproterozoic Kibaran orogen in central-eastern Africa. Unpublished, 23 pp.

Kampunzu, A.B., Armstrong, R., Chorowicz, J., Villeneuve, M., 2003b. Geology and detrital zircons from the Precambrian Itombwe supergroup (Congo): implications for the depositional age, provenance and the geotectonic evolution of the East African orogen during East-West Gondwana continental collision. Unpublished, 32 pp.

King P.B. (1969- 1972) - Tectonic maps of North America Scales : 1/ 5 000 000 and 1¨15 000 000. U.S. Geol. Surv.

Klerkx J., Lavreau J., Liégèois, J.P., Theunissen, K., 1984. Granitoides Kibariens précoces et tectonique tengentielle au Burundi: magmatisme bimodal lié à la distension crustale. In: Klerkx, J., Michot, J., (eds.), African Geology, Musée royal De l'Afrique centrale, Tervuren, Belgium, 29–46.

Klerkx, J., Liégeois, J.P., Lavreau, J., Claessen, W., 1987. Crustal Evolution of the Northern Kibaran Belt, eastern and central Africa. In: Kröner, A. (ed.), Proterozoic Lithospheric Evolution. American Geophysical Union, Geodynamics Series 17, 217–233.

Kokonyangi, J.W, Okudaira, T., Kampunzu, A.B.,Yoshida, M., 2001. Geological evolution of the Kibarides belt, Mitwaba, Democratic Republic of Congo, Central Africa, Gondwana Research 4, 663–664.

Kokonyangi, J.W., Armstrong, R.A., Kampunzu, A.B., Yoshida, M., Okudaira, T., 2004. U-Pb zircon geochronology and petrology of granitoids from Mitwaba (Katanga, Congo): implications for the evolution of the Mesoproterozoic Kibaran belt. Geological Magazine 142, 109–130.

Kokonynangi, J.W, Kampunzu, A.B, Armstrong, R., Yoshida, M., Okudaira, T., Arima, M., Ngulube, D.A., 2006. The Mesoproterozoic Kibaride belt (Katanga, SE D.R. Congo). Journal of African Earth Sciences 46, 1–35.

Kokonyangi, J.W., Kampunzu, A.B., Armstrong, R., Arima, M., Yoshida, M., Okudaira, T., 2007. U-Pb SHRIMP dating of detrital zircons from the Nzilo group (Kibaran belt): implications for the source of sediments and Mesoproterozoic evolution of central Africa. Journal of Geology 115, 99–113.

Koegelenberg, C., Kister, A.F.M., 2014. Tectonic wedging, back-thrusting and basin development in the frontal parts of the Mesoproterozoic Karagwe Ankole belt in NW Tanzania. Journal of African Earth Sciences 97, 87–98.

Lavreau, J., 1985. Le groupe de la Ruzizi (Ruzizien du Zaïre, Rwanda et Burundi) à la lumière des connaissances actuelles. Musée royal d'Afrique centrale, Tervuren, Belgique. Dept. Géologie Minéralogie, Rapport Annuel 1983-1984, 111–119.

Lavreau, J., Liègeois, J.P., 1982. Granites à étain et granito-gneiss burundiens (région de Kibuye): âge et signification. Annales de la Société géologique de Belgique 105, 289–294.

Legraye, M., 1939. Le complexe cristallophyllien et les formations du Kibali de la province Nord-Orientale du Congo-Belge, leurs relations avec les formations comparables des régions voisines. Annales de la Société géologique de Belgique.63B, 30–48.

Lenoir J.L., Liégeois J.P., Theunissen K., Klerkx J. (1994) – The Palaeoproterozoic Ubendian shear belt in Tanzania: geochronology and structure**.** Journal of African Earth Sciences, 19 (3), 169–184.

Lhoest A., 1940. Quelques grandes lignes de la Géologie de la concession Nord de la Compagnie Minière des Grands lacs Africains. Ann. Soc. Geol. Belgique, 63, 183–199.

Lhoest, A., 1946. Une coupe remarquable des couches de base de l'Urundi dans l'Itombwe. Annales de la Société géologique de Belgique 3, 183–199.

Lhoest, A., 1964. Précisions sur la stratigraphie des couches de base du systeme de l'Urundi dans la partie Nord du synclinal de l'Itombwe. Annales de la Société géologique de Belgique, 86, 10, 557–568.

Li, Z.X, Bogdanova, S.V., Collins, A.S., Davidson, A., De Waele, B., Ernst, R.E., Fitzsimons, I.C.W., Fuck, R.A., Gladkochub, D.P., Jacobs, J., Karlstrom, K.E., Lu, S., Natapov, L.M., Pease, V., Pisarevsky, S.A., Thrane, K., Vernikovsky, V. 2008. Assembly, configuration, and break-up history of Rodinia: Asynthesis. Precambrian Research 160, 179–210.

Link, K., Koehn, D., Barth, M.G., Tiberindwa, J.V., Barifaijo, E., Aanyu, K., Foley, S.F., 2010. Continuous cratonic crust between the Congo and Tanzania blocks in western Uganda. International Journal of Earth Sciences 99, 1559–1573.

Ludwig, K.R., 2001. User manual for Isoplot/Ex rev. 2.49. Berkeley Geochronology Center Special Publications 1a, 1–56.

Luvizotto, G.L., Zack, T., Meyer, H.P., Ludwig, T., Triebold, S., Kronz, A., Münker, C., Stockli, D.F., Prowatke, S., Klemme, S., Jacob, D.E., von Eynatten, H., 2009. Rutile crystals as

potential trace element and isotope mineral standards for microanalysis. Chemical Geology 261, 346–369.

Mc Lelland, J., Hamilton, M., Selleck, B., Mc Lelland, J., Walker, D., Orell, S., 2001. Zircon U-Pb geochronology of the Ottawan orogeny, Adirondack Highlands, New York: regional and tectonic implications. Precambrian Research 109, 39–72.

Magnée (de), I., 1935. Coupe géologique dans les monts Kibara. Annales de la Société géologique de Belgique 58, 70–82.

Monteyne–Poulaert, G., Delwiche, R., Safianikoff, A., Cahen, L., 1962. Age des minéralisations pegmatitiques et filoniennes du Kivu méridional (Congo oriental). Indications préliminaires sur les âges des phases pegmatitiques successives. Bulletin de la Société belge de géologie, de paléontologie et d'hydrologie 71, 272–295.

Mortelmans, G., 1951. Stratigraphie et tectonique des mont Kibara dans la région Mitwaba-Kina. Bulletin de la Société belge de géologie, de paléontologie et d'hydrologie 59, 359–382.

Mugaruka-Bibentyo T., Cirhuza-Cirimwani R., Mugisho-Birhengira E., Basimike-Tschangaboba J., Ganza-Bamulezi G., Kapajika-Badibanga C., Nzolang C., 2015. Petrographie et geochimie des gneiss kibariens à Bunyakiri, sud Kivu, R.D. Congo. Intern. Journ. of Innovation and Applied Sciences, 11(2), 376–382.

Nzojibwami, E., 1984. The west Mugere suprecrustal complex (Bujumbura): Evidence of an ancient basement complex remobilised during the Kibaran orogeny. UNESCO, Geology for Development, Newsletters 3, 5–12.

Pasteels, P., 1961. Géologie et pétrographie de la région de Kirotshe (Kivu). Académie royale des sciences d'outre-mer. Classe des sciences techniques 15, 115 pp.

Pasteels, P., Villeneuve, M., De Paepe, P., Klerkx, J., 1989. Timing of the volcanism of the southern Kivu province: implications for the evolution of the western branch of the East African Rift system. Earth and Planetary Science Letters 94, 353–363.

Peeters, L., 1956. Contribution à la géologie des terrains anciens du Rwanda-Urundi et Kivu. Annales du Musée royal du Congo belge, Tervuren, Belgique: Sciences géologiques 16, 197 pp.

Pöhl, W., 1992. Kibaran evolution and metallogeny of Central Africa: A synthesis at the end of the IGCP project 255. IGCP n°255 Newsletters 4, 1–8.

Pöhl, W., 1994. Metallogeny of the northeastern Kibara belt, central Africa-recent perspectives. Ore Geology Reviews 9, 105–130.

Pouclet, A., Bellon, H., Bram, K., 2016. The Cenozoic volcanism in the Kivu rift: assessment of the tectonic setting, geochemistry and geochronology of the volcanic activity in the south Kivu and Virunga regions. Journal of African Earth Sciences 121, 219–246.

Radulescu, I., 1981. Carte géologique et esquisse metallogénique du Burundi, 1/500 000, Projet de recherches minières, UNDP, Bujumbura.

Robert, M., 1938. Notice de la carte géologique du Katanga à l'échelle du 1.000.000. Note preliminaire. Bulletin de la Société belge de géologie, de paléontologie et d'hydrologie 48, 7–22.

Robert, M., 1944. Contribution à la géologie du Katanga. Le systeme des Kibaras et le complexe de base. Memoires de l'Institut Royal Colonial Belge 7, 92 pp.

Robert, M., 1951. Géologie du Katanga. Les formations du soubassement ancien. Comité Special du Katanga 19, 35 pp.

Rumvegeri, B.T., 1984. Etudes lithostratigraphique et structurale du Précambrien de la région de Bunyakiri (Kivu, Zaire); modèle d'évolution géodynamique de la chaine Kibarienne en Afrique centrale et orientale. DES Université Lubumbashi, Zaïre, 183 pp.

Rumvegeri, B.T., 1987. Le Précambrien de l'Ouest du lac Kivu (Zaire) et sa place dans l'évolution Géodynamique de l'Afrique centrale et orientale. These Doctoral, Université Lubumbashi, 313 pp.

Rumvegeri, B.T., 1989. Le Précambrien de l'Ouest du lac Kivu (Zaïre) et sa place dans l'évolution géodynamique de l'Afrique centrale et orientale. IGCP 255, Newsletter 2, 73–76.

Rumvegeri, B.T. 1991. Tectonic significance of Kibaran structures in Central and Eastern Africa. Journal of African Earth Sciences 13, 267–276.

Rumvegeri, B.T., Kampunzu, A.B., Caron, J.P.H., Lubala, R.T., 1985. Lithostratigraphie et evolution structurale de la chaine Kibarienne à l'Ouest du lac Kivu (Zaire). UNESCO, Geology for Economic Development, Newsletters 4, 83–90.

Safianikoff, A., 1950. Les systèmes de l'Urundi et de la Ruzizi au Kivu et les intrusions granitiques. Annales de la Société géologique de Belgique 63, 87–97.

Salée, A., 1928. Constitution géologique du Ruanda oriental. Mémoires de l'Institut géologique de l'Université Louvain 5, 47–166.

Schmitt, A.K., Zack, T., 2012. High-sensitivity U-Pb rutile dating by secondary ion mass spectrometry (SIMS) with an O2+ primary beam. Chemical Geology 332–333, 65–73.

Salée, A., Boutakoff, N., de la Vallée Poussin, J., 1939. Carte géologique de la région du Kivu, au 500.000". Institut Géologique de l'Université Louvain, Belgique 9, pl. V.

Sircombe, K.N., 2004. AGEDISPLAY: an EXCEL workbook to evaluate and display univariate geochronological data using binned frequency histograms and probability density distributions. Computers & Geosciences 30, 21–31.

Spencer, C.J., Kirkland, C.L., Taylor, R.J.M., 2016. Strategies towards statistically robust interpretation of in situ U-Pb zircon geochronology. Geoscience Frontiers 7, 581–589.

Stacey, J.S., Kramers, J.D., 1975. Approximation of terrestrial lead isotope evolution by a two-stage model. Earth and Planetary Science Letters 26, 207–221.

Tack, L., De Paepe, P., Liégeois, J.P., Nimpagaritse, G., Ntungicimpye, A., Midende, G., 1990. Late Kibaran magmatism in Burundi. Journal of African Earth Sciences 10, 733–738.

Tack, L., Liégeois, J.P., Deblond, A., Duchesne, J.C., 1994. Kibaran A-type granitoids and mafic rocks generated by to mantle sources in a late orogenic setting (Burundi). Precambrian Research 68, 323–356.

Tack, L., Wingate, M.T.D., De Waele, B., Meert, J., Belousava, E., Griffin, B., Tahon, A., Fernandez-Alonso, M., 2010. The 1375 Ma "Kibaran event" in Central Africa: Prominent

emplacement of bimodal magmatism under extensional regime. Precambrian Research 180, 63–84.

Tahon A., Fernandez-Alonso M., Tack L., Barritt S.D., 2004. New insights about the evolution of the Mesoproterozoic Northeastern Kibarabn belt (Central Africa). 20° colloque de Géologie Africaine, Orléans, France, p. 389.

Theunissen, K., 1984. Les principaux traits de la tectonique Kibarienne au Burundi. UNESCO, Geology for Development, Newsletters 3, 25–30.

Theunissen, K. 1988a. The Ufipa shear zone in the Ubendian belt at Karema (W. Tanzania): a NW oriented left lateral strike-slip of postulated late Kibaran age. UNESCO/IUGS GARS program in Africa (J. Lavreau and J.Bardinet edit.). Annales du Musée royal du Congo belge, Tervuren, Belgique 96, 63–77.

Theunissen, K. 1988b. Evidence for Upper Proterozoic conjugate strike-slips basins controlled by basement structures in NW Tanzania and Burundi. Bulletin de la Société belge de Géologie 97, 115–130.

Theunissen, K., 1989. Carte géologique du Burundi, Feuille Cibitoke, S3-20SW, République du Burundi, Ministère Energie et Mines. Bujumbura.

Theunissen, K., Klerkx, J., 1980. Considerations preliminaires sue l'evolution tectonique du «Burundien» au Burundi. Musée royal d'Afrique centrale, Tervuren, Belgique. Dept. Géologie Minéralogie, Rapport Annuel 1979, 207–214.

Theunissen, K., Hanon, M., Fernandez-Alonso, M., 1991. Carte géologique du Rwanda 1:200.000. Service géologique, Ministere de l'Industrie et de l'Artisanat, Kigali, Rwanda.

Theunissen, K., Lenoir, J.L., Liégeois, J.P., Delvaux, D., Mruma, A., 1992. Empreinte panafricaine majeure dans la chaine Ubendienne de Tanzanie sud-occidentale; géochronologie U-Pb Zircon et contexte structural. Comptes Rendus de l'Académie des Sciences, Paris 314, 1355–1362.

Theunissen, K., Klerkx, J., Melnikoff, A., Mruma, A., 1996. Mechanism of inheritance of rift faulting in the western branch of the East African Rift (Tanzania). Tectonics 15, 776–790.

Thibault, P.M., 1982. Carte géologique au 1/500 000 du Haut Zaïre et du Nord Kivu. Service géologique du Zaïre, Kinshasa.

Van de Steen, J., 1959. Le système des Kibaras. Bulletin Géologique du Congo-Belge et du Ruanda-Urundi. 1, 8–22.

Vernon-Chamberlain, V. E., Snelling, N.J., 1972. Age and isotope studies on the "arena" granites of SW Uganda. Annales du Musée royal du Congo belge, Tervuren, Belgique 73, 5–44.

Villeneuve, M., 1976. Mise en évidence d'une discordance angulaire majeure dans les terrains précambriens du Nord du synclinal de l'Itombwe (région du Kivu, République du Zaïre). Comptes Rendus de l'Académie des Sciences, Paris, 282D, 1709–1712.

Villeneuve, M., 1977. Le Précambrien du sud du lac Kivu (République du Zaïre). Thèse 3ème cycle, Université Aix-Marseille III, 195 p.

Villeneuve, M., 1978. La stratigraphie du Précambrien du sud du Lac Kivu (Zaïre oriental). Bulletin de la Société Géologique de France 7, 20, 6, 915–920.

Villeneuve, M., 1983a. Les formations précambriennes de Katana, au Kivu oriental (Zaïre). Musée royal d'Afrique centrale, Tervuren, Belgique. Dept. Géologie Minéralogie, Rapport Annuel 1981-1982 153–159.

Villeneuve, M., 1983b. Les sillons tectoniques du precambrien superieur dans l'Est du Zaire; comparaisons avec les directions du rift Est-African. Bulletin des Centres de Recherches Exploration-Production Elf-Aquitaine, Pau, France 7, 163–174.

Villeneuve, M., 1987. Géologie du synclinal de l'Itombwe (Zaïre Oriental) et le problème de l'existence d'un sillon plissé pan-africain. Journal of African Earth Sciences 6, 869–880.

Villeneuve, M., Chorowicz, J., 2004. Les sillons plissés du Brundien supérieur dans la chaine Kibarienne d'Afrique centrale. Comptes Rendus Geoscience 336, 807–814.

Villeneuve, M., Guyonnet-Benaize, C., 2006. Apports de l'imagerie spatiale à la résolution des structures géologiques en zone équatoriale: exemples du Précambrien au Kivu (Congo Oriental). Photo-Interprétation 4, 3–22.

Villeneuve M., Gärtner A., Delvaux D., Wazi N., Dewaele S., Fernandez-Alonso M. (in progress). The Kibaran «Kivu Belt (KVB)» in central Africa: New Insights. Journ. Afric. Earth Sci.,

Wayland, E.J., 1920. Geology of Uganda. Annual Report of the Geological Department of Uganda, Kampala.

Westerhof A.B., Harma P., Isabirye H ;, Katto E., Koistinen T., Kuosmanen, E;, Letho T., Lehtonen M;, Makitie H., Manninnen T, Manttari I.,Pekkala Y., Pokki J., saalmann K, Virransalo P., 2014. Geology and geodynamic Development of Uganda with explanation

of th 1.1 000.000 Scale Geological map, Geological Survey of Finland, Special Paper 0782-8535 55.

Ziserman, A., Zigirabili, J., Petricec, V., Baudin, B., 1983. Données sur la métallogenie du Rwanda. Enseignements tirés de la carte des gites mineraux. Chronique des Mines et de la Recherche Miniere 471, 31–40.

Zolnai G. 1986. Les aulacogènes du continent nord-americain. Bulletin de la Société Géologique de France 8, 2, 5, 809-818.

Sample coordinates:

NG1: (field sample 2/285) Bangwe Formation: N 2°41'39.9" / W 28°53'51.8"

NG2: (field sample 2/17) Mughera Formation: N2°42'43.8"/ W 28°50'19.5"

NG3: (field sample 2/28) Mukubio Formation: N 2°41'45.2" / W 28°51'39.9"

NG4: (field sample 2/48) Mughera Formation: N 2°43'19.5" / W 28°50'06.6"

NG5: (field sample 2-443a) Kamanyola Formation: N 2° 41' 86.0" / W 28° 57' 22.1"

NG6: (field sample 2-483) Kashenie Formation: N2° 42' 23.0" / W 28° 58' 55.2"

Figure Captions

Figure 1: Geological sketch map of the KAB (Kivu Belt) and KVB (Karagwe–Ankole Belt) areas.

1a) – Sketch map with location of KVB (Kivu Belt), KAB (Karagwe–Ankole Belt) and KIB (Kibaride Belt).

Legend: CC = Congo Craton, BB = Bangweulu Block, TzC = Tanzanian Craton. RC = Rhodesian Craton, KAB = Karagwe Ankole Belt, KVB = Kivu Belt, Kb = Kibaride Belt, Ib = Irumide Belt, Mb = Mozambique Belt.

1b) - Geological sketch map of the KVB and KAB.

Legend: 1 - Kibalian / Ruwenzorian basement (Archaean), 2 - Tanzanian basement (Archaean), 3 - Bukoba Group, 4 - unknown terranes, 5 - unit 1 (Kv1 and Ka1), 6 - unit 2 (Kv2 and Ka2), 7 - Unit 3 (Kv3), 8 - unit 4 (Kv4), 9 - units 1 and 2 reworked, 10 - post-Kibaran-Burundian formations, 11 - Great Lakes, 12 - Main rivers, 13 - main thrusts, 14 - Main strike slip faults. ED= Eastern Domain and WD = Western Domain of the KAB (Tack et al., 2010)

Basement massifs: a - Elila Massif, b - Bujumbura Massif, c - central massif, d - Kibuye structures, e - Lushasha Massif, f - Oso-Lubanga Massif. **Trenches**: 1 - Maniema trench, 2 - Kama trench. 3 - Shabunda trench. 4 - Luemba trench, 5 - Kayanza trench, 6 - Ngozi trench, 7 - Muyinga-Rwinkwavu trench, 8- Bugene trench, 9 - Rugera-Nyakuhara trench, 10 - Kagera trench, 11 - Byumba-Miyove trench, 12 - Mukungwa trench, 13 - Kibuye trench, 14 - Kirotshe trench, 15 - Masisi trench, 16 - Walikale trench, 17 - Kitole trench, 18 - Rwate-Bilati trench, 19 - Lubero trench, 20 - Luhule-Mobissio trench, 21 - Lindi trench, 22 - Lugulu trench, 23 - Bugarama-Nya-Ngezie trench, 24 - Itombwe Structure. AB = Southern cross section, CD = northern cross section. **Lakes**: EL = Edward Lake, KL = Kivu Lake, TL = Tanganiyka Lake, VL = Victoria Lake. **Cities**: Pan = Pangi, Buk = Bukavu, Ks = Kasika, Lu = Luemba, Buj = Bujumbura,

Figure 2 - Geology of the Nya-Ngezie area.

2a) - ***Geological sketch map of the Nya-Ngezie area.***

2b) ***- Lithostratigraphic succession of the Nya-Ngezie area with position of samples for detrital zircon age determination.*** 1 and 2: Major unconformities.

Figure 3 - Sedimentological marks of the Nya-Ngezie group.

Left - Ripple-mark axes and scour-mark directions.

Right) - Diagrams indicate the mean directions of ripple-marks and scour-marks of the Nya-Ngezie Group. 1 and 2 indicate the main unconformities.

Figure 4 - Diagram with the mean ages of inherited zircons in the Bugarama and Nya-Ngezie groups. See legend in fig. 2.

Figure 5 - Northern (CD) and southern (AB) geological sections across the KVB and the KAB. (See location in figure 1)

Legend: numbers 1 to 23 = trenches plotted in figure 1. Letters (a) to (f) = unit 1 massifs located in figure 1.

Captions: 1 – Tertiary sediments of the East African Rift, 2 – Karoo (at Walikale), 3 – pan-African sediments (Malagarasian), 4 – unit 3 (Masisi and Bugarama groups), 5 – unit 2, 6 – basal conglomerate of unit 2, 7 – unit 1, 8 – supposed Tanzanian basement and basic and ultrabasic intrusions of Musindosi, 9 – sediments of the Bukoba and Ruvubu groups, 10 – upper part of sediments of the Bukoba and Ruvubu groups, 11 – Tanzanian basement (Archaean), 12 – examples of granitic intrusions, 13 – Main faults.

Table I - ***Correlations throughout the Kibaran Belts, from Katanga (SE Congo) to Uganda.***

Legend: Kv (Kv1 to Kv4) = lithostratigraphic units in the KVB, Ki (Ki1 to Ki4) = Lithostratigraphic units in the Kibaride belt (KIB). K1 to K5 = Common Lithostratigraphic units

for the Kibaran Orogen, Un1 to Un5 = Major unconformities. Kai. gr. = Kiaora Group, Nzilo gr. = Nzilo Group, Haka.gr. = Hakansson Group, Lub.gr. = Lubudi Group, Banji Group = Banji Group, Luiko gr. = Luiko Group. Wak.T. = Wakole Terranes, It. gr. = Itiaso Group, Ubend. = Ubendian basement, Ukiga gr. = Ukiga Group, Rug.gr = Rugezi Group, Cyo.gr. = Cyohoha Group, Pin.gr. = Pindura Group, Gik.gr = Gikoro Group, Tanz.bas = Tanzanian basement, Buk.gr. = Bukoba Group, Ruv.gr = Ruvubu Group, Muy.gr. = Muyaga Group, Igara bas. = Igara basement,

Table II- ***Synopsis of the Kibaran Orogen evolution including tectonostratigraphic cycles, tectonic, granitic and metamorphic events. Cartoons of the geodynamic evolution of the Kibaran Orogen through time***

Legend: K/Cy = tectonostratigraphic cycles, Un = major unconformities, D = tectonic events, G = main granitic events, M = Main metamorphic events (explanation in text), Yellow circles = Main stages of the geodynamic evolution (see explanations in text). 1 - Extensional tectonic regime, 2 - compressional tectonic regime.

NG1 to NG6 samples dated by detrital zircons and located in figs 2 and 4.

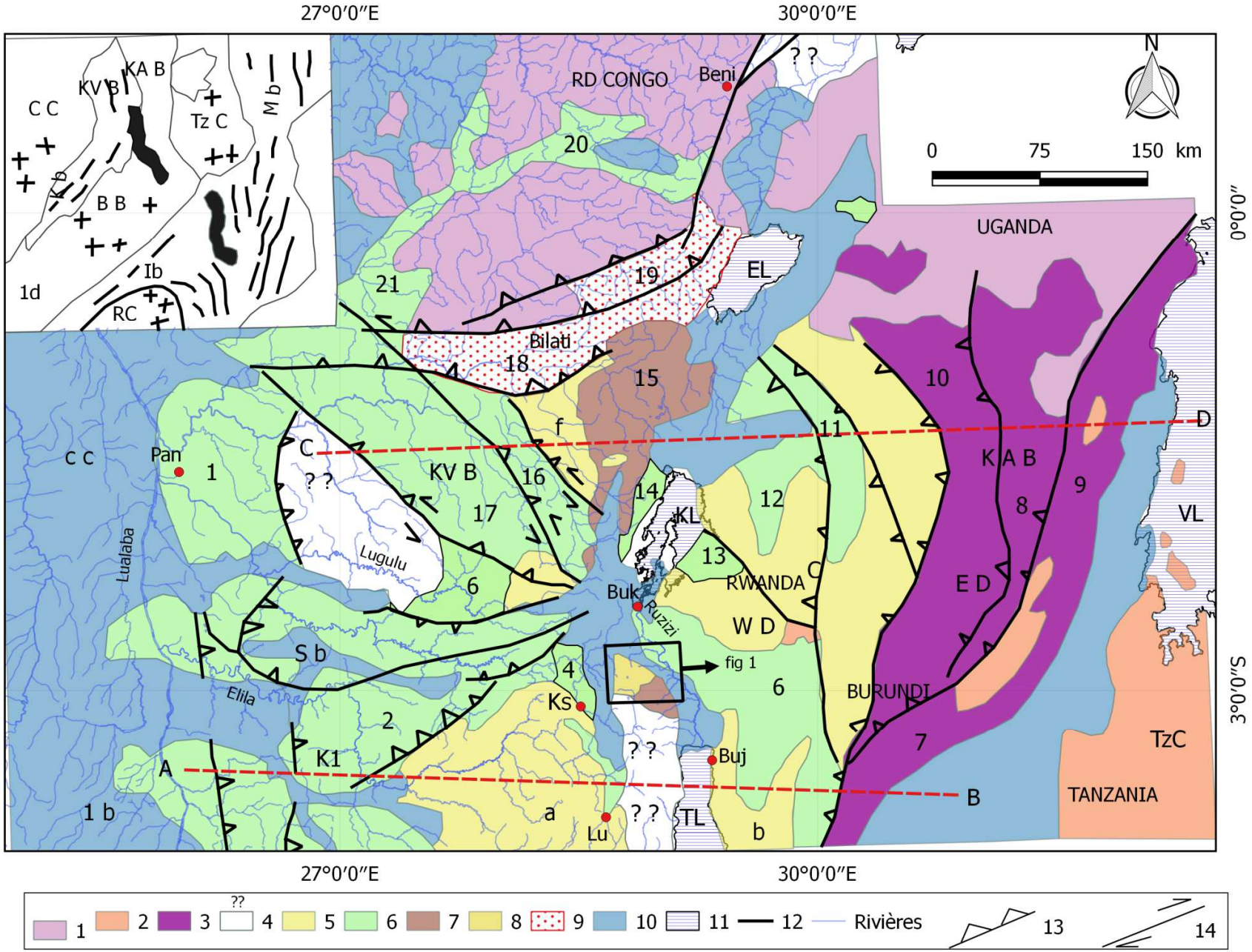
27°0′0″E
30°0′0″E
0°0′0″
3°0′0″S
N
0 75 150 km
RD CONGO
Beni
UGANDA
RWANDA
BURUNDI
TANZANIA
Bilati
Pan
Buk
Ruzizi
Lualaba
Lugulu
Elila
Ks
Lu
Buj
fig 1
KV B
KA B
Tz C
M b
K b
B B
Ib
RC
1d
1 b
EL
KL
VL
TL
TzC
E D
W D
S b
K1
A
B
C
D
f
a
b
1
2
3
4
5
6
7
8
9
10
11
12
13
14
Rivières

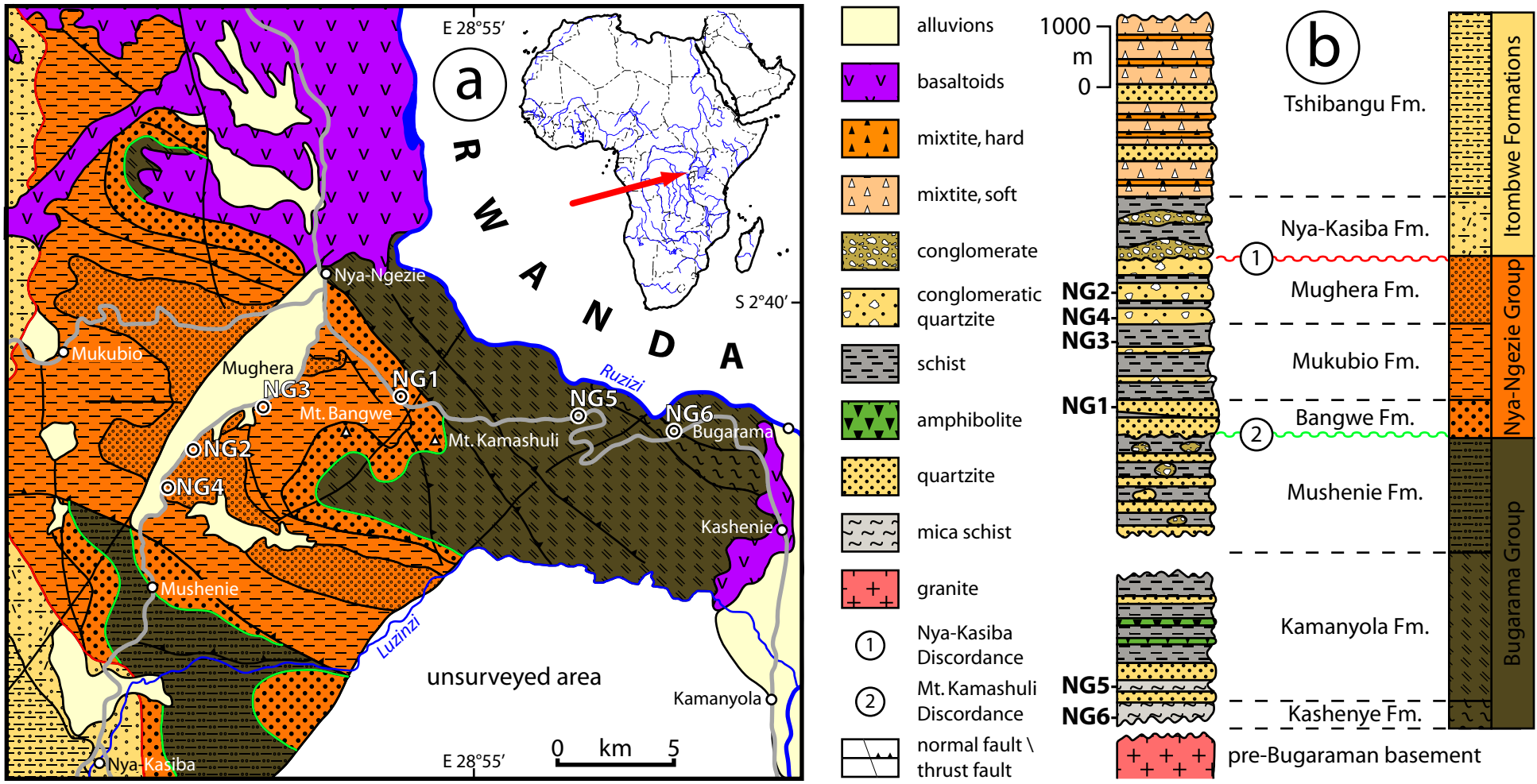
a
E 28°55′
S 2°40′
RWANDA
Nya-Ngezie
Mukubio
Mughera
NG3
NG1
Mt. Bangwe
NG5
NG6
Bugarama
Mt. Kamashuli
NG2
NG4
Kashenie
Mushenie
Luzinzi
Ruzizi
unsurveyed area
Kamanyola
Nya-Kasiba
E 28°55′
0 km 5
alluvions
basaltoids
mixtite, hard
mixtite, soft
conglomerate
conglomeratic quartzite
schist
amphibolite
quartzite
mica schist
granite
① Nya-Kasiba Discordance
② Mt. Kamashuli Discordance
normal fault \ thrust fault
b
1000 m 0
Tshibangu Fm.
Nya-Kasiba Fm.
Mughera Fm.
Mukubio Fm.
Bangwe Fm.
Mushenie Fm.
Kamanyola Fm.
Kashenye Fm.
pre-Bugaraman basement
Itombwe Formations
Nya-Ngezie Group
Bugarama Group

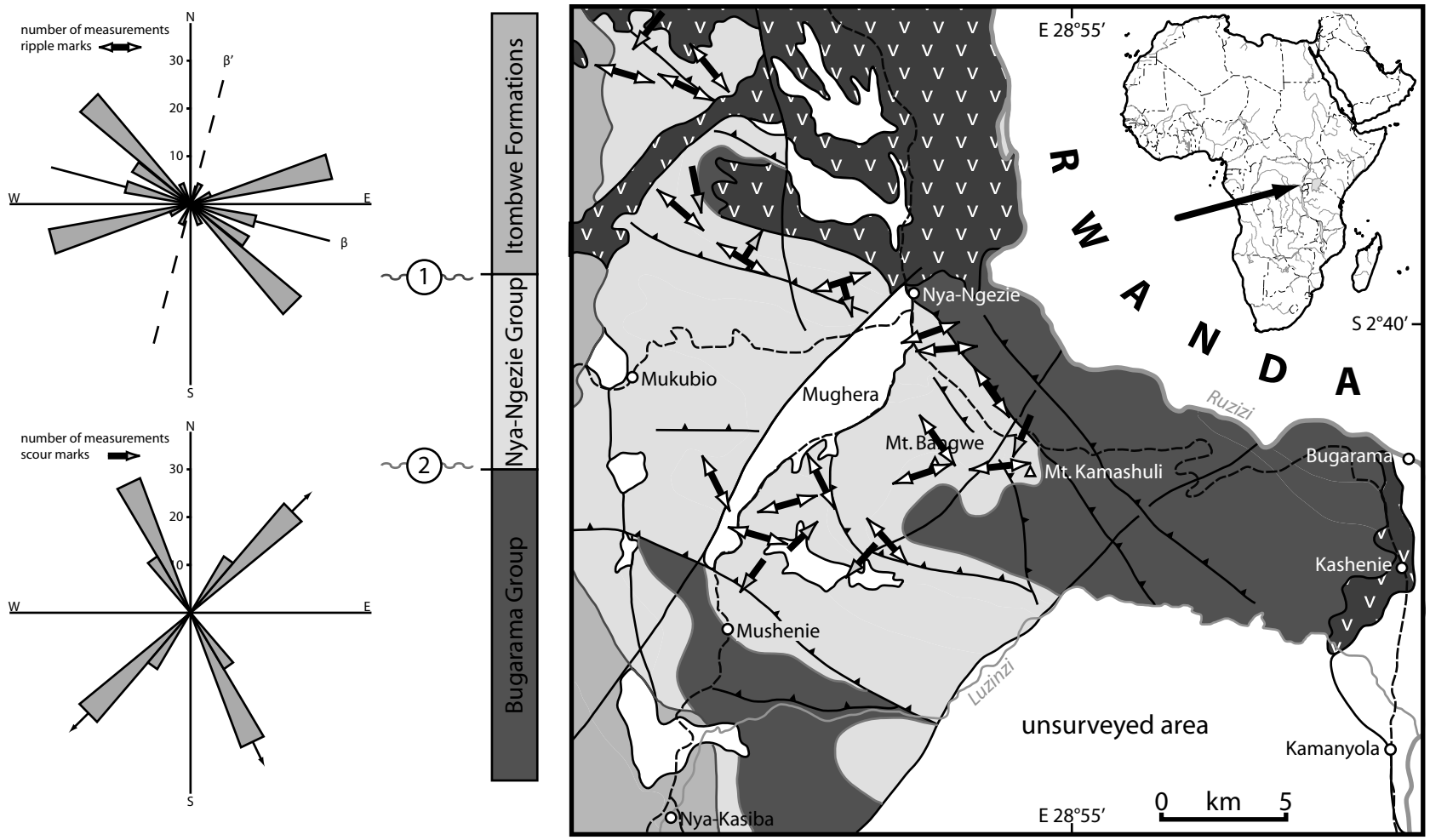
number of measurements
ripple marks
N
30
20
10
W
E
S
β′
β
number of measurements
scour marks
N
30
20
0
W
E
S
1
2
Itombwe Formations
Nya-Ngezie Group
Bugarama Group
E 28°55′
S 2°40′
R W A N D A
Nya-Ngezie
Mukubio
Mughera
Mt. Bangwe
Mt. Kamashuli
Ruzizi
Bugarama
Kashenie
Mushenie
Luzinzi
unsurveyed area
Kamanyola
Nya-Kasiba
E 28°55′
0 km 5

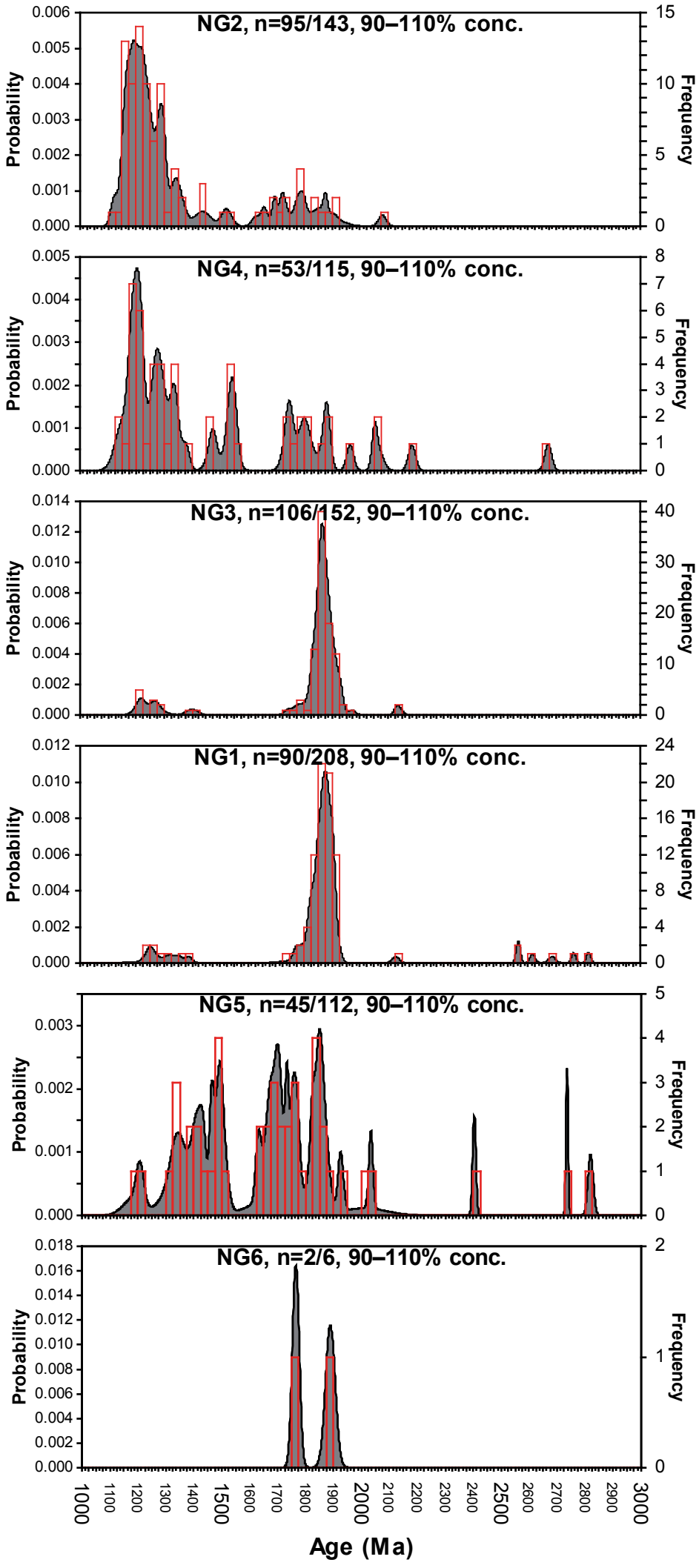
NG2, n=95/143, 90–110% conc.
NG4, n=53/115, 90–110% conc.
NG3, n=106/152, 90–110% conc.
NG1, n=90/208, 90–110% conc.
NG5, n=45/112, 90–110% conc.
NG6, n=2/6, 90–110% conc.
Probability
Frequency
Age (Ma)

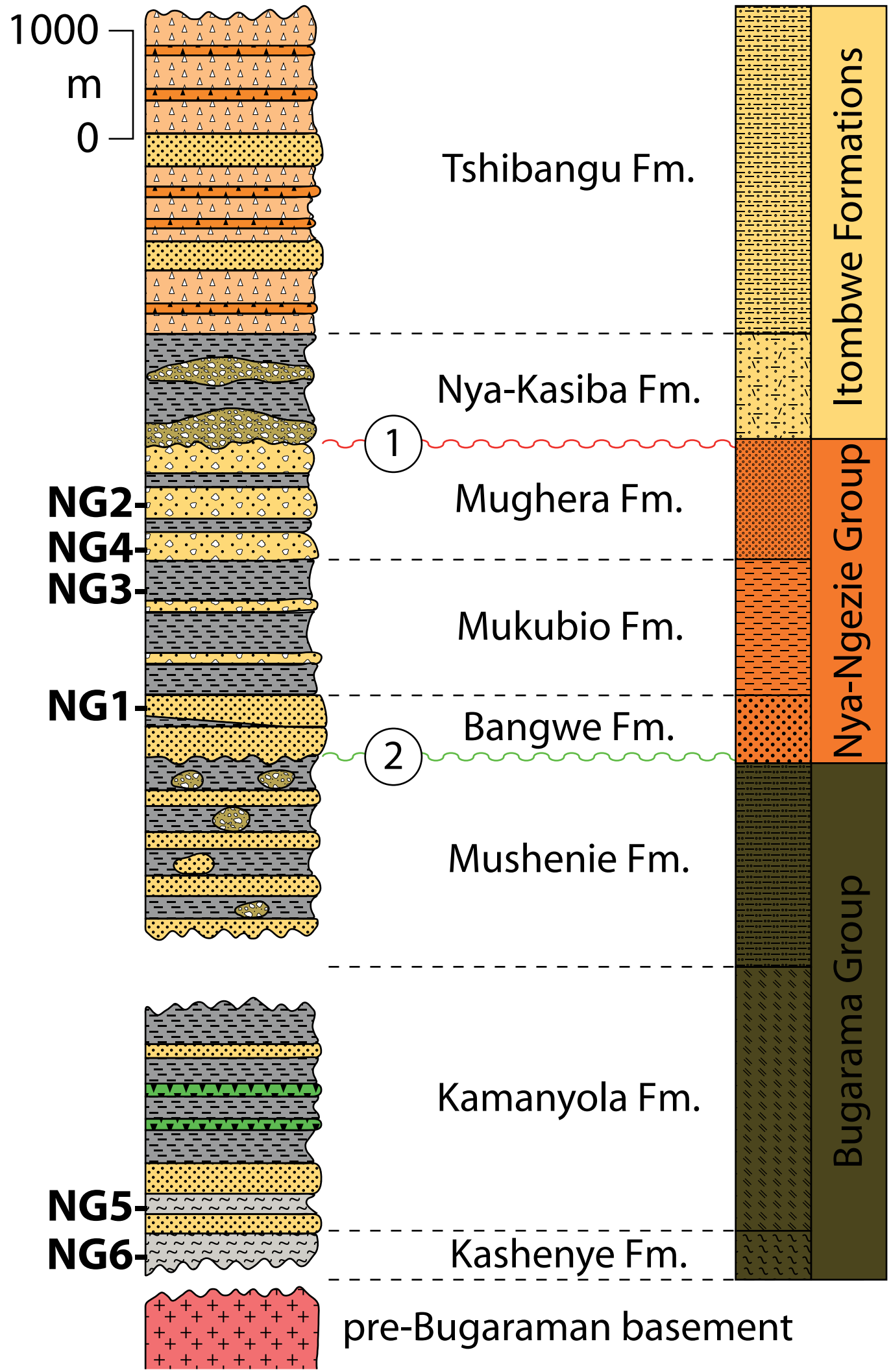
1000
m
0
Tshibangu Fm.
Nya-Kasiba Fm.
1
Mughera Fm.
NG2-
NG4-
NG3-
Mukubio Fm.
NG1-
Bangwe Fm.
2
Mushenie Fm.
Kamanyola Fm.
NG5-
NG6-
Kashenye Fm.
pre-Bugaraman basement
Itombwe Formations
Nya-Ngezie Group
Bugaraman Group

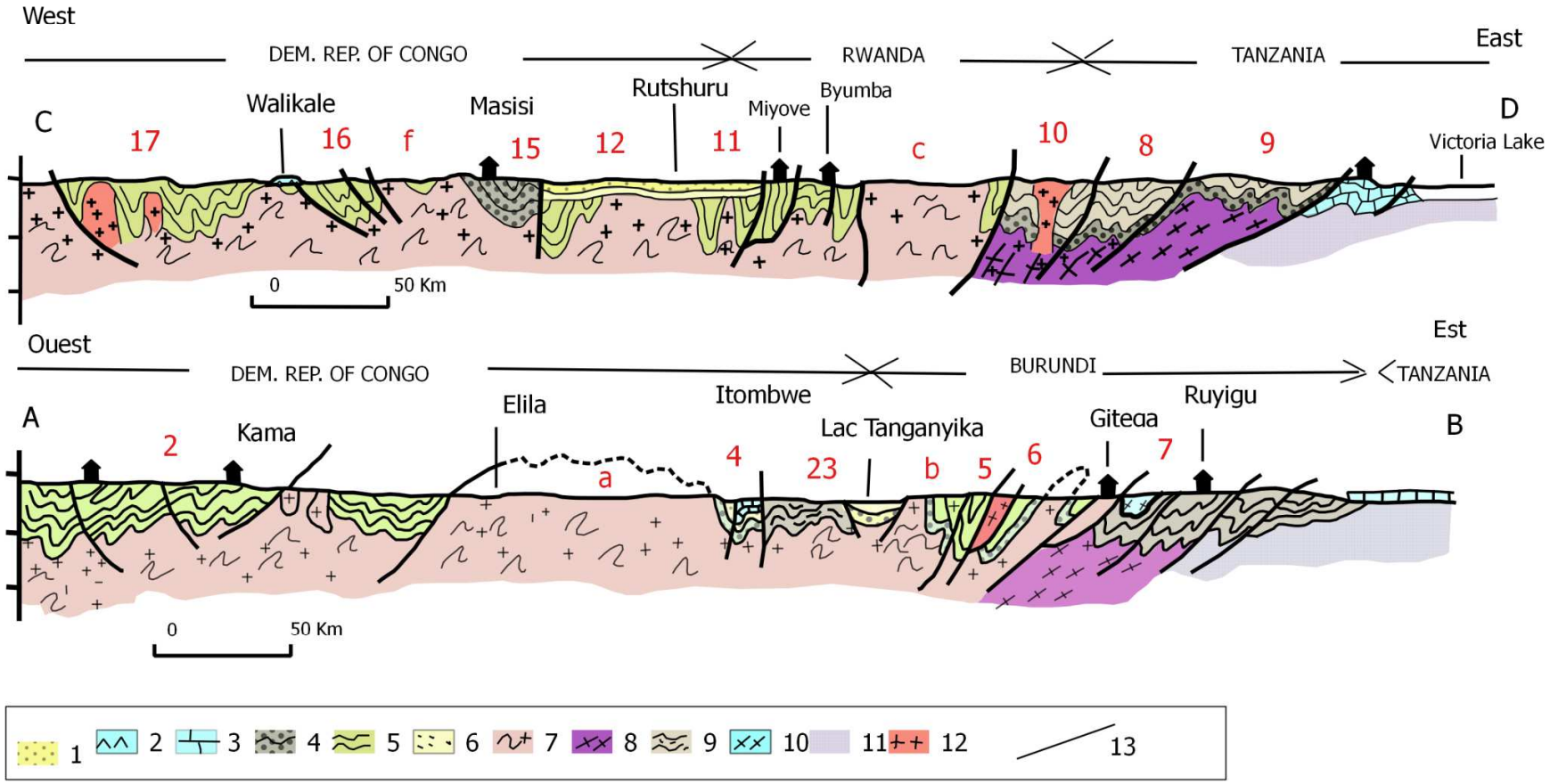
West
DEM. REP. OF CONGO
RWANDA
TANZANIA
East
C
D
Walikale
Masisi
Rutshuru
Miyove
Byumba
Victoria Lake
17
16
f
15
12
11
c
10
8
9
0
50 Km
Ouest
DEM. REP. OF CONGO
BURUNDI
TANZANIA
Est
A
B
Kama
Elila
Itombwe
Lac Tanganyika
Gitega
Ruyigu
2
a
4
23
b
5
6
7
0
50 Km
1
2
3
4
5
6
7
8
9
10
11
12
13

Tab. 2: U-Pb-Th data of zircon from sample NG1, n = 90 of 208 measured zircon grains (90-110 % conc.), quartzitic sandstone with ripple marks, South Kivu Province, DR Congo

Number	^{207}Pb (cps)	U^a (ppm)	Pb^a (ppm)	$\frac{Th^c}{U}$	$\frac{^{206}Pb}{^{204}Pb}$	$\frac{^{206}Pb^e}{^{238}U}$	2 σ %	$\frac{^{207}Pb^e}{^{235}U}$	2 σ %	$\frac{^{207}Pb^e}{^{206}Pb}$	2 σ %	rho	$\frac{^{206}Pb}{^{238}U}$	2 σ (Ma)	$\frac{^{207}Pb}{^{235}U}$	2 σ (Ma)	$\frac{^{207}Pb}{^{206}Pb}$	2 σ (Ma)	conc %
NG1-seq1-a01	101687	147	59	0.83	20181	0.33517	2.0	5.17342	2.5	0.11195	1.5	0.81	1863	33	1848	22	1831	27	**102**
NG1-seq1-a02	1859	6	2	1.80	2303	0.21367	5.7	2.41641	9.2	0.08202	7.2	0.62	1248	65	1247	68	1246	140	**100**
NG1-seq1-a03	18020	54	11	0.46	1334	0.19529	3.3	2.40667	3.9	0.08938	2.0	0.85	1150	35	1245	28	1412	39	81
NG1-seq1-a04	156639	251	69	0.53	1158	0.24225	3.2	3.97488	3.5	0.11900	1.4	0.91	1398	40	1629	29	1941	25	72
NG1-seq1-a05	182203	260	74	0.64	327	0.22729	2.3	3.54657	3.0	0.11317	1.9	0.77	1320	28	1538	24	1851	34	71
NG1-seq1-a06	87796	274	64	1.02	4489	0.19337	2.2	3.02394	2.5	0.11342	1.2	0.88	1140	23	1414	19	1855	22	61
NG1-seq1-a07	8954	13	6	1.46	8228	0.32395	2.4	4.93552	3.8	0.11050	3.0	0.64	1809	39	1808	33	1808	54	**100**
NG1-seq1-a08	119328	187	76	0.84	15957	0.33775	1.7	5.43328	2.3	0.11667	1.5	0.75	1876	28	1890	20	1906	28	**98**
NG1-seq1-a09	35525	163	26	0.92	6515	0.13681	2.6	1.98351	2.8	0.10515	1.0	0.93	827	20	1110	19	1717	19	48
NG1-seq1-a10	162667	689	101	0.22	2198	0.12796	3.0	1.97985	3.6	0.11222	2.0	0.83	776	22	1109	25	1836	37	42
NG1-seq1-a11	106369	157	57	0.44	32995	0.33385	2.4	5.30820	2.7	0.11532	1.1	0.91	1857	40	1870	23	1885	20	**99**
NG1-seq1-a12	98063	168	68	0.89	86597	0.33703	2.1	5.33121	2.4	0.11473	1.2	0.87	1872	34	1874	21	1876	21	**100**
NG1-seq1-a13	50761	119	20	0.75	9242	0.12093	7.6	1.85275	7.8	0.11112	1.5	0.98	736	53	1064	53	1818	27	40
NG1-seq1-a14	80989	205	69	1.02	21580	0.28953	1.8	4.32253	2.1	0.10828	1.1	0.85	1639	26	1698	17	1771	20	**93**
NG1-seq1-a15	24152	104	21	1.06	4401	0.17050	3.7	2.66590	4.0	0.11340	1.5	0.93	1015	34	1319	30	1855	27	55
NG1-seq1-a16	50322	88	34	0.83	11153	0.32617	2.5	5.18201	2.9	0.11523	1.5	0.85	1820	40	1850	25	1883	28	**97**
NG1-seq1-a17	121851	226	83	0.71	32440	0.31181	2.0	4.86319	2.2	0.11312	0.9	0.90	1750	31	1796	19	1850	17	**95**
NG1-seq1-a18	61565	216	57	0.85	11671	0.23816	2.2	3.66578	2.5	0.11163	1.3	0.86	1377	27	1564	20	1826	24	75
NG1-seq1-a19	95454	202	67	0.39	65968	0.32835	3.3	5.19702	3.4	0.11479	1.0	0.96	1830	53	1852	30	1877	18	**98**
NG1-seq1-a20	74903	139	52	0.60	66424	0.32992	2.1	5.17822	2.6	0.11383	1.4	0.83	1838	34	1849	22	1861	26	**99**
NG1-seq1-a21	36131	166	52	2.39	16241	0.21092	1.8	2.39194	2.2	0.08225	1.3	0.81	1234	20	1240	16	1251	25	**99**
NG1-seq1-a22	60840	173	45	1.04	27838	0.21112	3.4	3.35069	3.6	0.11511	1.0	0.96	1235	39	1493	28	1882	18	66
NG1-seq1-a23	34598	88	27	0.99	7773	0.25444	2.4	3.96982	2.8	0.11316	1.4	0.87	1461	32	1628	23	1851	25	79
NG1-seq1-a24	25158	185	23	0.38	5752	0.12481	2.2	1.46834	2.7	0.08532	1.6	0.81	758	16	917	16	1323	31	57
NG1-seq1-a25	45534	93	35	0.70	12776	0.32879	1.8	5.23896	2.3	0.11557	1.4	0.79	1832	29	1859	20	1889	25	**97**
NG1-seq1-a26	101955	210	83	0.78	89032	0.33545	2.0	5.35590	2.3	0.11580	1.1	0.88	1865	33	1878	20	1892	20	**99**
NG1-seq1-a27	22042	46	18	0.85	19115	0.33161	2.1	5.34542	2.8	0.11691	1.9	0.75	1846	34	1876	24	1909	33	**97**
NG1-seq1-a28	40474	103	35	0.77	6566	0.29684	2.9	4.74559	3.3	0.11595	1.7	0.87	1676	42	1775	28	1895	30	88
NG1-seq1-a29	64759	164	58	1.20	12527	0.27252	2.7	4.42250	3.8	0.11770	2.6	0.72	1554	38	1717	32	1922	47	81
NG1-seq1-a30	67137	170	68	1.32	27487	0.32295	1.8	5.13677	2.1	0.11536	1.0	0.87	1804	28	1842	18	1885	18	**96**
NG1-seq1-a31	34446	161	34	0.42	40357	0.20090	2.3	2.39795	2.9	0.08657	1.7	0.81	1180	25	1242	21	1351	32	87

NG1-seq1-a32	99433	317	71	0.85	14373	0.16637	3.3	2.54221	3.6	0.11082	1.3	0.93	992	30	1284	26	1813	24	55
NG1-seq1-a33	13270	157	14	0.92	819	0.07307	4.5	1.16918	5.2	0.11605	2.6	0.87	455	20	786	29	1896	46	24
NG1-seq1-a34	72431	239	69	0.92	22600	0.25370	1.8	3.96518	2.0	0.11336	0.9	0.90	1458	23	1627	16	1854	16	79
NG1-seq1-a35	31571	120	37	1.11	1299	0.26687	2.5	4.09899	2.7	0.11140	1.2	0.90	1525	34	1654	22	1822	21	84
NG1-seq1-a36	62342	219	67	0.93	32588	0.27155	2.0	4.25175	2.2	0.11356	1.0	0.90	1549	28	1684	19	1857	17	83
NG1-seq1-a37	49620	280	50	0.69	7645	0.16718	2.1	2.63867	2.4	0.11447	1.3	0.85	997	19	1311	18	1872	23	53
NG1-seq1-a38	86579	349	109	0.94	9710	0.27812	1.6	4.36496	1.9	0.11383	1.0	0.85	1582	23	1706	16	1861	18	85
NG1-seq1-a39	129139	333	124	1.00	1271	0.31348	1.8	4.82755	2.0	0.11169	0.8	0.91	1758	28	1790	17	1827	14	**96**
NG1-seq1-a40	3837	66	4	0.89	4590	0.05974	3.3	0.67261	4.7	0.08165	3.3	0.71	374	12	522	19	1237	65	30
NG1-seq1-a41	39720	157	41	0.94	36933	0.22975	3.5	3.44979	3.8	0.10890	1.4	0.93	1333	43	1516	30	1781	26	75
NG1-seq1-a42	23583	52	22	1.09	20359	0.33360	1.9	5.21262	2.4	0.11332	1.5	0.78	1856	31	1855	21	1853	27	**100**
NG1-seq1-a43	67720	243	57	0.99	5993	0.19661	2.0	3.04559	2.2	0.11235	0.9	0.91	1157	22	1419	17	1838	17	63
NG1-seq1-a44	21847	72	24	1.41	13393	0.25879	2.4	4.07625	2.8	0.11424	1.4	0.86	1484	32	1650	23	1868	26	79
NG1-seq1-a45	12614	90	9	1.11	2264	0.08417	3.8	1.26167	4.5	0.10872	2.4	0.84	521	19	829	26	1778	44	29
NG1-seq1-a46	69799	408	48	0.60	6839	0.10385	3.1	1.55236	3.2	0.10841	1.0	0.95	637	19	951	20	1773	18	36
NG1-seq1-a47	25507	46	20	1.13	22170	0.34772	2.0	5.57967	2.7	0.11638	1.8	0.75	1924	33	1913	23	1901	32	**101**
NG1-seq1-a48	59595	139	42	0.81	31383	0.25787	4.5	4.19944	4.6	0.11811	1.2	0.96	1479	60	1674	39	1928	22	77
NG1-seq1-a49	18179	67	17	0.71	4843	0.22317	2.1	2.62356	2.5	0.08526	1.4	0.83	1299	24	1307	19	1321	27	**98**
NG1-seq1-a50	52550	111	47	2.16	46991	0.30391	1.8	4.74645	2.0	0.11327	0.9	0.89	1711	27	1775	17	1853	17	**92**
NG1-seq1-a51	18577	44	16	1.32	16466	0.27631	2.8	4.35979	3.5	0.11444	2.0	0.81	1573	40	1705	29	1871	36	84
NG1-seq1-a52	37294	80	26	1.01	13261	0.25542	2.0	3.98389	2.2	0.11312	0.9	0.92	1466	27	1631	18	1850	16	79
NG1-seq1-a53	65273	509	65	0.76	2192	0.12158	2.7	1.80916	3.0	0.10792	1.4	0.89	740	19	1049	20	1765	25	42
NG1-seq1-a54	34910	75	22	1.16	11924	0.21532	3.2	3.32866	3.4	0.11212	1.1	0.94	1257	36	1488	27	1834	20	69
NG1-seq1-a55	21378	120	16	0.81	2955	0.12793	3.8	1.76220	4.3	0.09990	2.0	0.89	776	28	1032	28	1622	37	48
NG1-seq1-a56	49575	93	33	0.53	44107	0.32567	2.7	5.11080	3.0	0.11382	1.4	0.89	1817	42	1838	26	1861	25	**98**
NG1-seq1-a57	38018	86	28	0.95	15609	0.26251	2.0	4.15298	2.4	0.11474	1.3	0.83	1503	26	1665	20	1876	24	80
NG1-seq1-a58	28553	50	20	0.97	16060	0.33986	2.3	5.29410	2.7	0.11298	1.5	0.84	1886	38	1868	24	1848	27	**102**
NG1-seq1-a59	25041	58	24	1.56	7553	0.32611	2.3	5.02547	3.0	0.11177	2.0	0.76	1819	37	1824	26	1828	36	**100**
NG1-seq1-a60	58544	114	49	1.23	51336	0.33895	2.4	5.38229	2.9	0.11517	1.6	0.83	1882	39	1882	25	1883	29	**100**
NG1-seq2-b01	78072	97	28	0.49	26468	0.25467	2.7	4.07760	2.9	0.11613	1.0	0.94	1463	35	1650	24	1897	18	77
NG1-seq2-b02	14627	36	9	0.48	17592	0.23184	2.5	2.68214	3.4	0.08391	2.4	0.72	1344	30	1324	26	1290	46	**104**
NG1-seq2-b03	142723	170	60	0.36	25299	0.32923	2.3	5.22546	2.6	0.11511	1.2	0.89	1835	37	1857	22	1882	21	**98**
NG1-seq2-b04	52276	172	48	1.43	3950	0.19840	2.2	2.57261	2.6	0.09405	1.5	0.83	1167	23	1293	19	1509	28	77
NG1-seq2-b05	270981	126	79	0.50	23697	0.54250	2.3	14.86811	2.5	0.19877	1.0	0.92	2794	52	2807	24	2816	16	**99**
NG1-seq2-b06	83500	108	46	0.96	73692	0.34158	2.5	5.39457	2.9	0.11454	1.5	0.85	1894	41	1884	25	1873	28	**101**
NG1-seq2-b07	94647	125	54	1.01	41968	0.34244	2.4	5.49081	2.7	0.11629	1.3	0.88	1898	40	1899	24	1900	24	**100**

NG1-seq2-b08	232407	516	150	0.49	8852	0.27796	1.9	4.24789	2.1	0.11084	0.9	0.90	1581	26	1683	17	1813	17	87
NG1-seq2-b09	91682	120	48	0.80	25846	0.33750	2.2	5.32428	2.5	0.11442	1.2	0.88	1875	36	1873	21	1871	21	**100**
NG1-seq2-b10	167861	276	94	0.51	151598	0.31251	1.8	4.81645	2.2	0.11178	1.2	0.83	1753	28	1788	18	1829	22	**96**
NG1-seq2-b11	151336	209	82	0.81	134218	0.33008	2.2	5.18368	2.6	0.11390	1.5	0.82	1839	35	1850	22	1863	27	**99**
NG1-seq2-b12	35715	183	22	0.62	3929	0.11088	6.1	1.28207	6.4	0.08386	1.7	0.96	678	40	838	37	1289	33	53
NG1-seq2-b13	8379	24	7	1.18	2100	0.21879	2.6	2.48003	3.4	0.08221	2.3	0.75	1275	30	1266	25	1251	44	**102**
NG1-seq2-b14	60110	78	37	1.37	52249	0.34156	1.9	5.47054	2.5	0.11616	1.6	0.77	1894	32	1896	22	1898	29	**100**
NG1-seq2-b15	22042	37	14	0.96	3254	0.30876	2.2	4.77678	3.2	0.11220	2.3	0.69	1735	34	1781	27	1835	42	**95**
NG1-seq2-b16	81186	118	43	0.54	40995	0.32369	2.0	4.95033	2.4	0.11092	1.4	0.83	1808	32	1811	21	1815	25	**100**
NG1-seq2-b17	123381	1412	72	0.07	1236	0.04355	2.8	0.53174	3.0	0.08855	1.0	0.94	275	8	433	11	1394	19	20
NG1-seq2-b18	41330	60	24	0.67	28496	0.33748	2.1	5.33153	2.3	0.11458	1.0	0.90	1875	34	1874	20	1873	18	**100**
NG1-seq2-b19	102818	145	59	0.97	28643	0.32779	2.3	5.19075	2.6	0.11485	1.1	0.90	1828	37	1851	22	1878	21	**97**
NG1-seq2-b20	72657	110	43	0.77	19073	0.32779	2.5	5.18363	3.0	0.11469	1.7	0.83	1828	40	1850	26	1875	30	**97**
NG1-seq2-b21	84725	123	51	0.90	30673	0.33881	3.9	5.40940	4.7	0.11579	2.6	0.84	1881	65	1886	41	1892	46	**99**
NG1-seq2-b22	62064	95	44	1.32	55216	0.34738	2.2	5.44526	2.8	0.11369	1.7	0.79	1922	36	1892	24	1859	31	**103**
NG1-seq2-b23	86502	147	53	0.76	898	0.29533	2.7	4.83420	3.0	0.11872	1.2	0.91	1668	40	1791	26	1937	22	86
NG1-seq2-b24	-	-	-	-	-	-	-	-	-	-	-	-	-	-	-	-	-	-	-
NG1-seq2-b25	35346	238	25	1.03	5545	0.07986	3.1	0.90156	3.2	0.08188	0.9	0.96	495	15	653	16	1243	18	40
NG1-seq2-b26	72230	147	42	1.10	12612	0.23082	3.2	3.61320	3.3	0.11353	0.7	0.98	1339	39	1552	27	1857	13	72
NG1-seq2-b27	106340	197	71	0.52	31317	0.34481	1.7	5.53855	2.0	0.11650	1.0	0.86	1910	29	1907	17	1903	18	**100**
NG1-seq2-b28	140179	358	112	0.95	5970	0.28342	2.0	4.44610	2.1	0.11378	0.7	0.94	1609	28	1721	18	1861	13	86
NG1-seq2-b29	103746	164	63	0.60	91059	0.33712	2.4	5.35144	2.8	0.11513	1.6	0.83	1873	38	1877	24	1882	28	**100**
NG1-seq2-b30	76975	149	62	1.52	6693	0.32513	2.9	5.12304	3.3	0.11428	1.6	0.87	1815	46	1840	29	1869	29	**97**
NG1-seq2-b31	80000	146	46	0.66	8991	0.27403	3.5	4.42950	4.2	0.11724	2.2	0.84	1561	49	1718	35	1915	40	82
NG1-seq2-b32	34033	104	36	1.05	5600	0.31315	2.0	4.91436	2.4	0.11382	1.4	0.83	1756	31	1805	21	1861	24	**94**
NG1-seq2-b33	16934	81	20	1.59	1558	0.17086	2.4	1.96425	3.9	0.08338	3.1	0.60	1017	22	1103	27	1278	61	80
NG1-seq2-b34	148030	325	114	0.41	25020	0.33167	2.7	5.25191	2.9	0.11484	1.1	0.93	1846	44	1861	25	1877	19	**98**
NG1-seq2-b35	59062	102	41	1.07	9639	0.32599	2.1	5.07283	2.5	0.11286	1.2	0.87	1819	34	1832	21	1846	22	**99**
NG1-seq2-b36	41730	101	37	0.88	12779	0.31879	2.2	4.92583	2.7	0.11206	1.6	0.80	1784	34	1807	23	1833	29	**97**
NG1-seq2-b37	270040	180	107	0.44	30431	0.51727	2.4	13.09566	2.9	0.18362	1.5	0.85	2688	54	2687	28	2686	25	**100**
NG1-seq2-b38	21815	32	15	1.14	9458	0.39017	2.2	6.21818	2.7	0.11559	1.5	0.83	2124	40	2007	24	1889	27	112
NG1-seq2-b39	57784	230	54	0.65	6410	0.22771	2.3	2.71941	2.7	0.08661	1.3	0.87	1323	28	1334	20	1352	25	**98**
NG1-seq2-b40	71385	163	37	0.51	10142	0.19247	5.3	2.97848	5.6	0.11223	1.5	0.96	1135	56	1402	43	1836	27	62
NG1-seq2-b41	27452	26	12	0.46	21031	0.40429	2.1	7.36855	2.6	0.13219	1.4	0.84	2189	40	2157	23	2127	24	**103**
NG1-seq2-b42	21953	69	15	0.64	2956	0.20645	4.6	2.56225	5.1	0.09001	2.2	0.90	1210	51	1290	38	1426	41	85
NG1-seq2-b43	102453	131	52	0.80	77523	0.33448	2.7	5.24806	2.9	0.11380	1.2	0.92	1860	43	1860	25	1861	21	**100**

NG1-seq2-b44	77654	103	42	0.87	9457	0.33793	3.9	5.40584	4.3	0.11602	1.7	0.92	1877	65	1886	37	1896	30	**99**
NG1-seq2-b45	123322	147	59	0.96	108749	0.32579	2.4	5.14445	2.7	0.11452	1.3	0.88	1818	38	1843	23	1872	23	**97**
NG1-seq2-b46	26051	85	9	1.06	3980	0.08570	2.9	1.36436	3.3	0.11546	1.6	0.87	530	15	874	19	1887	29	28
NG1-seq2-b47	58933	68	26	0.78	54435	0.32594	2.1	4.92094	3.2	0.10950	2.4	0.65	1819	33	1806	27	1791	44	**102**
NG1-seq2-b48	44156	46	18	1.63	11783	0.27048	2.5	4.29497	2.8	0.11517	1.4	0.87	1543	34	1692	24	1882	25	82
NG1-seq2-b49	102364	123	42	0.93	9020	0.31139	1.9	4.90049	2.0	0.11414	0.7	0.94	1748	29	1802	17	1866	12	**94**
NG1-seq2-b50	33477	30	13	1.55	29147	0.32081	1.9	5.13210	2.1	0.11602	1.0	0.89	1794	29	1841	18	1896	17	**95**
NG1-seq2-b51	39850	33	14	0.85	15851	0.34831	2.0	5.65490	2.4	0.11775	1.3	0.83	1927	33	1925	21	1922	24	**100**
NG1-seq2-b52	31787	62	20	1.13	5896	0.29549	2.7	4.71685	3.4	0.11577	2.0	0.80	1669	40	1770	29	1892	36	88
NG1-seq2-b53	46977	48	20	1.32	8510	0.33728	2.3	5.35032	2.5	0.11505	0.9	0.94	1874	38	1877	22	1881	16	**100**
NG1-seq2-b54	17039	52	7	0.76	5491	0.13120	3.7	1.71920	4.1	0.09504	1.7	0.91	795	28	1016	27	1529	33	52
NG1-seq2-b55	155485	121	29	0.71	6565	0.21871	3.7	5.38556	3.8	0.17859	0.8	0.98	1275	43	1883	33	2640	13	48
NG1-seq2-b56	66931	70	22	1.36	7061	0.26409	2.0	4.12585	2.2	0.11331	1.0	0.90	1511	27	1659	18	1853	18	82
NG1-seq2-b57	168998	329	48	0.61	2928	0.13424	2.1	2.16483	2.2	0.11696	0.6	0.96	812	16	1170	15	1910	10	43
NG1-seq2-b58	65045	72	21	0.70	10261	0.27571	2.6	4.32254	2.8	0.11371	1.0	0.93	1570	37	1698	24	1860	19	84
NG1-seq2-b59	127198	117	33	0.42	50013	0.27177	2.3	4.31913	2.4	0.11527	0.9	0.93	1550	31	1697	20	1884	17	82
NG1-seq2-b60	315424	126	65	0.45	47249	0.46458	2.1	10.95351	2.3	0.17100	0.8	0.93	2460	43	2519	21	2567	14	**96**
NG1-seq3-c01	437132	987	158	0.26	2288	0.15391	2.9	3.43131	3.2	0.16169	1.4	0.90	923	25	1512	25	2473	24	37
NG1-seq3-c02	137103	260	77	1.02	25094	0.25286	2.3	3.95262	2.5	0.11337	1.1	0.90	1453	30	1625	21	1854	20	78
NG1-seq3-c03	82763	182	60	1.40	26542	0.27119	2.0	4.07432	2.3	0.10897	1.1	0.88	1547	27	1649	19	1782	20	87
NG1-seq3-c04	121088	208	82	0.99	35769	0.33313	2.5	5.23093	2.7	0.11388	1.0	0.93	1854	40	1858	23	1862	18	**100**
NG1-seq3-c05	111814	193	116	1.16	12340	0.54422	1.7	8.99510	1.9	0.11987	1.0	0.86	2801	38	2338	18	1954	17	143
NG1-seq3-c06	348352	286	139	0.79	157	0.33609	2.0	5.27100	2.4	0.11374	1.4	0.81	1868	32	1864	21	1860	26	**100**
NG1-seq3-c07	145837	931	110	0.12	3043	0.09124	2.3	1.39199	2.6	0.11065	1.1	0.91	563	13	886	15	1810	20	31
NG1-seq3-c08	69783	242	52	0.68	80511	0.20022	1.8	2.40994	2.0	0.08730	1.0	0.88	1176	19	1246	15	1367	18	86
NG1-seq3-c09	48626	137	29	1.09	6558	0.17348	4.4	2.74657	4.5	0.11482	1.1	0.97	1031	42	1341	34	1877	20	55
NG1-seq3-c10	10009	40	8	1.27	1559	0.16954	2.8	2.62396	3.3	0.11225	1.8	0.83	1010	26	1307	25	1836	33	55
NG1-seq3-c11	99174	167	68	1.23	88343	0.33074	2.1	5.15596	2.3	0.11306	1.0	0.90	1842	33	1845	20	1849	18	**100**
NG1-seq3-c12	103307	183	60	0.68	7225	0.29992	1.8	4.88445	1.9	0.11812	0.7	0.94	1691	27	1800	17	1928	12	88
NG1-seq3-c13	283504	296	126	0.81	10309	0.37347	1.7	8.62542	1.8	0.16750	0.5	0.96	2046	30	2299	16	2533	8	81
NG1-seq3-c14	94680	320	61	0.54	5766	0.17369	1.7	2.62855	2.0	0.10976	1.1	0.84	1032	16	1309	15	1795	20	58
NG1-seq3-c15	45699	179	31	0.79	4185	0.15240	2.8	2.38283	3.8	0.11340	2.5	0.75	914	24	1237	27	1855	45	49
NG1-seq3-c16	158880	302	112	0.58	113361	0.33054	3.0	5.32136	3.1	0.11676	0.8	0.96	1841	48	1872	27	1907	15	**97**
NG1-seq3-c17	23123	93	27	1.63	21180	0.20425	2.3	2.31147	2.9	0.08208	1.7	0.79	1198	25	1216	20	1247	34	**96**
NG1-seq3-c18	283433	626	150	0.24	23514	0.23617	2.4	3.89750	5.0	0.11969	4.4	0.48	1367	30	1613	41	1952	78	70
NG1-seq3-c19	49921	153	37	0.97	1768	0.21650	2.6	3.58834	3.3	0.12021	2.0	0.79	1263	29	1547	26	1959	36	64

NG1-seq3-c20	146686	315	105	0.91	35265	0.28739	2.2	4.58091	2.5	0.11560	1.1	0.90	1628	32	1746	21	1889	19	86
NG1-seq3-c21	62237	234	42	0.89	8589	0.15532	2.9	2.42213	3.1	0.11310	1.1	0.93	931	25	1249	22	1850	20	50
NG1-seq3-c22	50187	154	37	0.93	6818	0.22113	2.8	3.40689	3.1	0.11174	1.3	0.91	1288	33	1506	25	1828	24	70
NG1-seq3-c23	21053	145	24	1.41	3818	0.12765	2.1	1.44264	3.0	0.08197	2.0	0.72	774	16	907	18	1245	40	62
NG1-seq3-c24	141185	572	104	0.75	9857	0.16214	1.8	2.52622	2.0	0.11300	1.0	0.88	969	16	1280	15	1848	18	52
NG1-seq3-c25	97114	297	64	0.72	10042	0.19637	3.0	3.16026	3.1	0.11672	0.7	0.97	1156	32	1448	24	1907	13	61
NG1-seq3-c26	108467	299	65	0.64	14278	0.19290	2.1	3.11203	2.4	0.11701	1.2	0.86	1137	22	1436	19	1911	22	60
NG1-seq3-c27	93940	164	66	0.89	36507	0.33284	2.5	5.28364	2.7	0.11513	1.0	0.93	1852	41	1866	23	1882	18	**98**
NG1-seq3-c28	85804	149	56	0.53	74278	0.33716	2.2	5.40707	2.4	0.11631	0.8	0.94	1873	36	1886	21	1900	15	**99**
NG1-seq3-c29	67063	321	72	1.36	12563	0.17734	2.5	2.03067	2.7	0.08305	1.1	0.92	1052	25	1126	19	1270	21	83
NG1-seq3-c30	102983	205	84	1.72	40312	0.30278	1.9	4.70895	2.1	0.11280	0.9	0.90	1705	28	1769	18	1845	17	**92**
NG1-seq3-c31	94327	287	77	1.03	19422	0.20823	5.1	3.20639	6.6	0.11168	4.1	0.78	1219	57	1459	52	1827	74	67
NG1-seq3-c32	109552	243	83	1.03	26492	0.26240	1.9	4.10820	2.5	0.11355	1.5	0.77	1502	25	1656	20	1857	28	81
NG1-seq3-c33	95653	395	78	0.45	7081	0.19261	1.9	3.01282	2.0	0.11345	0.7	0.94	1135	20	1411	15	1855	12	61
NG1-seq3-c34	71868	188	49	0.80	10018	0.22929	2.0	3.66713	2.3	0.11599	1.0	0.90	1331	24	1564	18	1895	17	70
NG1-seq3-c35	69652	362	69	0.58	7005	0.18471	2.1	2.25455	2.2	0.08852	0.8	0.93	1093	21	1198	16	1394	16	78
NG1-seq3-c36	142482	369	104	0.26	12499	0.27973	3.8	4.38877	4.0	0.11379	1.5	0.93	1590	53	1710	34	1861	27	85
NG1-seq3-c37	56496	128	53	1.83	3844	0.31358	1.9	4.79863	2.1	0.11098	0.7	0.94	1758	30	1785	17	1816	13	**97**
NG1-seq3-c38	56422	110	33	1.17	1538	0.22266	2.5	3.45923	3.1	0.11268	1.9	0.80	1296	29	1518	25	1843	34	70
NG1-seq3-c39	361888	259	127	1.18	87	0.30250	2.8	4.46132	5.4	0.10697	4.6	0.51	1704	41	1724	46	1748	85	**97**
NG1-seq3-c40	115484	253	74	1.25	15171	0.24016	1.9	3.75986	2.1	0.11355	0.7	0.94	1388	24	1584	17	1857	13	75
NG1-seq3-c41	35324	128	17	0.97	6229	0.11325	2.5	1.89192	2.9	0.12117	1.4	0.86	692	16	1078	19	1973	26	35
NG1-seq3-c42	116197	182	47	0.45	25103	0.23202	3.3	3.93707	3.5	0.12307	1.2	0.94	1345	41	1621	29	2001	22	67
NG1-seq3-c43	47839	65	23	0.78	17273	0.29626	2.6	4.57038	2.8	0.11189	1.0	0.93	1673	39	1744	24	1830	19	**91**
NG1-seq3-c44	57183	117	34	1.05	9434	0.25960	2.5	3.80091	2.7	0.10619	1.0	0.93	1488	33	1593	22	1735	17	86
NG1-seq3-c45	48159	82	25	2.11	7446	0.22351	2.4	3.54467	2.6	0.11502	1.2	0.89	1300	28	1537	21	1880	22	69
NG1-seq3-c46	55384	113	26	1.41	21538	0.17574	3.9	2.75787	4.2	0.11381	1.3	0.95	1044	38	1344	32	1861	24	56
NG1-seq3-c47	34228	36	17	1.50	29537	0.34290	1.8	5.51773	2.3	0.11671	1.5	0.77	1901	29	1903	20	1906	26	**100**
NG1-seq3-c48	82605	335	30	0.63	3538	0.07855	3.7	1.13197	3.9	0.10451	1.3	0.95	487	17	769	21	1706	23	29
NG1-seq3-c49	42071	90	19	0.66	17526	0.18794	2.6	2.77372	2.9	0.10704	1.3	0.90	1110	27	1348	22	1750	23	63
NG1-seq3-c50	58978	250	31	0.68	4443	0.11939	2.0	1.46865	2.4	0.08922	1.2	0.86	727	14	918	14	1409	23	52
NG1-seq3-c51	102094	101	43	1.07	15670	0.33757	1.9	5.29427	2.4	0.11375	1.4	0.80	1875	31	1868	21	1860	26	**101**
NG1-seq3-c52	261261	147	79	0.60	1112	0.47512	4.7	11.17175	4.8	0.17053	0.8	0.99	2506	99	2538	46	2563	14	**98**
NG1-seq3-c53	81605	121	29	0.89	9285	0.21666	2.1	3.42218	2.4	0.11456	1.2	0.86	1264	24	1510	19	1873	22	67
NG1-seq3-c54	55271	70	26	0.88	15531	0.31893	3.0	4.81171	3.3	0.10942	1.5	0.90	1785	47	1787	28	1790	27	**100**
NG1-seq3-c55	46058	73	17	0.55	10306	0.22676	1.9	3.17304	2.4	0.10149	1.5	0.78	1318	23	1451	19	1651	28	80

NG1-seq3-c56	126483	207	35	0.47	7618	0.15969	2.0	2.54322	2.4	0.11550	1.3	0.85	955	18	1284	17	1888	23	51
NG1-seq3-c57	63245	95	29	1.20	9130	0.26701	2.4	4.13876	2.6	0.11242	1.0	0.92	1526	33	1662	21	1839	19	83
NG1-seq3-c58	-	-	-	-	-	-	-	-	-	-	-	-	-	-	-	-	-	-	-
NG1-seq3-c59	114558	121	35	1.03	10368	0.24880	1.7	3.83196	1.9	0.11171	0.7	0.92	1432	22	1599	15	1827	13	78
NG1-seq3-c60	30004	28	8	1.24	26663	0.22612	3.2	3.53341	3.8	0.11333	1.9	0.86	1314	38	1535	30	1854	35	71
NG1-seq4-d01	55360	182	51	0.84	19379	0.23790	1.9	2.89369	2.3	0.08822	1.3	0.82	1376	24	1380	18	1387	26	**99**
NG1-seq4-d02	62568	172	48	0.94	10560	0.25401	1.8	4.00867	2.1	0.11446	1.1	0.86	1459	24	1636	17	1871	19	78
NG1-seq4-d03	43735	199	45	1.49	4184	0.17775	1.8	2.78934	2.2	0.11381	1.1	0.85	1055	18	1353	16	1861	20	57
NG1-seq4-d04	7647	31	7	1.04	2732	0.19937	2.6	3.11799	3.7	0.11343	2.7	0.71	1172	28	1437	29	1855	48	63
NG1-seq4-d05	63222	126	53	1.94	2320	0.31705	4.5	4.83938	5.7	0.11070	3.5	0.78	1775	70	1792	49	1811	64	**98**
NG1-seq4-d06	14084	26	12	1.61	12490	0.33306	2.2	5.25330	3.3	0.11439	2.5	0.67	1853	36	1861	29	1870	44	**99**
NG1-seq4-d07	36733	68	29	1.22	5661	0.33279	1.9	5.23800	2.4	0.11416	1.5	0.79	1852	30	1859	21	1867	26	**99**
NG1-seq4-d08	89554	167	63	0.91	5558	0.31285	2.0	4.88692	2.3	0.11329	1.2	0.85	1755	30	1800	20	1853	22	**95**
NG1-seq4-d09	37694	141	27	0.67	6948	0.16802	5.4	2.65783	5.6	0.11473	1.6	0.96	1001	50	1317	42	1876	29	53
NG1-seq4-d10	64794	219	46	1.28	3197	0.16581	1.9	2.61477	2.1	0.11438	0.9	0.91	989	17	1305	15	1870	15	53
NG1-seq4-d11	78303	158	57	0.57	19378	0.32348	3.7	5.18763	3.9	0.11631	1.0	0.97	1807	59	1851	34	1900	18	**95**
NG1-seq4-d12	42428	77	29	0.60	18388	0.33088	2.2	5.31746	2.6	0.11655	1.3	0.86	1843	36	1872	22	1904	24	**97**
NG1-seq4-d13	124179	391	80	0.60	9136	0.18823	2.7	2.94146	2.8	0.11334	0.8	0.96	1112	27	1393	21	1854	14	60
NG1-seq4-d14	16857	27	13	1.16	3786	0.37933	1.6	5.97306	2.3	0.11420	1.6	0.71	2073	29	1972	20	1867	29	111
NG1-seq4-d15	38034	171	33	0.86	9678	0.17334	3.6	2.73793	3.8	0.11456	1.2	0.95	1030	34	1339	28	1873	22	55
NG1-seq4-d16	66094	186	45	0.49	8750	0.24301	1.8	3.79596	2.1	0.11329	1.0	0.88	1402	23	1592	17	1853	17	76
NG1-seq4-d17	88549	57	35	0.55	46442	0.53233	2.9	14.12664	3.1	0.19247	1.0	0.95	2751	66	2758	30	2763	16	**100**
NG1-seq4-d18	92107	209	79	0.74	33261	0.33015	2.5	5.27066	2.7	0.11578	1.1	0.91	1839	40	1864	23	1892	20	**97**
NG1-seq4-d19	14566	99	13	0.92	5934	0.12519	2.8	1.44820	3.3	0.08390	1.8	0.84	760	20	909	20	1290	34	59
NG1-seq4-d20	134112	246	90	0.69	65753	0.31835	2.2	5.02368	2.5	0.11445	1.3	0.87	1782	34	1823	22	1871	23	**95**
NG1-seq4-d21	147446	377	119	1.19	914	0.23967	3.3	3.56334	3.4	0.10783	0.8	0.97	1385	41	1541	27	1763	15	79
NG1-seq4-d22	160410	215	86	0.49	63196	0.36152	2.0	8.46951	2.4	0.16991	1.3	0.83	1989	34	2283	22	2557	22	78
NG1-seq4-d23	33802	60	26	1.01	12897	0.34531	1.8	5.52036	2.4	0.11595	1.6	0.76	1912	30	1904	21	1895	28	**101**
NG1-seq4-d24	12325	38	10	1.14	12412	0.21923	4.2	3.03270	4.9	0.10033	2.5	0.86	1278	49	1416	38	1630	47	78
NG1-seq4-d25	128575	256	97	0.88	5382	0.31221	2.1	4.82236	2.4	0.11202	1.1	0.89	1752	33	1789	20	1832	20	**96**
NG1-seq4-d26	146231	141	75	0.57	20881	0.47588	2.2	11.55161	2.4	0.17605	1.0	0.90	2509	45	2569	23	2616	17	**96**
NG1-seq4-d27	66010	115	48	0.85	57016	0.34703	1.7	5.58610	2.2	0.11675	1.3	0.80	1920	29	1914	19	1907	23	**101**
NG1-seq4-d28	116872	433	83	0.31	5749	0.19114	4.2	3.00082	4.3	0.11387	1.0	0.97	1128	43	1408	33	1862	18	61

[a] within-run background-corrected mean ^{207}Pb signal in counts per second

[b] U and Pb content and Th/U ratio were calculated relative to GJ-1 and are accurate to approximately 10%.

[c] corrected for background, mass bias, laser induced U-Pb fractionation and common Pb (if detectable, see analytical method) using Stacey & Kramers (1975) model Pb composition. $^{207}Pb/^{235}U$ calculated using $^{207}Pb/^{206}Pb/(^{238}U/^{206}Pb \times 1/137.88)$. Errors are propagated by quadratic addition of within-run errors (2SE) and the reproducibility of GJ-1 (2SD).

[d] Rho is the error correlation defined as $err^{206}Pb/^{238}U/err^{207}Pb/^{235}U$.

Tab. 3: U-Pb-Th data of zircon from sample NG2, n = 95 of 143 measured zircon grains (90-110 % conc.), quartzite, South Kivu Province, DR Congo

Number	^{207}Pb (cps)	U^a (ppm)	Pb^a (ppm)	$\frac{Th^c}{U}$	$\frac{^{206}Pb}{^{204}Pb}$	$\frac{^{206}Pb^e}{^{238}U}$	2 σ %	$\frac{^{207}Pb^e}{^{235}U}$	2 σ %	$\frac{^{207}Pb^e}{^{206}Pb}$	2 σ %	rho	$\frac{^{206}Pb}{^{238}U}$	2 σ (Ma)	$\frac{^{207}Pb}{^{235}U}$	2 σ (Ma)	$\frac{^{207}Pb}{^{206}Pb}$	2 σ (Ma)	conc %
NG2-seq1-a01	320809	694	200	0.58	45808	0.23717	3.3	4.40563	4.5	0.13473	3.1	0.73	1372	41	1713	38	2160	54	64
NG2-seq1-a02	20980	97	24	1.04	17435	0.19807	3.2	2.15950	3.5	0.07908	1.6	0.89	1165	34	1168	25	1174	32	**99**
NG2-seq1-a03	45354	247	48	0.70	21862	0.18902	3.4	2.03744	3.5	0.07818	0.9	0.97	1116	35	1128	24	1151	18	**97**
NG2-seq1-a04	172631	291	117	0.65	31616	0.36761	2.8	6.52007	3.2	0.12864	1.5	0.88	2018	49	2049	28	2079	27	**97**
NG2-seq1-a05	77687	159	64	0.76	20928	0.33990	2.6	5.23839	4.2	0.11177	3.2	0.64	1886	43	1859	36	1828	58	**103**
NG2-seq1-a06	40312	201	41	0.36	28356	0.19726	2.9	2.13997	3.3	0.07868	1.6	0.88	1161	31	1162	23	1164	31	**100**
NG2-seq1-a07	69742	177	65	0.95	8757	0.30043	2.3	4.28922	3.2	0.10355	2.2	0.72	1693	34	1691	26	1689	40	**100**
NG2-seq1-a08	36398	143	34	0.99	9898	0.22092	1.7	2.44172	2.1	0.08016	1.2	0.81	1287	20	1255	15	1201	24	**107**
NG2-seq1-a09	48277	254	56	1.59	11214	0.20002	1.7	2.23305	2.5	0.08097	1.8	0.69	1175	18	1191	17	1221	35	**96**
NG2-seq1-a10	103543	576	102	0.38	9200	0.16983	2.6	1.89633	2.8	0.08098	1.1	0.91	1011	24	1080	19	1221	23	83
NG2-seq1-a11	24038	116	28	1.40	13483	0.21017	2.7	2.36881	3.1	0.08174	1.6	0.86	1230	30	1233	22	1239	30	**99**
NG2-seq1-a12	20891	98	24	1.38	25188	0.21384	1.7	2.46396	2.1	0.08357	1.2	0.82	1249	19	1262	15	1283	23	**97**
NG2-seq1-a13	67937	163	68	1.85	15268	0.33863	3.2	5.31922	3.6	0.11393	1.7	0.88	1880	52	1872	31	1863	31	**101**
NG2-seq1-a14	79777	449	92	0.78	8281	0.19717	2.4	2.41298	2.6	0.08876	1.0	0.91	1160	25	1246	19	1399	20	83
NG2-seq1-a15	89213	670	96	0.74	14565	0.14255	2.3	1.57931	2.5	0.08035	0.8	0.94	859	19	962	16	1206	16	71
NG2-seq1-a16	45429	208	53	0.35	16969	0.25244	2.5	2.93152	2.7	0.08422	1.0	0.93	1451	32	1390	20	1298	19	112
NG2-seq1-a17	20765	109	24	1.33	5409	0.21109	2.1	2.38245	3.1	0.08186	2.2	0.70	1235	24	1237	22	1242	43	**99**
NG2-seq1-a18	53168	194	53	0.67	59259	0.24402	2.4	3.05097	3.4	0.09068	2.4	0.71	1408	30	1420	26	1440	45	**98**
NG2-seq1-a19	20103	93	19	0.29	6438	0.19610	3.7	2.14986	4.3	0.07951	2.2	0.86	1154	39	1165	31	1185	44	**97**
NG2-seq1-a20	-	-	-	-	-	-	-	-	-	-	-	-	-	-	-	-	-	-	-
NG2-seq1-a21	23729	120	28	1.08	11812	0.21641	2.0	2.51399	2.6	0.08425	1.7	0.77	1263	23	1276	19	1298	33	**97**
NG2-seq1-a22	63355	303	66	0.44	49501	0.21522	1.8	2.43956	2.1	0.08221	1.1	0.86	1257	20	1254	15	1251	21	**100**
NG2-seq1-a23	83639	415	84	0.57	8142	0.19060	2.1	2.17971	2.4	0.08294	1.3	0.86	1125	22	1175	17	1268	24	89
NG2-seq1-a24	46296	238	54	0.63	34683	0.21362	2.4	2.42844	3.2	0.08245	2.1	0.74	1248	27	1251	23	1256	42	**99**
NG2-seq1-a25	93666	586	123	0.54	19280	0.20726	1.9	2.29359	2.2	0.08026	1.0	0.88	1214	21	1210	16	1203	20	**101**
NG2-seq1-a26	56225	498	69	0.41	5511	0.13426	2.7	1.51248	2.9	0.08170	0.9	0.95	812	21	935	18	1238	18	66
NG2-seq1-a27	58759	151	54	0.86	20528	0.32304	2.3	4.83573	3.0	0.10857	1.9	0.77	1805	36	1791	25	1776	34	**102**
NG2-seq1-a28	32459	181	37	0.75	27311	0.20105	1.8	2.21545	2.4	0.07992	1.6	0.75	1181	20	1186	17	1195	32	**99**
NG2-seq1-a29	32957	76	35	1.82	28337	0.33593	4.1	5.45561	5.7	0.11779	3.9	0.72	1867	67	1894	50	1923	70	**97**
NG2-seq1-a30	79805	2725	143	0.14	1107	0.03308	1.9	0.38934	2.1	0.08537	0.7	0.95	210	4	334	6	1324	13	16
NG2-seq1-a31	63714	369	72	1.37	16314	0.19513	2.0	2.17861	2.2	0.08098	1.0	0.88	1149	21	1174	16	1221	21	**94**
NG2-seq1-a32	68051	216	71	0.94	65662	0.29605	2.0	4.24052	2.2	0.10389	0.8	0.93	1672	30	1682	18	1695	15	**99**

NG2-seq1-a33	81804	495	92	0.83	18914	0.16500	2.5	1.92311	2.9	0.08453	1.6	0.83	985	22	1089	20	1305	32	75
NG2-seq1-a34	56546	254	59	0.36	3835	0.21576	2.4	2.48789	2.7	0.08363	1.4	0.87	1259	27	1269	20	1284	26	**98**
NG2-seq1-a35	42603	203	49	0.41	22260	0.22375	3.0	2.55997	4.1	0.08298	2.8	0.74	1302	35	1289	30	1269	54	**103**
NG2-seq1-a36	59436	307	61	0.92	3703	0.17869	6.4	2.65638	7.0	0.10782	2.8	0.91	1060	63	1316	53	1763	52	60
NG2-seq1-a37	39675	591	63	0.35	2093	0.07742	2.8	0.87279	3.7	0.08176	2.4	0.76	481	13	637	17	1240	46	39
NG2-seq1-a38	16763	94	20	1.48	20235	0.18861	1.7	2.11165	3.3	0.08120	2.8	0.53	1114	18	1153	23	1226	55	**91**
NG2-seq1-a39	63943	311	66	0.39	15396	0.21600	2.5	2.38819	2.8	0.08019	1.2	0.90	1261	28	1239	20	1202	24	**105**
NG2-seq1-a40	49574	550	66	0.60	2490	0.11103	3.2	1.29488	3.8	0.08458	2.0	0.85	679	21	843	22	1306	39	52
NG2-seq1-a41	26784	108	29	1.81	9149	0.20885	1.7	2.37791	2.2	0.08258	1.4	0.77	1223	19	1236	16	1259	28	**97**
NG2-seq1-a42	64115	265	57	0.70	16920	0.20670	2.1	2.33001	2.6	0.08175	1.5	0.82	1211	24	1221	19	1240	29	**98**
NG2-seq1-a43	30722	144	30	2.72	16933	0.19315	1.8	2.12034	2.2	0.07962	1.3	0.80	1138	19	1155	15	1188	26	**96**
NG2-seq1-a44	55879	211	45	0.38	11714	0.21154	2.0	2.30955	2.7	0.07918	1.8	0.76	1237	23	1215	19	1177	35	**105**
NG2-seq1-a45	35950	122	28	0.73	20881	0.21360	2.5	2.47757	3.0	0.08412	1.7	0.82	1248	28	1266	22	1295	34	**96**
NG2-seq1-a46	71758	262	55	0.61	42186	0.19973	2.0	2.25798	2.8	0.08199	1.9	0.73	1174	22	1199	20	1245	37	**94**
NG2-seq1-a47	125544	216	63	1.03	114711	0.27250	1.6	4.13998	1.8	0.11019	0.7	0.91	1553	22	1662	15	1803	13	86
NG2-seq1-a48	72129	217	42	0.60	85520	0.18220	2.1	2.13578	2.3	0.08502	0.9	0.92	1079	21	1160	16	1316	17	82
NG2-seq1-a49	44842	148	30	0.94	14605	0.19860	1.6	2.17932	1.8	0.07959	0.9	0.88	1168	17	1174	13	1187	17	**98**
NG2-seq1-a50	22730	75	16	0.80	15485	0.21050	2.1	2.30200	3.2	0.07931	2.4	0.66	1231	24	1213	23	1180	47	**104**
NG2-seq1-a51	77232	140	49	1.13	35978	0.28867	2.3	3.99066	2.8	0.10026	1.6	0.82	1635	34	1632	23	1629	30	**100**
NG2-seq1-a52	6965	25	5	4.19	2234	0.16554	2.1	1.80068	3.0	0.07889	2.1	0.70	987	19	1046	20	1169	42	84
NG2-seq1-a53	68236	295	55	0.21	5121	0.15818	2.1	1.78709	2.5	0.08194	1.4	0.84	947	19	1041	16	1244	26	76
NG2-seq1-a54	65578	84	30	0.90	60158	0.31890	2.6	4.83367	2.8	0.10993	1.1	0.92	1784	41	1791	24	1798	20	**99**
NG2-seq1-a55	22442	56	13	1.05	26958	0.21607	1.7	2.50004	2.1	0.08392	1.2	0.82	1261	20	1272	15	1291	24	**98**
NG2-seq1-a56	55100	169	26	0.67	12096	0.15088	2.2	1.60943	2.8	0.07737	1.8	0.77	906	18	974	18	1131	36	80
NG2-seq1-a57	15746	38	8	0.42	8485	0.19672	2.5	2.12609	3.1	0.07838	1.8	0.82	1158	27	1157	22	1157	35	**100**
NG2-seq1-a58	43671	130	21	0.83	10760	0.15886	1.8	1.76358	2.2	0.08052	1.2	0.84	950	16	1032	14	1210	23	79
NG2-seq1-a59	46432	101	21	0.43	40766	0.20616	3.1	2.30223	3.4	0.08099	1.2	0.93	1208	35	1213	24	1221	24	**99**
NG2-seq1-a60	27451	24	10	0.91	7584	0.33374	2.2	5.35449	2.9	0.11636	1.9	0.74	1856	35	1878	25	1901	35	**98**
NG2-seq2-b01	27116	87	19	1.64	16861	0.20868	1.9	2.31663	2.5	0.08052	1.6	0.75	1222	21	1217	18	1210	32	**101**
NG2-seq2-b02	171473	823	138	0.13	1874	0.12014	5.9	1.32161	7.0	0.07978	3.9	0.84	731	41	855	42	1192	76	61
NG2-seq2-b03	36507	91	20	0.64	17438	0.20866	3.6	2.34671	4.0	0.08157	1.9	0.88	1222	40	1227	29	1235	38	**99**
NG2-seq2-b04	51160	162	39	0.81	46129	0.22580	2.9	2.62319	3.1	0.08426	1.0	0.94	1312	34	1307	23	1298	19	**101**
NG2-seq2-b05	39796	97	26	0.53	46146	0.23659	2.0	2.84620	2.5	0.08725	1.4	0.82	1369	25	1368	19	1366	27	**100**
NG2-seq2-b06	31187	124	29	1.79	15348	0.18807	2.1	2.04699	2.5	0.07894	1.3	0.84	1111	21	1131	17	1171	26	**95**
NG2-seq2-b07	64340	85	34	1.66	59711	0.33916	2.0	5.09040	2.3	0.10886	1.3	0.83	1883	32	1835	20	1780	24	**106**
NG2-seq2-b08	167472	992	119	0.10	4597	0.10930	5.4	1.18567	5.8	0.07868	2.2	0.93	669	34	794	32	1164	43	57

NG2-seq2-b09	29391	116	24	0.80	14187	0.20067	1.8	2.18392	2.2	0.07893	1.3	0.81	1179	19	1176	15	1170	25	**101**
NG2-seq2-b10	57444	213	51	1.44	15091	0.18277	2.1	2.06913	2.5	0.08211	1.4	0.84	1082	21	1139	18	1248	27	87
NG2-seq2-b11	77004	402	57	0.68	104222	0.12828	3.6	1.32275	4.0	0.07479	1.7	0.90	778	26	856	23	1063	35	73
NG2-seq2-b12	21027	71	15	0.43	9256	0.19581	1.9	2.18832	2.5	0.08105	1.5	0.79	1153	21	1177	17	1223	30	**94**
NG2-seq2-b13	15155	59	13	0.98	5337	0.20448	2.0	2.28757	2.5	0.08114	1.6	0.78	1199	22	1208	18	1225	31	**98**
NG2-seq2-b14	18873	68	14	0.36	23356	0.20285	3.3	2.29130	4.2	0.08192	2.6	0.79	1191	36	1210	30	1244	51	**96**
NG2-seq2-b15	12029	34	10	1.03	1245	0.24952	3.4	3.11439	5.1	0.09052	3.8	0.66	1436	43	1436	40	1437	72	**100**
NG2-seq2-b16	65656	137	46	0.97	48948	0.29624	2.4	4.30580	2.6	0.10542	1.0	0.92	1673	35	1694	22	1722	19	**97**
NG2-seq2-b17	50653	210	43	0.61	13640	0.19430	1.9	2.14264	2.2	0.07998	1.1	0.87	1145	20	1163	16	1196	22	**96**
NG2-seq2-b18	22888	82	17	4.08	2391	0.15507	2.8	2.30714	3.2	0.10791	1.5	0.88	929	24	1214	23	1764	28	53
NG2-seq2-b19	91766	166	52	1.27	15702	0.25881	3.8	4.04637	4.1	0.11339	1.4	0.94	1484	51	1644	34	1854	26	80
NG2-seq2-b20	16217	54	14	0.85	19244	0.22696	2.5	2.67168	3.2	0.08538	2.0	0.78	1319	30	1321	24	1324	38	**100**
NG2-seq2-b21	52026	118	39	1.09	5371	0.29975	2.8	4.37419	3.7	0.10584	2.5	0.74	1690	41	1707	31	1729	46	**98**
NG2-seq2-b22	49797	340	48	1.20	5420	0.12993	2.2	1.51903	2.5	0.08479	1.2	0.88	787	17	938	16	1311	23	60
NG2-seq2-b23	39233	142	34	0.61	45823	0.22971	2.1	2.74591	3.2	0.08670	2.5	0.64	1333	25	1341	24	1354	48	**98**
NG2-seq2-b24	340271	1247	298	0.15	143	0.11892	3.0	1.14070	3.9	0.06957	2.5	0.76	724	20	773	21	916	52	79
NG2-seq2-b25	28544	139	26	1.31	16362	0.17747	2.0	1.97574	2.3	0.08074	1.3	0.84	1053	19	1107	16	1215	25	87
NG2-seq2-b26	54872	291	51	0.85	12424	0.17150	1.7	1.89987	2.0	0.08035	1.0	0.87	1020	16	1081	13	1206	19	85
NG2-seq2-b27	90632	492	79	0.57	108696	0.15210	2.1	1.77064	2.7	0.08443	1.7	0.78	913	18	1035	18	1303	33	70
NG2-seq2-b28	52140	283	54	0.58	15207	0.19368	1.9	2.09921	2.3	0.07861	1.4	0.80	1141	20	1149	16	1162	28	**98**
NG2-seq2-b29	99685	242	86	1.11	9040	0.29883	2.5	4.36416	2.9	0.10592	1.4	0.87	1685	37	1706	24	1730	26	**97**
NG2-seq2-b30	25888	132	29	0.80	32812	0.20382	1.9	2.24324	2.3	0.07982	1.3	0.82	1196	20	1195	16	1193	26	**100**
NG2-seq2-b31	55422	364	50	0.85	12245	0.12762	2.4	1.43349	2.8	0.08146	1.4	0.85	774	17	903	17	1233	28	63
NG2-seq2-b32	49545	261	56	0.75	53169	0.19842	2.1	2.20890	2.4	0.08074	1.2	0.87	1167	23	1184	17	1215	23	**96**
NG2-seq2-b33	25911	92	27	1.09	27576	0.25981	2.2	3.40895	2.8	0.09516	1.7	0.78	1489	29	1506	22	1531	33	**97**
NG2-seq2-b34	142716	399	108	0.61	17967	0.25654	2.2	4.02190	2.6	0.11370	1.5	0.83	1472	29	1639	22	1859	27	79
NG2-seq2-b35	17375	79	21	1.36	5479	0.22444	2.1	2.56174	3.1	0.08278	2.2	0.69	1305	25	1290	23	1264	43	**103**
NG2-seq2-b36	46212	278	54	0.78	9091	0.19323	1.9	2.10101	2.2	0.07886	1.2	0.85	1139	20	1149	16	1169	23	**97**
NG2-seq2-b37	56347	236	59	0.72	9407	0.23234	2.4	2.76798	2.9	0.08640	1.6	0.83	1347	29	1347	22	1347	31	**100**
NG2-seq2-b38	34386	158	35	0.93	5634	0.21207	1.7	2.46246	2.0	0.08421	1.0	0.87	1240	20	1261	15	1298	20	**96**
NG2-seq2-b39	38885	184	37	0.36	8664	0.19159	2.3	2.03934	2.5	0.07720	1.0	0.92	1130	24	1129	17	1126	19	**100**
NG2-seq2-b40	44546	215	45	1.20	11365	0.19305	1.9	2.09682	2.1	0.07877	0.9	0.89	1138	19	1148	14	1166	19	**98**
NG2-seq2-b41	26564	119	27	1.28	32890	0.21077	1.9	2.37324	2.5	0.08166	1.6	0.77	1233	21	1235	18	1237	31	**100**
NG2-seq2-b42	51767	190	47	1.19	1654	0.21856	2.3	2.74257	3.2	0.09101	2.2	0.73	1274	27	1340	24	1447	42	88
NG2-seq2-b43	157250	706	134	0.19	7960	0.17721	3.5	2.17105	4.5	0.08886	2.8	0.77	1052	34	1172	32	1401	54	75
NG2-seq2-b44	41490	179	38	0.97	11219	0.19505	2.4	2.06394	2.6	0.07675	1.0	0.92	1149	25	1137	18	1115	20	**103**

NG2-seq2-b45	36477	123	33	1.63	8555	0.21258	1.9	2.51376	2.6	0.08576	1.8	0.74	1243	22	1276	19	1333	34	**93**
NG2-seq2-b46	52941	202	37	0.67	15973	0.16975	2.6	1.83965	3.1	0.07860	1.7	0.83	1011	24	1060	21	1162	34	87
NG2-seq2-b47	71176	134	36	0.81	14104	0.26021	2.8	4.02976	3.3	0.11232	1.7	0.86	1491	38	1640	27	1837	30	81
NG2-seq2-b48	38198	66	25	1.42	10767	0.30275	2.4	4.56403	3.4	0.10934	2.4	0.70	1705	35	1743	29	1788	44	**95**
NG2-seq2-b49	81450	143	47	0.84	46408	0.29340	1.9	4.11894	2.2	0.10182	1.1	0.88	1658	28	1658	18	1658	19	**100**
NG2-seq2-b50	43245	113	25	0.55	5791	0.21701	2.4	2.50150	2.7	0.08360	1.2	0.90	1266	28	1272	20	1283	23	**99**
NG2-seq2-b51	91946	139	52	1.24	20346	0.32424	2.2	5.13217	2.4	0.11480	0.8	0.94	1810	35	1841	20	1877	15	**96**
NG2-seq2-b52	47367	77	29	2.85	7520	0.28378	2.1	4.51006	2.4	0.11527	1.2	0.86	1610	30	1733	21	1884	22	85
NG2-seq2-b53	85040	399	58	0.24	5251	0.13361	2.5	1.48291	3.2	0.08049	1.9	0.80	808	19	923	19	1209	38	67
NG2-seq2-b54	15754	53	12	1.54	4619	0.20434	2.1	2.27541	2.8	0.08076	1.7	0.78	1199	24	1205	20	1216	34	**99**
NG2-seq2-b55	30659	80	17	1.21	16361	0.19731	1.7	2.13640	2.5	0.07853	1.8	0.69	1161	18	1161	17	1160	36	**100**
NG2-seq2-b56	11420	33	7	0.71	4121	0.19972	2.8	2.17707	3.5	0.07906	2.1	0.80	1174	30	1174	25	1174	42	**100**
NG2-seq2-b57	30922	73	19	1.06	12295	0.21643	2.6	2.50777	2.9	0.08404	1.3	0.89	1263	29	1274	21	1293	25	**98**
NG2-seq2-b58	76145	164	38	1.13	15467	0.23096	2.9	3.13095	3.8	0.09832	2.4	0.77	1340	36	1440	30	1593	45	84
NG2-seq2-b59	40345	94	21	0.84	6775	0.21711	3.9	2.56503	5.0	0.08569	3.0	0.79	1267	45	1291	37	1331	59	**95**
NG2-seq2-b60	41078	22	13	0.79	86	0.34982	3.5	13.35640	20.2	0.27691	19.9	0.17	1934	58	2705	212	3346	312	58
NG2-seq3-c01	22620	125	27	0.68	6802	0.21008	2.0	2.35988	3.1	0.08147	2.3	0.65	1229	22	1231	22	1233	46	**100**
NG2-seq3-c02	42754	293	57	0.60	10754	0.19202	3.1	2.06931	3.5	0.07816	1.6	0.89	1132	32	1139	24	1151	32	**98**
NG2-seq3-c03	27340	173	38	1.36	10409	0.20527	2.2	2.27062	3.0	0.08023	2.0	0.74	1204	24	1203	22	1203	40	**100**
NG2-seq3-c04	76759	783	128	0.20	4209	0.14258	6.4	1.63038	6.5	0.08293	1.0	0.99	859	52	982	42	1268	20	68
NG2-seq3-c05	7660	39	11	0.93	2745	0.28903	2.5	3.56841	5.1	0.08954	4.4	0.49	1637	36	1543	41	1416	85	116
NG2-seq3-c06	39387	248	49	0.34	44329	0.19362	2.6	2.11725	3.1	0.07931	1.7	0.83	1141	27	1154	22	1180	34	**97**
NG2-seq3-c07	87266	339	91	0.30	23503	0.26099	1.9	3.39792	2.5	0.09442	1.6	0.76	1495	26	1504	20	1517	31	**99**
NG2-seq3-c08	24175	150	33	3.15	5687	0.19259	1.6	2.16305	2.0	0.08146	1.2	0.81	1135	17	1169	14	1233	23	**92**
NG2-seq3-c09	49710	318	63	0.65	8782	0.17671	3.3	1.95014	4.0	0.08004	2.3	0.82	1049	32	1098	27	1198	46	88
NG2-seq3-c10	43998	279	60	0.49	17981	0.21336	2.6	2.45063	3.2	0.08330	1.8	0.83	1247	30	1258	23	1276	35	**98**
NG2-seq3-c11	85717	1101	116	0.16	1450	0.09522	5.7	1.18616	6.1	0.09035	2.1	0.94	586	32	794	34	1433	41	41
NG2-seq3-c12	63010	186	66	0.84	6329	0.32796	3.4	5.08067	4.1	0.11236	2.1	0.85	1828	55	1833	35	1838	39	**99**
NG2-seq3-c13	55241	394	72	0.63	8059	0.18914	2.4	2.20266	2.6	0.08446	1.0	0.93	1117	25	1182	19	1303	19	86
NG2-seq3-c14	39838	150	56	2.47	2065	0.23722	2.0	3.58808	3.3	0.10970	2.6	0.60	1372	25	1547	27	1794	48	76
NG2-seq3-c15	24812	138	35	1.14	7755	0.23204	1.7	2.75674	2.1	0.08617	1.2	0.82	1345	21	1344	16	1342	23	**100**
NG2-seq3-c16	4046	44	6	4.17	2428	0.08822	3.5	0.92870	4.9	0.07635	3.5	0.70	545	18	667	24	1104	70	49
NG2-seq3-c17	41513	260	59	0.63	24301	0.20827	2.7	2.38766	3.0	0.08314	1.4	0.89	1220	30	1239	22	1273	27	**96**
NG2-seq3-c18	6394	34	9	1.52	3159	0.24993	4.9	3.11199	6.2	0.09030	3.8	0.79	1438	63	1436	49	1432	73	**100**
NG2-seq3-c19	35444	228	48	0.90	9311	0.20450	1.8	2.28513	2.2	0.08104	1.4	0.79	1199	19	1208	16	1222	27	**98**
NG2-seq3-c20	84951	603	123	0.58	8985	0.18877	2.1	2.05522	2.6	0.07896	1.6	0.79	1115	21	1134	18	1171	32	**95**

NG2-seq3-c21	68975	728	113	0.37	6503	0.14484	2.0	1.67786	4.2	0.08402	3.8	0.47	872	16	1000	27	1293	73	67
NG2-seq3-c22	17050	126	27	0.98	21460	0.19832	1.9	2.19430	2.6	0.08025	1.7	0.75	1166	20	1179	18	1203	33	**97**
NG2-seq3-c23	34158	278	57	1.04	9255	0.19482	2.4	2.13744	2.6	0.07957	1.1	0.90	1147	25	1161	18	1186	23	**97**

[a] within-run background-corrected mean ^{207}Pb signal in counts per second

[b] U and Pb content and Th/U ratio were calculated relative to GJ-1 and are accurate to approximately 10%.

[c] corrected for background, mass bias, laser induced U-Pb fractionation and common Pb (if detectable, see analytical method) using Stacey & Kramers (1975) model Pb composition. $^{207}Pb/^{235}U$ calculated using $^{207}Pb/^{206}Pb/(^{238}U/^{206}Pb \times 1/137.88)$. Errors are propagated by quadratic addition of within-run errors (2SE) and the reproducibility of GJ-1 (2SD).

[d] Rho is the error correlation defined as $err^{206}Pb/^{238}U/err^{207}Pb/^{235}U$.

Tab. 4: U-Pb-Th data of zircon from sample NG3, n = 106 of 152 measured zircon grains (90-110 % conc.), quartzite, South Kivu Province, DR Congo

Number	^{207}Pb (cps)	U^{a} (ppm)	Pb^{a} (ppm)	$\frac{Th^{c}}{U}$	$\frac{^{206}Pb}{^{204}Pb}$	$\frac{^{206}Pb^{e}}{^{238}U}$	2 σ %	$\frac{^{207}Pb^{e}}{^{235}U}$	2 σ %	$\frac{^{207}Pb^{e}}{^{206}Pb}$	2 σ %	rho	$\frac{^{206}Pb}{^{238}U}$	2 σ (Ma)	$\frac{^{207}Pb}{^{235}U}$	2 σ (Ma)	$\frac{^{207}Pb}{^{206}Pb}$	2 σ (Ma)
NG3-seq1-a01	59813	107	40	0.86	52731	0.32022	2.8	5.04319	3.0	0.11422	1.0	0.94	1791	44	1827	26	1868	19
NG3-seq1-a02	163214	314	103	0.55	145935	0.29890	2.0	4.65767	2.2	0.11302	0.9	0.92	1686	30	1760	18	1848	15
NG3-seq1-a03	34273	62	22	0.58	8782	0.32317	2.6	5.15889	3.1	0.11578	1.6	0.86	1805	42	1846	26	1892	28
NG3-seq1-a04	18214	34	15	1.45	3324	0.34320	2.7	5.50957	3.3	0.11643	1.8	0.83	1902	45	1902	28	1902	32
NG3-seq1-a05	25741	51	19	0.75	23801	0.31636	2.4	4.77039	3.2	0.10936	2.1	0.75	1772	37	1780	27	1789	38
NG3-seq1-a06	14570	74	17	1.31	3653	0.19946	2.2	2.20686	2.8	0.08025	1.6	0.81	1172	24	1183	19	1203	32
NG3-seq1-a07	46695	95	33	0.96	41599	0.29189	3.4	4.57015	3.5	0.11356	0.9	0.96	1651	49	1744	30	1857	17
NG3-seq1-a08	57413	145	46	1.49	20900	0.23942	3.4	3.87726	3.8	0.11745	1.6	0.91	1384	43	1609	31	1918	28
NG3-seq1-a09	21297	44	18	1.40	18835	0.31582	2.2	4.94222	2.7	0.11350	1.5	0.83	1769	34	1809	23	1856	27
NG3-seq1-a10	16766	32	13	1.10	10779	0.33233	2.7	5.21351	3.1	0.11378	1.5	0.88	1850	44	1855	27	1861	27
NG3-seq1-a11	57507	127	44	0.80	51068	0.30437	2.5	4.75670	2.8	0.11334	1.2	0.90	1713	38	1777	24	1854	22
NG3-seq1-a12	27963	144	40	2.19	11760	0.19839	2.3	2.21285	2.7	0.08090	1.3	0.87	1167	25	1185	19	1219	26
NG3-seq1-a13	63767	147	60	1.29	55919	0.31884	2.4	5.05905	2.7	0.11508	1.1	0.90	1784	38	1829	23	1881	21
NG3-seq1-a14	144215	399	108	0.73	3956	0.23836	2.9	3.67603	3.2	0.11185	1.4	0.89	1378	36	1566	26	1830	26
NG3-seq1-a15	18324	39	17	1.36	16127	0.32594	2.9	5.16908	3.8	0.11502	2.4	0.78	1819	46	1848	33	1880	43
NG3-seq1-a16	112460	257	89	0.52	99741	0.31939	2.4	5.01795	2.5	0.11395	0.9	0.94	1787	37	1822	21	1863	16
NG3-seq1-a17	10695	41	11	0.92	6412	0.23549	3.0	2.89659	3.6	0.08921	1.9	0.84	1363	37	1381	27	1409	37
NG3-seq1-a18	79929	186	74	1.09	57799	0.32118	2.7	5.04354	2.9	0.11389	1.0	0.94	1795	42	1827	25	1862	18
NG3-seq1-a19	31080	63	24	0.82	16806	0.33875	2.3	5.65113	2.7	0.12099	1.4	0.85	1881	38	1924	24	1971	25
NG3-seq1-a20	87376	206	76	0.71	78771	0.32489	2.6	5.01900	2.8	0.11204	1.0	0.94	1814	42	1823	24	1833	17
NG3-seq1-a21	21152	57	21	1.24	11528	0.32318	2.1	5.05968	2.4	0.11355	1.2	0.88	1805	33	1829	20	1857	21
NG3-seq1-a22	50566	127	56	1.54	34248	0.33121	2.3	5.19243	2.6	0.11370	1.2	0.88	1844	38	1851	23	1859	22
NG3-seq1-a23	69987	218	75	0.84	25629	0.29417	2.2	4.32457	2.6	0.10662	1.4	0.83	1662	32	1698	22	1742	26
NG3-seq1-a24	59802	158	69	1.78	11921	0.32341	2.4	5.25460	2.8	0.11784	1.4	0.86	1806	38	1862	24	1924	26
NG3-seq1-a25	27411	68	31	2.03	16032	0.31991	2.5	5.46642	2.9	0.12393	1.4	0.87	1789	39	1895	25	2014	25
NG3-seq1-a26	31474	77	31	0.95	10387	0.33292	3.0	5.27828	3.6	0.11499	2.0	0.83	1853	48	1865	31	1880	36
NG3-seq1-a27	140948	437	134	0.61	12272	0.27103	2.3	4.23026	2.8	0.11320	1.6	0.83	1546	32	1680	23	1851	28
NG3-seq1-a28	47966	119	42	0.85	24454	0.31300	3.3	5.39675	3.9	0.12505	2.0	0.86	1755	51	1884	34	2030	35
NG3-seq1-a29	51213	138	58	1.31	17043	0.32682	2.3	5.13832	3.0	0.11403	1.9	0.77	1823	37	1842	26	1865	35
NG3-seq1-a30	134743	744	162	0.52	3907	0.19313	2.2	3.07075	2.5	0.11532	1.2	0.88	1138	23	1425	20	1885	21
NG3-seq1-a31	61942	175	71	1.13	22938	0.33401	2.5	5.31428	2.8	0.11540	1.3	0.89	1858	41	1871	25	1886	24
NG3-seq1-a32	46339	302	72	0.89	48939	0.20650	2.3	2.36453	2.7	0.08305	1.4	0.85	1210	26	1232	20	1270	28

NG3-seq1-a33	46427	138	55	0.96	25197	0.33453	2.7	5.22467	3.1	0.11327	1.5	0.87	1860	44	1857	27	1853	27
NG3-seq1-a34	30767	202	48	0.76	8936	0.21011	2.6	2.41195	3.2	0.08326	1.8	0.82	1229	29	1246	23	1275	36
NG3-seq1-a35	24302	80	31	1.13	2745	0.31660	3.3	4.77061	4.0	0.10929	2.1	0.85	1773	52	1780	34	1788	38
NG3-seq1-a36	60717	185	73	0.95	39951	0.32828	2.6	5.24399	2.8	0.11586	1.1	0.92	1830	41	1860	24	1893	20
NG3-seq1-a37	35654	102	35	0.57	26366	0.31929	2.9	5.07515	3.3	0.11528	1.7	0.86	1786	45	1832	29	1884	31
NG3-seq1-a38	58130	168	51	0.39	22415	0.28266	2.2	4.55589	2.8	0.11690	1.8	0.77	1605	31	1741	24	1909	32
NG3-seq1-a39	58621	178	64	1.04	12665	0.31368	2.0	4.80043	2.3	0.11099	1.1	0.89	1759	31	1785	19	1816	19
NG3-seq1-a40	6583	39	11	2.07	7347	0.21441	2.4	2.48899	3.3	0.08419	2.3	0.73	1252	28	1269	24	1297	44
NG3-seq1-a41	109044	307	103	0.58	31591	0.30464	2.4	4.78634	2.7	0.11395	1.3	0.87	1714	36	1783	23	1863	24
NG3-seq1-a42	14151	84	21	1.08	11893	0.21142	2.2	2.35947	3.0	0.08094	2.0	0.74	1236	25	1230	21	1220	39
NG3-seq1-a43	81194	200	76	0.90	34046	0.31843	2.7	4.96645	3.0	0.11312	1.4	0.89	1782	42	1814	26	1850	25
NG3-seq1-a44	40548	235	55	1.03	2198	0.20899	2.7	2.33181	3.1	0.08092	1.5	0.88	1223	30	1222	22	1220	29
NG3-seq1-a45	11935	42	9	0.74	2629	0.20408	3.1	3.10895	3.8	0.11049	2.2	0.81	1197	34	1435	30	1807	40
NG3-seq1-a46	4605	10	6	3.13	1899	0.32647	3.1	5.12613	4.1	0.11388	2.8	0.74	1821	49	1840	36	1862	51
NG3-seq1-a47	23271	87	24	0.76	17269	0.23912	2.0	2.91478	2.9	0.08841	2.0	0.71	1382	25	1386	22	1391	38
NG3-seq1-a48	23545	50	21	1.28	13022	0.33542	2.9	5.25791	3.2	0.11369	1.4	0.89	1865	47	1862	28	1859	26
NG3-seq1-a49	43232	91	34	1.01	12182	0.31667	2.3	5.07253	2.6	0.11617	1.3	0.88	1773	36	1832	22	1898	23
NG3-seq1-a50	59322	119	39	0.39	29528	0.31596	2.3	4.95672	2.7	0.11378	1.5	0.85	1770	36	1812	23	1861	26
NG3-seq1-a51	43636	263	49	1.23	7653	0.14910	3.7	1.71144	4.2	0.08325	2.0	0.88	896	31	1013	27	1275	40
NG3-seq1-a52	27337	64	20	1.10	11494	0.25080	2.9	3.87478	3.5	0.11205	1.9	0.83	1443	37	1608	28	1833	35
NG3-seq1-a53	24586	59	23	1.67	21662	0.31488	2.4	4.97677	2.8	0.11463	1.5	0.84	1765	36	1815	24	1874	27
NG3-seq1-a54	67889	127	51	0.91	20072	0.33130	2.8	5.21320	3.0	0.11412	1.0	0.94	1845	45	1855	26	1866	18
NG3-seq1-a55	21345	92	23	1.33	13704	0.18464	2.9	2.10121	3.3	0.08254	1.7	0.85	1092	29	1149	23	1258	34
NG3-seq1-a56	42011	76	30	0.74	27450	0.33741	2.8	5.32697	3.2	0.11450	1.5	0.88	1874	46	1873	28	1872	27
NG3-seq1-a57	19410	85	19	0.99	22790	0.19223	2.4	2.22994	2.8	0.08413	1.5	0.84	1133	25	1190	20	1296	30
NG3-seq1-a58	9429	17	6	0.83	8325	0.32859	2.6	5.19045	3.2	0.11456	1.9	0.81	1832	42	1851	28	1873	35
NG3-seq1-a59	34765	66	25	0.99	27394	0.31935	2.5	5.09907	3.0	0.11580	1.6	0.84	1787	39	1836	25	1892	29
NG3-seq1-a60	60248	111	43	0.91	25646	0.32332	2.5	5.06598	2.7	0.11364	1.1	0.91	1806	39	1830	23	1858	20
NG3-seq2-b01	55645	109	47	1.34	18107	0.32446	2.4	5.11229	2.8	0.11428	1.4	0.86	1811	38	1838	24	1868	25
NG3-seq2-b02	207899	361	148	0.42	158231	0.39107	2.7	7.13790	2.9	0.13238	1.0	0.94	2128	50	2129	26	2130	18
NG3-seq2-b03	191052	679	140	0.77	2370	0.17800	2.5	2.72861	2.9	0.11118	1.5	0.86	1056	25	1336	22	1819	27
NG3-seq2-b04	54280	158	39	0.51	3602	0.23505	1.9	3.17793	4.6	0.09806	4.2	0.41	1361	23	1452	36	1588	78
NG3-seq2-b05	52692	109	43	1.13	19312	0.31839	2.3	5.05487	2.6	0.11515	1.3	0.87	1782	36	1829	22	1882	23
NG3-seq2-b06	40955	87	32	0.78	36058	0.32286	2.9	5.09788	3.3	0.11452	1.5	0.89	1804	46	1836	28	1872	27
NG3-seq2-b07	41126	233	40	0.88	4159	0.16043	2.7	1.89934	3.0	0.08586	1.4	0.89	959	24	1081	20	1335	27
NG3-seq2-b08	51478	109	43	1.29	11310	0.29813	1.8	4.66709	2.4	0.11354	1.6	0.76	1682	27	1761	20	1857	28

NG3-seq2-b09	83898	181	63	0.46	55170	0.32017	2.2	4.99651	2.5	0.11318	1.1	0.89	1791	34	1819	21	1851	21
NG3-seq2-b10	63702	139	60	1.28	55768	0.34177	2.1	5.39061	2.5	0.11439	1.2	0.87	1895	35	1883	21	1870	22
NG3-seq2-b11	100566	716	107	0.80	2658	0.12877	2.2	1.55432	2.5	0.08754	1.1	0.89	781	16	952	16	1373	22
NG3-seq2-b12	79057	78	48	1.51	12618	0.40366	3.2	11.33359	3.8	0.20363	2.1	0.84	2186	60	2551	37	2856	34
NG3-seq2-b13	71651	157	57	0.57	33068	0.33069	2.2	5.40521	2.4	0.11855	0.9	0.92	1842	35	1886	20	1934	16
NG3-seq2-b14	48172	258	45	1.14	4762	0.16257	1.8	1.96607	2.0	0.08771	0.9	0.90	971	17	1104	14	1376	17
NG3-seq2-b15	136960	300	128	1.44	12423	0.32889	2.1	5.27440	2.5	0.11631	1.3	0.85	1833	34	1865	22	1900	24
NG3-seq2-b16	43897	95	39	1.05	37864	0.33353	2.5	5.37223	2.7	0.11682	1.0	0.92	1855	41	1880	24	1908	19
NG3-seq2-b17	66124	174	47	0.56	24698	0.24731	2.6	3.78186	3.0	0.11091	1.5	0.86	1425	33	1589	24	1814	27
NG3-seq2-b18	55372	125	55	1.61	48640	0.33145	2.0	5.24329	2.4	0.11473	1.2	0.85	1845	32	1860	20	1876	22
NG3-seq2-b19	60973	133	55	1.35	21064	0.32065	2.3	5.09494	2.6	0.11524	1.1	0.90	1793	36	1835	22	1884	21
NG3-seq2-b20	58274	139	52	0.96	14414	0.33609	2.2	5.46393	2.4	0.11791	1.1	0.89	1868	35	1895	21	1925	20
NG3-seq2-b21	29652	170	47	1.94	11450	0.19187	3.7	2.26354	5.1	0.08556	3.5	0.73	1132	39	1201	37	1328	67
NG3-seq2-b22	79819	186	60	0.14	69303	0.32425	2.4	5.13546	2.7	0.11487	1.2	0.89	1810	39	1842	24	1878	22
NG3-seq2-b23	109538	351	77	1.27	3832	0.16589	2.9	2.65044	3.7	0.11588	2.3	0.79	989	27	1315	28	1894	41
NG3-seq2-b24	114051	340	122	0.51	8028	0.34072	2.9	5.51101	3.2	0.11731	1.5	0.89	1890	47	1902	28	1916	27
NG3-seq2-b25	66167	459	95	1.30	7621	0.15614	3.3	1.74688	3.6	0.08114	1.3	0.93	935	29	1026	23	1225	26
NG3-seq2-b26	162446	563	163	0.83	7103	0.26434	2.3	4.07002	2.6	0.11167	1.0	0.92	1512	32	1648	21	1827	19
NG3-seq2-b27	195387	1072	161	0.46	1484	0.13814	2.5	2.07652	3.1	0.10902	1.8	0.81	834	20	1141	22	1783	33
NG3-seq2-b28	9411	21	8	0.88	3782	0.34427	2.5	5.55629	3.1	0.11705	1.9	0.78	1907	41	1909	27	1912	35
NG3-seq2-b29	76211	197	71	0.76	31104	0.31764	2.1	5.07105	2.5	0.11579	1.3	0.86	1778	33	1831	21	1892	23
NG3-seq2-b30	50237	125	51	1.39	28698	0.31784	2.4	5.04716	2.9	0.11517	1.5	0.85	1779	38	1827	24	1883	27
NG3-seq2-b31	9092	46	11	0.96	3817	0.21156	2.2	2.40113	3.0	0.08231	2.0	0.75	1237	25	1243	22	1253	39
NG3-seq2-b32	83492	222	86	1.18	73989	0.32292	2.3	5.06445	2.8	0.11374	1.6	0.81	1804	36	1830	24	1860	29
NG3-seq2-b33	127541	331	114	0.43	108940	0.31879	2.1	5.18966	2.4	0.11807	1.3	0.85	1784	32	1851	21	1927	23
NG3-seq2-b34	57393	169	60	0.73	18931	0.32099	2.3	5.05250	2.8	0.11416	1.6	0.81	1795	35	1828	24	1867	30
NG3-seq2-b35	160734	764	157	0.88	2629	0.19048	2.9	2.83249	3.4	0.10785	1.9	0.84	1124	30	1364	26	1763	34
NG3-seq2-b36	34676	97	36	1.30	29723	0.29920	3.2	4.85321	3.6	0.11764	1.7	0.88	1687	47	1794	31	1921	31
NG3-seq2-b37	121567	336	107	0.58	17142	0.30483	1.9	4.69990	2.1	0.11182	0.9	0.91	1715	28	1767	17	1829	16
NG3-seq2-b38	37790	98	34	1.25	5380	0.26902	3.0	4.11383	3.5	0.11091	1.8	0.85	1536	41	1657	29	1814	33
NG3-seq2-b39	75168	170	61	1.04	15754	0.29132	2.4	4.62689	2.7	0.11519	1.3	0.88	1648	35	1754	23	1883	24
NG3-seq2-b40	7624	15	7	1.51	1478	0.33582	2.5	5.41767	3.1	0.11701	1.8	0.82	1867	41	1888	27	1911	32
NG3-seq2-b41	39643	87	28	0.54	13643	0.29722	2.5	4.60651	2.7	0.11241	1.0	0.92	1678	37	1750	23	1839	19
NG3-seq2-b42	39710	81	31	1.18	34604	0.30842	2.2	4.85743	2.7	0.11422	1.6	0.81	1733	33	1795	23	1868	28
NG3-seq2-b43	38638	74	30	0.99	13732	0.33496	2.2	5.17457	2.7	0.11204	1.6	0.82	1862	36	1848	23	1833	29
NG3-seq2-b44	44440	79	32	1.33	23294	0.32706	1.8	5.16654	2.2	0.11457	1.1	0.86	1824	29	1847	19	1873	20

NG3-seq2-b45	44217	72	33	1.54	19544	0.33663	2.1	5.42882	2.6	0.11696	1.5	0.82	1870	35	1889	23	1910	27
NG3-seq2-b46	15542	56	13	1.05	13734	0.20809	2.7	2.36994	3.1	0.08260	1.5	0.87	1219	30	1234	23	1260	30
NG3-seq2-b47	36176	52	20	0.88	4437	0.32640	1.9	5.14952	2.3	0.11442	1.2	0.85	1821	31	1844	19	1871	21
NG3-seq2-b48	97437	225	56	0.96	6932	0.22447	2.3	3.46520	2.4	0.11196	0.9	0.93	1305	27	1519	19	1831	17
NG3-seq2-b49	156542	276	66	0.23	7682	0.23405	2.6	3.68160	2.9	0.11408	1.4	0.88	1356	32	1567	24	1865	25
NG3-seq2-b50	53206	75	28	0.97	2712	0.31385	2.3	4.91760	2.7	0.11364	1.5	0.84	1760	35	1805	23	1858	26
NG3-seq2-b51	37604	49	19	0.91	10093	0.32118	2.9	5.05768	3.2	0.11421	1.4	0.90	1795	45	1829	28	1867	26
NG3-seq2-b52	82277	109	43	0.96	69873	0.32552	2.7	5.03433	3.1	0.11217	1.6	0.87	1817	43	1825	27	1835	29
NG3-seq2-b53	51096	78	20	0.53	6017	0.23531	3.4	3.63896	3.6	0.11216	1.0	0.96	1362	42	1558	29	1835	18
NG3-seq2-b54	64205	82	29	0.65	18695	0.31748	2.4	4.99812	2.9	0.11418	1.6	0.83	1777	38	1819	25	1867	29
NG3-seq2-b55	175251	221	64	0.71	3212	0.24808	2.6	4.41611	2.8	0.12911	1.2	0.91	1429	33	1715	24	2086	21
NG3-seq2-b56	44475	115	24	0.54	21414	0.19539	2.7	2.28623	3.2	0.08486	1.8	0.83	1150	28	1208	23	1312	35
NG3-seq2-b57	30450	36	13	1.04	12309	0.28636	2.2	4.57133	2.7	0.11578	1.7	0.79	1623	31	1744	23	1892	30
NG3-seq2-b58	185512	251	62	0.67	6138	0.21980	2.7	3.57723	3.3	0.11803	1.9	0.83	1281	32	1544	26	1927	33
NG3-seq2-b59	79500	82	30	0.54	28901	0.33329	2.6	5.18081	2.9	0.11274	1.3	0.89	1854	42	1849	25	1844	24
NG3-seq2-b60	25003	25	10	1.11	8029	0.32888	2.3	5.28880	2.9	0.11663	1.7	0.80	1833	37	1867	25	1905	31
NG3-seq3-c01	46378	112	45	1.07	14660	0.31757	2.7	5.16064	3.0	0.11786	1.4	0.89	1778	42	1846	26	1924	25
NG3-seq3-c02	104686	273	99	0.80	32533	0.31378	2.1	4.96179	2.5	0.11469	1.4	0.83	1759	32	1813	22	1875	25
NG3-seq3-c03	10529	29	9	1.77	1554	0.25931	2.5	4.07082	3.1	0.11386	1.8	0.82	1486	34	1648	26	1862	32
NG3-seq3-c04	46990	84	36	0.54	3740	0.39621	2.8	6.04933	3.2	0.11073	1.5	0.89	2152	52	1983	28	1811	27
NG3-seq3-c05	111996	279	96	0.41	47164	0.32116	1.9	4.95784	2.2	0.11196	1.0	0.89	1795	30	1812	18	1832	18
NG3-seq3-c06	46403	452	40	1.39	1701	0.07862	3.9	1.08475	4.0	0.10007	0.8	0.98	488	18	746	21	1625	16
NG3-seq3-c07	42560	107	40	0.90	6847	0.31480	1.6	4.88197	2.1	0.11248	1.3	0.79	1764	25	1799	18	1840	23
NG3-seq3-c08	50956	142	57	1.30	45094	0.33448	1.9	5.23281	2.2	0.11347	1.0	0.88	1860	31	1858	19	1856	19
NG3-seq3-c09	52153	145	51	0.75	22568	0.31125	2.4	4.81429	3.5	0.11218	2.6	0.68	1747	37	1787	30	1835	47
NG3-seq3-c10	42994	105	43	1.06	12251	0.33070	2.3	5.11237	2.9	0.11212	1.8	0.79	1842	36	1838	25	1834	32
NG3-seq3-c11	99143	179	79	0.79	26468	0.38025	1.6	6.99525	2.0	0.13342	1.2	0.79	2077	28	2111	18	2143	21
NG3-seq3-c12	26209	115	27	0.78	4795	0.22926	1.8	3.01095	2.2	0.09525	1.2	0.83	1331	22	1410	17	1533	23
NG3-seq3-c13	70582	181	72	1.01	61850	0.32743	2.2	5.17471	2.7	0.11462	1.6	0.81	1826	34	1848	23	1874	28
NG3-seq3-c14	62687	261	62	0.70	3116	0.21019	3.4	3.26155	3.8	0.11254	1.6	0.91	1230	39	1472	30	1841	29
NG3-seq3-c15	19167	54	19	0.39	4835	0.32347	2.5	5.02362	3.3	0.11264	2.2	0.75	1807	39	1823	28	1842	39
NG3-seq3-c16	36978	101	39	1.19	5601	0.33206	2.4	5.31780	2.6	0.11615	1.1	0.90	1848	38	1872	23	1898	20
NG3-seq3-c17	31602	81	32	0.81	10024	0.33705	2.3	5.31044	2.6	0.11427	1.3	0.87	1872	37	1871	23	1868	23
NG3-seq3-c18	7993	50	15	2.50	9932	0.20048	1.9	2.23419	3.1	0.08083	2.5	0.61	1178	20	1192	22	1217	48
NG3-seq3-c19	8962	29	10	1.22	3116	0.28854	2.1	4.31337	3.2	0.10842	2.4	0.66	1634	31	1696	27	1773	44
NG3-seq3-c20	9791	37	13	2.32	6048	0.29562	1.8	4.45663	2.9	0.10934	2.3	0.62	1670	27	1723	25	1788	42

NG3-seq3-c21	11629	30	16	2.88	4043	0.32765	2.3	5.19435	2.9	0.11498	1.8	0.78	1827	36	1852	25	1880	33
NG3-seq3-c22	50657	134	53	1.01	28170	0.32219	2.1	5.07258	2.5	0.11419	1.4	0.83	1800	33	1832	22	1867	25
NG3-seq3-c23	67096	450	84	0.87	3411	0.15859	2.3	1.80548	2.8	0.08257	1.5	0.83	949	20	1047	18	1259	30
NG3-seq3-c24	42995	112	43	0.68	16573	0.33749	2.2	5.28039	2.8	0.11348	1.6	0.81	1875	36	1866	24	1856	30
NG3-seq3-c25	58379	161	55	0.46	44651	0.32034	2.2	5.10869	2.6	0.11566	1.4	0.84	1791	34	1838	22	1890	25
NG3-seq3-c26	57330	162	62	0.99	51323	0.31382	1.9	4.85648	2.6	0.11224	1.7	0.76	1760	30	1795	22	1836	30
NG3-seq3-c27	85170	287	83	0.81	16624	0.26718	1.8	4.20866	2.1	0.11424	1.0	0.87	1526	25	1676	17	1868	19
NG3-seq3-c28	25838	73	24	1.77	7201	0.26024	1.8	4.07569	2.2	0.11359	1.2	0.84	1491	24	1649	18	1858	21
NG3-seq3-c29	83437	252	120	2.26	28463	0.31663	2.2	4.95477	2.6	0.11349	1.3	0.85	1773	34	1812	22	1856	24
NG3-seq3-c30	112596	358	101	0.70	7148	0.26527	2.0	4.13547	2.2	0.11307	1.0	0.89	1517	27	1661	18	1849	19
NG3-seq3-c31	51329	136	52	0.85	43884	0.31753	2.5	5.10193	3.0	0.11653	1.7	0.83	1778	39	1836	26	1904	30
NG3-seq3-c32	20828	75	21	1.36	7913	0.22678	4.4	3.57375	4.7	0.11429	1.8	0.93	1318	52	1544	38	1869	32

[a] within-run background-corrected mean ^{207}Pb signal in counts per second

[b] U and Pb content and Th/U ratio were calculated relative to GJ-1 and are accurate to approximately 10%.

[c] corrected for background, mass bias, laser induced U-Pb fractionation and common Pb (if detectable, see analytical method) using Stacey & Kramers (1975) model Pb composition. $^{207}Pb/^{235}U$ calculated using $^{207}Pb/^{206}Pb/(^{238}U/^{206}Pb \times 1/137.88)$. Errors are propagated by quadratic addition of within-run errors (2SE) and the reproducibility of GJ-1 (2SD).

[d] Rho is the error correlation defined as $err^{206}Pb/^{238}U/err^{207}Pb/^{235}U$.

conc %
96
91
95
100
99
97
89
72
95
99
92
96
95
75
97
96
97
96
95
99
97
99
95
94
89
99
84
86
98
60
98
95

100
96
99
97
95
84
97
97
92
101
96
100
66
98
99
100
93
95
70
79
94
99
87
100
87
98
94
97
97
100
58
86
95
96
72
91

97
101
57
77
95
71
96
97
79
98
95
97
85
96
52
99
76
83
47
100
94
95
99
97
93
96
64
88
94
85
88
98
91
93
102
97

98
97
97
71
73
95
96
99
74
95
68
88
86
66
101
96
92
94
80
119
98
30
96
100
95
100
97
87
97
67
98
97
100
97
92
93

97
96
75
101
95
96
82
80
96
82
93
71

Tab. 5: U-Pb-Th data of zircon from sample NG4, n = 53 of 115 measured zircon grains (90-110 % conc.), quartzite, South Kivu Province, DR Congo

Number	^{207}Pb (cps)	U^a (ppm)	Pb^a (ppm)	$\frac{Th^c}{U}$	$\frac{^{206}Pb}{^{204}Pb}$	$\frac{^{206}Pb^e}{^{238}U}$	2 σ %	$\frac{^{207}Pb^e}{^{235}U}$	2 σ %	$\frac{^{207}Pb^e}{^{206}Pb}$	2 σ %	rho	$\frac{^{206}Pb}{^{238}U}$	2 σ (Ma)	$\frac{^{207}Pb}{^{235}U}$	2 σ (Ma)	$\frac{^{207}Pb}{^{206}Pb}$	2 σ (Ma)	conc %
NG4-seq1-a01	45576	87	33	1.19	14364	0.33515	1.8	5.56885	2.3	0.12051	1.4	0.79	1863	29	1911	20	1964	25	**95**
NG4-seq1-a02	-	-	-	-	-	-	-	-	-	-	-	-	-	-	-	-	-	-	-
NG4-seq1-a03	13855	82	6	2.36	3085	0.06412	4.0	0.81589	5.5	0.09229	3.8	0.72	401	15	606	26	1473	73	27
NG4-seq1-a04	-	-	-	-	-	-	-	-	-	-	-	-	-	-	-	-	-	-	-
NG4-seq1-a05	37038	353	38	0.95	8434	0.10037	3.9	1.13049	4.7	0.08169	2.5	0.85	617	23	768	25	1238	48	50
NG4-seq1-a06	29120	145	33	1.87	31500	0.18917	3.2	2.15535	3.9	0.08263	2.2	0.82	1117	33	1167	27	1261	44	89
NG4-seq1-a07	32735	127	30	2.20	38738	0.22333	3.0	2.63817	3.4	0.08568	1.6	0.88	1299	35	1311	25	1331	32	**98**
NG4-seq1-a08	39519	90	29	1.43	16017	0.27579	3.7	4.10035	4.1	0.10783	1.7	0.91	1570	52	1654	34	1763	31	89
NG4-seq1-a09	33581	115	24	0.33	41129	0.20468	2.3	2.32634	3.0	0.08243	1.9	0.77	1200	25	1220	21	1256	37	**96**
NG4-seq1-a10	23324	60	16	0.77	8866	0.24401	2.1	3.10528	2.5	0.09230	1.3	0.85	1408	27	1434	19	1474	25	**96**
NG4-seq1-a11	10490	36	11	2.16	12420	0.22262	2.0	2.57677	2.8	0.08395	1.9	0.72	1296	24	1294	21	1291	38	**100**
NG4-seq1-a12	40668	177	37	1.19	48596	0.18557	2.2	2.16336	2.6	0.08455	1.4	0.84	1097	22	1169	18	1305	28	84
NG4-seq1-a13	35658	158	32	0.38	15931	0.20618	2.8	2.26725	3.1	0.07975	1.3	0.91	1208	31	1202	22	1191	25	**101**
NG4-seq1-a14	65063	733	47	0.52	7782	0.06413	2.7	0.72804	3.2	0.08234	1.7	0.85	401	11	555	14	1254	34	32
NG4-seq1-a15	11165	118	16	2.47	3085	0.12028	6.9	1.35415	7.4	0.08165	2.7	0.93	732	48	869	44	1237	54	59
NG4-seq1-a16	15714	26	14	2.13	6618	0.47133	3.4	5.45100	4.1	0.08388	2.3	0.83	2489	71	1893	36	1290	45	193
NG4-seq1-a17	25774	127	25	0.76	9377	0.19190	1.8	2.10236	2.2	0.07946	1.3	0.80	1132	18	1150	15	1184	26	**96**
NG4-seq1-a18	26793	368	27	0.48	7286	0.06582	2.5	0.73184	2.9	0.08065	1.4	0.87	411	10	558	13	1213	28	34
NG4-seq1-a19	46993	299	39	1.03	11320	0.11832	2.1	1.32476	2.8	0.08120	1.9	0.74	721	14	857	16	1226	37	59
NG4-seq1-a20	21058	247	39	1.14	2826	0.16004	6.0	1.85214	7.0	0.08394	3.6	0.86	957	54	1064	47	1291	70	74
NG4-seq1-a21	40736	229	50	0.87	7496	0.20580	4.1	2.28007	4.5	0.08035	1.8	0.91	1206	45	1206	32	1206	36	**100**
NG4-seq1-a22	20115	85	19	0.95	10158	0.20294	1.9	2.27570	2.4	0.08133	1.6	0.77	1191	20	1205	17	1229	31	**97**
NG4-seq1-a23	91555	301	77	0.74	69217	0.24081	2.8	3.21186	3.3	0.09673	1.7	0.85	1391	35	1460	26	1562	33	89
NG4-seq1-a24	42281	59	30	1.61	3972	0.38369	2.7	7.23110	3.0	0.13669	1.5	0.87	2093	48	2140	28	2186	26	**96**
NG4-seq1-a25	16613	79	14	1.86	9772	0.13261	5.0	1.73804	5.5	0.09506	2.3	0.91	803	38	1023	36	1529	43	52
NG4-seq1-a26	17602	113	22	1.13	22938	0.19244	3.1	2.06827	3.7	0.07795	1.9	0.85	1135	32	1138	25	1146	38	**99**
NG4-seq1-a27	2981	45	6	1.94	2852	0.10935	19.7	2.51018	72.1	0.16649	69.4	0.27	669	126	1275	736	2523	1165	27
NG4-seq1-a28	45220	258	43	1.24	7206	0.16123	3.0	2.26212	3.5	0.10176	1.8	0.85	964	27	1201	25	1656	34	58
NG4-seq1-a29	45262	211	45	0.43	19652	0.20909	2.3	2.40173	2.6	0.08331	1.3	0.87	1224	25	1243	19	1276	26	**96**
NG4-seq1-a30	76537	537	144	0.73	10794	0.27569	1.7	3.38053	2.1	0.08893	1.2	0.82	1570	24	1500	17	1403	23	112
NG4-seq1-a31	26040	107	22	0.38	18459	0.20481	1.9	2.26668	2.6	0.08027	1.7	0.74	1201	21	1202	18	1204	34	**100**
NG4-seq1-a32	67530	1212	55	0.15	5846	0.04218	5.9	0.53787	6.3	0.09249	2.2	0.94	266	15	437	23	1477	41	18

NG4-seq1-a33	75744	198	45	1.05	67354	0.17441	3.3	2.72584	3.5	0.11335	1.2	0.94	1036	32	1336	27	1854	22	56
NG4-seq1-a34	15346	51	15	2.11	663	0.19868	18.8	5.15806	75.2	0.18829	72.8	0.25	1168	204	1846	1010	2727	1200	43
NG4-seq1-a35	9345	88	16	0.87	12304	0.16576	42.6	1.87320	59.0	0.08196	40.8	0.72	989	403	1072	493	1245	800	79
NG4-seq1-a36	-	-	-	-	-	-	-	-	-	-	-	-	-	-	-	-	-	-	-
NG4-seq1-a37	-	-	-	-	-	-	-	-	-	-	-	-	-	-	-	-	-	-	-
NG4-seq1-a38	-	-	-	-	-	-	-	-	-	-	-	-	-	-	-	-	-	-	-
NG4-seq1-a39	37823	345	16	1.04	47198	0.03395	12.2	0.37890	12.3	0.08095	1.0	1.00	215	26	326	35	1220	21	18
NG4-seq1-a40	13802	84	13	1.23	9408	0.15602	2.0	1.76771	2.9	0.08217	2.1	0.68	935	17	1034	19	1250	42	75
NG4-seq1-a41	29280	94	23	0.51	15048	0.22993	1.9	2.72340	2.3	0.08591	1.3	0.81	1334	22	1335	17	1336	26	**100**
NG4-seq1-a42	27091	98	20	1.91	6207	0.20228	2.5	3.07206	2.8	0.11015	1.3	0.89	1188	27	1426	22	1802	24	66
NG4-seq1-a43	33077	146	23	0.14	31994	0.16499	2.5	1.80533	2.9	0.07936	1.4	0.87	984	23	1047	19	1181	29	83
NG4-seq1-a44	42747	140	29	0.41	14543	0.20145	2.5	2.23920	2.9	0.08062	1.5	0.85	1183	27	1193	20	1212	30	**98**
NG4-seq1-a45	21731	73	20	1.72	20172	0.20346	2.3	2.26198	2.7	0.08063	1.4	0.85	1194	25	1201	19	1212	28	**98**
NG4-seq1-a46	42539	81	28	1.01	40071	0.31378	2.6	4.64198	3.0	0.10730	1.4	0.88	1759	41	1757	25	1754	26	**100**
NG4-seq1-a47	51602	359	38	0.85	5252	0.10068	2.2	1.18469	2.5	0.08535	1.1	0.90	618	13	793	14	1323	21	47
NG4-seq1-a48	39014	70	20	0.60	41265	0.26801	2.0	3.53042	2.6	0.09554	1.5	0.80	1531	28	1534	20	1539	29	**99**
NG4-seq1-a49	23974	58	14	0.89	28885	0.22408	2.2	2.59371	2.6	0.08395	1.5	0.83	1303	26	1299	19	1291	28	**101**
NG4-seq1-a50	30299	57	19	1.60	31815	0.26270	2.4	3.48519	2.7	0.09622	1.3	0.88	1504	32	1524	22	1552	25	**97**
NG4-seq1-a51	17796	62	13	1.19	22725	0.19763	2.4	2.15827	2.8	0.07920	1.5	0.86	1163	26	1168	20	1177	29	**99**
NG4-seq1-a52	27701	46	13	0.49	9489	0.27150	2.6	3.58621	3.0	0.09580	1.5	0.87	1548	36	1546	24	1544	28	**100**
NG4-seq1-a53	57878	209	45	0.78	5534	0.20883	4.4	2.37936	5.3	0.08263	2.9	0.83	1223	49	1236	39	1261	57	**97**
NG4-seq1-a54	100503	115	50	1.44	88374	0.33871	2.7	5.36660	3.0	0.11491	1.3	0.91	1880	45	1880	26	1879	23	**100**
NG4-seq1-a55	15740	121	9	2.02	19047	0.06627	5.3	0.76305	5.7	0.08351	2.0	0.93	414	21	576	25	1281	39	32
NG4-seq1-a56	30659	55	15	0.75	18550	0.23720	2.0	2.86991	2.5	0.08775	1.4	0.83	1372	25	1374	19	1377	27	**100**
NG4-seq1-a57	3979	25	3	1.50	5068	0.10359	6.5	1.13032	7.5	0.07914	3.7	0.87	635	39	768	41	1176	74	54
NG4-seq1-a58	25914	71	13	0.82	32763	0.17117	2.6	1.88639	3.2	0.07993	1.9	0.81	1019	25	1076	22	1195	37	85
NG4-seq1-a59	11749	25	5	0.88	14946	0.16565	1.9	1.81504	2.9	0.07947	2.2	0.66	988	18	1051	19	1184	43	83
NG4-seq1-a60	19706	47	8	1.50	17405	0.15383	15.7	2.36849	15.9	0.11167	2.8	0.98	922	136	1233	120	1827	52	50
NG4-seq2-b01	8257	68	7	2.79	7444	0.09528	3.5	1.47100	4.0	0.11197	1.9	0.88	587	20	919	24	1832	35	32
NG4-seq2-b02	216139	219	119	0.71	119834	0.47607	2.4	11.95275	2.8	0.18209	1.5	0.85	2510	50	2601	27	2672	24	**94**
NG4-seq2-b03	32165	68	30	1.69	28182	0.32724	2.5	5.19819	2.8	0.11521	1.3	0.88	1825	40	1852	24	1883	24	**97**
NG4-seq2-b04	86079	163	67	0.64	642	0.38741	2.0	6.82525	2.8	0.12777	1.9	0.72	2111	37	2089	25	2068	34	**102**
NG4-seq2-b05	-	-	-	-	-	-	-	-	-	-	-	-	-	-	-	-	-	-	-
NG4-seq2-b06	77335	218	59	0.97	21665	0.22235	7.6	3.46111	7.8	0.11290	1.4	0.98	1294	90	1518	63	1847	25	70
NG4-seq2-b07	23365	123	24	0.34	13477	0.19848	2.9	2.18473	4.3	0.07983	3.2	0.66	1167	31	1176	31	1193	64	**98**
NG4-seq2-b08	36572	539	40	0.88	6630	0.06668	2.4	0.74800	3.0	0.08136	1.8	0.80	416	10	567	13	1230	35	34

NG4-seq2-b09	22462	142	27	0.62	11386	0.19471	2.1	2.14408	2.9	0.07986	1.9	0.73	1147	22	1163	20	1194	38	**96**
NG4-seq2-b10	53469	117	42	0.77	11545	0.35561	2.3	6.21044	2.5	0.12666	1.0	0.91	1961	39	2006	22	2052	18	**96**
NG4-seq2-b11	31896	186	36	0.98	5491	0.17993	2.7	2.10668	2.9	0.08492	1.2	0.92	1067	27	1151	20	1314	23	81
NG4-seq2-b12	16861	79	19	1.01	8773	0.23106	2.6	2.74469	2.9	0.08615	1.4	0.87	1340	31	1341	22	1342	28	**100**
NG4-seq2-b13	6180	32	7	0.83	4184	0.19320	2.7	2.08611	3.7	0.07831	2.6	0.72	1139	28	1144	26	1155	51	**99**
NG4-seq2-b14	51164	294	61	0.49	63721	0.20340	3.3	2.26583	3.5	0.08079	1.1	0.95	1194	36	1202	25	1216	21	**98**
NG4-seq2-b15	18281	183	20	0.99	8631	0.10777	2.6	1.22549	3.4	0.08247	2.2	0.76	660	16	812	19	1257	43	52
NG4-seq2-b16	35754	199	31	0.65	12208	0.14603	4.4	1.65839	5.1	0.08236	2.6	0.86	879	37	993	33	1254	51	70
NG4-seq2-b17	4351	10	4	1.73	3981	0.32290	2.4	4.90923	3.8	0.11027	2.9	0.63	1804	38	1804	32	1804	53	**100**
NG4-seq2-b18	28101	179	23	0.51	33959	0.12486	5.1	1.43945	5.3	0.08361	1.5	0.96	759	36	905	32	1283	29	59
NG4-seq2-b19	8036	25	8	0.87	8328	0.27715	2.5	3.63827	3.8	0.09521	2.8	0.66	1577	35	1558	30	1532	53	**103**
NG4-seq2-b20	38415	102	39	1.16	15854	0.31440	1.9	4.62655	2.3	0.10673	1.3	0.84	1762	30	1754	20	1744	23	**101**
NG4-seq2-b21	14891	77	17	0.60	18770	0.20528	2.1	2.26654	2.7	0.08008	1.7	0.77	1204	23	1202	19	1199	33	**100**
NG4-seq2-b22	39315	105	28	0.76	491	0.19376	6.9	2.27379	7.7	0.08511	3.3	0.90	1142	73	1204	56	1318	65	87
NG4-seq2-b23	32448	88	32	1.27	11882	0.29583	3.2	4.32907	3.7	0.10613	1.7	0.88	1671	48	1699	31	1734	31	**96**
NG4-seq2-b24	38550	157	41	0.75	23681	0.23898	2.6	3.20024	3.2	0.09712	1.9	0.81	1381	33	1457	25	1570	35	88
NG4-seq2-b25	19840	68	21	0.69	21002	0.27873	2.0	3.66347	2.6	0.09532	1.6	0.78	1585	28	1563	21	1534	30	**103**
NG4-seq2-b26	8776	43	9	0.41	10545	0.21143	2.1	2.45101	2.8	0.08408	1.9	0.73	1236	23	1258	21	1294	38	**96**
NG4-seq2-b27	41528	292	42	0.92	49854	0.13751	3.3	1.59503	4.1	0.08413	2.5	0.80	831	25	968	26	1295	48	64
NG4-seq2-b28	18832	132	20	0.74	4460	0.14315	6.6	1.62715	7.5	0.08244	3.5	0.89	862	54	981	48	1256	68	69
NG4-seq2-b29	52205	177	45	1.22	18005	0.23773	3.3	3.75655	3.5	0.11461	1.0	0.96	1375	41	1584	28	1874	18	73
NG4-seq2-b30	13208	59	17	2.67	1848	0.21287	7.7	3.73668	15.5	0.12731	13.5	0.50	1244	88	1579	132	2061	237	60
NG4-seq2-b31	21338	164	28	0.72	22966	0.16763	3.4	2.12821	6.2	0.09208	5.2	0.55	999	31	1158	44	1469	99	68
NG4-seq2-b32	36320	235	55	0.87	43353	0.22573	3.3	2.63247	4.1	0.08458	2.5	0.80	1312	39	1310	31	1306	49	**100**
NG4-seq2-b33	21455	60	23	1.25	3334	0.31266	2.4	4.72387	3.0	0.10958	1.8	0.80	1754	36	1771	25	1792	33	**98**
NG4-seq2-b34	41603	270	57	0.85	20121	0.20196	1.9	2.31045	2.4	0.08297	1.4	0.81	1186	21	1216	17	1269	27	**93**
NG4-seq2-b35	31818	364	53	1.44	7440	0.13862	2.4	1.61704	2.7	0.08460	1.2	0.89	837	19	977	17	1306	24	64
NG4-seq2-b36	14866	141	24	1.13	18881	0.17106	2.0	1.87213	2.7	0.07937	1.8	0.75	1018	19	1071	18	1181	35	86
NG4-seq2-b37	32260	195	42	0.36	16555	0.21307	2.3	2.35828	2.6	0.08027	1.3	0.86	1245	26	1230	19	1204	26	**103**
NG4-seq2-b38	50259	341	59	0.67	25978	0.16859	4.8	2.02348	5.3	0.08705	2.1	0.92	1004	45	1123	36	1362	41	74
NG4-seq2-b39	3963	23	5	0.83	4490	0.19968	23.3	2.82758	37.9	0.10270	29.8	0.62	1174	255	1363	333	1674	552	70
NG4-seq2-b40	54500	480	68	1.03	5059	0.12990	3.7	1.40098	3.9	0.07822	1.3	0.94	787	28	889	24	1152	26	68
NG4-seq2-b41	27541	169	32	0.74	3721	0.18860	2.1	2.18134	2.8	0.08388	1.9	0.74	1114	21	1175	20	1290	37	86
NG4-seq2-b42	26483	87	21	0.25	6811	0.24334	2.5	3.09237	3.3	0.09217	2.2	0.75	1404	31	1431	25	1471	41	**95**
NG4-seq2-b43	53146	92	32	1.03	23489	0.28007	2.4	4.47499	2.6	0.11589	1.1	0.92	1592	34	1726	22	1894	19	84
NG4-seq2-b44	21575	94	18	0.36	6604	0.19090	3.0	2.09179	3.5	0.07947	1.9	0.85	1126	31	1146	25	1184	37	**95**

NG4-seq2-b45	60387	112	44	1.10	19029	0.34664	2.6	5.46249	3.4	0.11429	2.1	0.78	1919	44	1895	29	1869	38	**103**
NG4-seq2-b46	72706	137	62	0.55	63819	0.44316	2.6	7.02683	2.8	0.11500	1.0	0.93	2365	51	2115	25	1880	19	126
NG4-seq2-b47	21510	92	18	0.82	27762	0.18383	2.2	1.96629	3.4	0.07758	2.5	0.66	1088	23	1104	23	1136	50	**96**
NG4-seq2-b48	18495	72	15	0.88	22588	0.20552	2.4	2.34241	2.8	0.08266	1.4	0.86	1205	27	1225	20	1261	28	**96**
NG4-seq2-b49	26103	116	17	1.47	3312	0.13169	2.6	1.48032	3.6	0.08153	2.5	0.72	797	19	922	22	1234	49	65
NG4-seq2-b50	16685	25	10	1.11	13015	0.31478	6.2	4.72950	7.3	0.10897	3.9	0.84	1764	96	1772	63	1782	72	**99**
NG4-seq2-b51	6099	17	5	2.20	7253	0.23006	2.7	2.71379	3.9	0.08555	2.7	0.70	1335	33	1332	29	1328	53	**101**
NG4-seq2-b52	39125	63	17	0.97	20283	0.22665	2.6	3.43870	2.8	0.11003	1.1	0.92	1317	31	1513	23	1800	20	73
NG4-seq2-b53	19367	68	10	0.82	5929	0.14167	6.8	1.90621	20.8	0.09759	19.6	0.33	854	55	1083	149	1579	367	54
NG4-seq2-b54	34173	50	18	0.95	2519	0.30994	2.5	4.73500	3.1	0.11080	1.9	0.79	1740	38	1773	27	1813	35	**96**
NG4-seq2-b55	50401	403	31	0.17	2212	0.06535	2.4	0.87021	3.0	0.09657	1.8	0.80	408	9	636	14	1559	33	26

[a] within-run background-corrected mean ^{207}Pb signal in counts per second

[b] U and Pb content and Th/U ratio were calculated relative to GJ-1 and are accurate to approximately 10%.

[c] corrected for background, mass bias, laser induced U-Pb fractionation and common Pb (if detectable, see analytical method) using Stacey & Kramers (1975) model Pb composition. $^{207}Pb/^{235}U$ calculated using $^{207}Pb/^{206}Pb/(^{238}U/^{206}Pb \times 1/137.88)$. Errors are propagated by quadratic addition of within-run errors (2SE) and the reproducibility of GJ-1 (2SD).

[d] Rho is the error correlation defined as $err^{206}Pb/^{238}U/err^{207}Pb/^{235}U$.